Pontifícia Universidade Católica do Rio Grande do Sul
Faculdade de Biociências
Programa de Pós-Graduação em Biologia Celular e Molecular

# Estudo *in silico* de inibidores de SIRT1

Tese apresentada ao Programa de Pós-Graduação em Biologia Celular e Molecular como requisito para a obtenção do grau de Doutor.

Autor
Graziela Heberlé

Orientador
Dr. Walter Filgueira de Azevedo Jr.

Porto Alegre, RS
2011

DEDICATÓRIA

Ao meu orientador, Dr. Walter Filgueira de Azevedo Jr.,
que me deu a oportunidade de realizar este trabalho.

AGRADECIMENTOS

À Pontifícia Universidade Católica do Rio Grande do Sul e ao
Programa de Pós-Graduação em Biologia Celular e Molecular, pelo curso ofertado.
À CAPES, pela bolsa de estudos concedida.
Aos professores e colegas de curso, pelo conhecimento construído.
Ao meu orientador, pela confiança e dedicação.
Aos colegas do LabioQuest-PUCRS, pelo auxílio e feliz convivência.
Aos amigos e familiares, por apoiarem as minhas escolhas.
Aos colegas de trabalho da UNIVATES, pelo incentivo e apoio.
Aos meus alunos, que deram mais sentido a esta busca.

# ÍNDICE

# RESUMO

A natureza como fonte de inspiração provou ter grande impacto benéfico no desenvolvimento de novas metodologias computacionais. Neste cenário, análises de interações entre uma proteína alvo e um ligante podem ser simuladas por algoritmos inspirados biologicamente (BIA). Neste trabalho, os algoritmos inspirados biologicamente, especialmente algoritmos evolutivos, são aplicados a simulações de *docking* molecular, que podem ser usadas na busca de novos fármacos. Estes algoritmos de *docking* foram aplicados a sirtuínas, que compõem uma importante família de proteínas - desacetilases dependentes de NAD - que regulam o silenciamento genético, inibição transcricional, estabilidade cromossômica, ciclo de divisão celular e apoptótico e resposta célular a agentes causadores de danos no DNA. Essas proteínas tem sido alvos moleculares emergentes no desenvolvimento farmacêutico de medicamentos para o tratamento de doenças humanas. Em função da importância estrutural das proteínas, neste trabalho foi realizada a modelagem por homologia molecular de SIRT1 humana, utilizando-se a estrutura cristalográfica de Sir2 de *Thermotoga maritima* como modelo. Além disso, foi aplicado o procedimento de *virtual screening* para a SIRT1 modelada contra duas bases de dados. Uma foi baseada em estruturas derivadas da nicotinamida e outra composta por moléculas da Sigma-Aldrich. Com base nos resultados obtidos no *virtual screening*, foram utilizados os acoplamentos com valores mais baixos de energia livre de ligação (*Plant Score*) para a seleção das melhores moléculas. Foi empregada a Similarity Ensemble Approach Tool (SEA), uma abordagem estratégica para analisar as relações entre as estruturas e a atividade farmacológica. Os resultados indicam que algumas moléculas apresentaram alta afinidade com a SIRT1, sugerindo novos inibidores de SIRT1, e essas moléculas mostram um elevado número de referências de atividades farmacológicas. Nossos resultados sugerem novos compostos inibidores de SIRT1 que apresentam potencial aplicação terapêutica.



Palavras-chave: sirtuínas, SIRT1, inibidores, moléculas, *virtual screening*, atividades farmacológicas.

# ABSTRACT

Nature as a source of inspiration has been shown to have a great beneficial impact on the development of new computational methodologies. In this scenario, analyses of the interactions between a protein target and a ligand can be simulated by biologically inspired algorithms. In this work, bioinspired algorithms, evolutionary algorithms specially, are applied to molecular docking simulations that can be used in the search for new drugs. These docking algorithms were applied to sirtuins, which compose an important family of proteins, nicotine adenine dinucleotide (NAD) deacetylases that regulate gene silencing, transcriptional repression, recombination, the cell apoptosis division cycle, chromosomal stability, and cellular responses to DNA-damaging agents. These proteins are emerging as molecular targets for pharmaceutical development of drugs for treating human diseases. On the basis of the structural importance of these proteins, in this work we carried out the molecular homology modeling of human SIRT1, using *Thermotoga maritima* Sir2 crystallographic structure as template. Furthermore, we also performed a virtual screening procedure for SIRT1 model against two databases. One based on a nicotinamide derivatives and the other composed of molecules from Sigma-Aldrich vendor. Based on the virtual screening results we used the lowest free binding energy (Plant Score) molecules to select the bet hits. We employed a Similarity Ensemble Approach Tool (SEA) for assessing the ligand structure and protein pharmacological activity relationships. Our results indicate some molecules presented high affinity against SIRT1, which suggest new of SIRT1 inhibitors. These molecules show a high number of pharmacological activity references. Our results suggest new compounds for development of SIRT1 inhibitors with potential therapeutic application.

# CAPÍTULO 1

## INTRODUÇÃO E OBJETIVOS

# 1. INTRODUÇÃO E OBJETIVOS

## 1.1. Introdução

### 1.1.1. Sirtuínas

As sirtuínas (SIRT) são uma importante família de proteínas, desacetilases dependentes de $NAD^+$ (nicotinamida adenina dinucleotídeo) que catalisam reações de desacetilação e ADP-ribosiltranferase. São proteínas amplamente distribuídas e conservadas em todos os filos da vida, desde em leveduras até em seres humanos. Micro-organismos como bactérias e leveduras codificam apenas uma sirtuína (Sir2), entretanto os eucariotos possuem várias. A família das sirtuínas em mamíferos é constituída de sete membros (SIRT1-7) homólogos da Sir2. Cada sirtuína é caracterizada por um domínio catalítico com uma sequência conservada de 275 aminoácidos e também por uma única sequência adicional N- e/ou C-terminal de comprimento variável. As primeiras sirtuínas encontradas, Sir2 em levedura ou SIRT1 em mamíferos, são consideradas moléculas chaves que afetam a longevidade, embora por mecanismos diferentes. Como mecanismos são sugeridos a regulação de reparos no DNA, silenciamento de genes e aumento da estabilidade cromossomal (Sauve, Wolberger *et al.*, 2006; Michan e Sinclair, 2007; Sedding e Haendeler, 2007; Yamamoto, Schoonjans *et al.*, 2007; Neugebauer, Uchiechowska *et al.*, 2008).

Estas proteínas foram classificadas em 4 grupos filogenéticos, com base na similaridade das suas sequências. As SIRT1, SIRT2 e SIRT3 compõem a classe I; a SIRT4 constitui a classe II; a SIRT5 a classe III; e as SIRT6 e SIRT7 formam a classe IV. As distintas localizações das sirtuínas nas células contribuem para as suas diferentes funções. As SIRT1, SIRT6 e SIRT7 estão predominantes no núcleo, estando envolvidas na estabilidade genômica e proliferação celular, enquanto a SIRT2 é a sirtuína que reside mais proeminente no citoplasma e está envolvida na

mitose. As SIRT3, SIRT4 e SIRT5 têm sido descritas como sirtuínas mitocondriais e apresentam um papel no metabolismo energético e resposta ao estresse oxidativo. Todas as 7 sirtuínas são expressas em tecidos humanos, sendo que níveis mais altos são detectados no cérebro para a maioria delas (Baur, Pearson *et al.*, 2006; Michan e Sinclair, 2007; Yamamoto, Schoonjans *et al.*, 2007). O papel das desacetilases de histonas (HDACs) e o potencial destas enzimas, como alvos terapêuticos, para o câncer, doenças neurodegenerativas e uma série de outras doenças é uma área de investigação que tem expandido rapidamente (Marks e Xu, 2009).

O papel vital das sirtuínas no controle metabólico e celular indica que elas têm função importante no metabolismo e podem proteger contra muitas doenças crônicas decorrentes de diversas disfunções metabólicas (Yamamoto, Schoonjans *et al.*, 2007). Portanto estas proteínas têm recebido considerável atenção, sendo relacionadas à busca de novos tratamentos para doenças associadas ao envelhecimento e, possivelmente, ao aumento da longevidade humana.

#### 1.1.1.1. Mecanismos de ação de sirtuínas

As sirtuínas estão inseridas na família das desacetilases de histonas. A atividade enzimática das sirtuínas afeta o estado conformacional e as atividades das proteínas substratos. As HDACs catalisam a remoção de grupos acetila das histonas resultando na compactação da cromatina (heterocromatina), regulando a expressão gênica. Desta forma, silenciam a transcrição por impedir o contato de fatores de transcrição, complexos regulatórios e RNA polimerase com o DNA. A reação inversa, de promoção da transcrição, pode ocorrer, por acetilação quando a eucromatina é formada: uma estrutura de conformação mais aberta, que promove o contato com os fatores de transcrição. Três classes de desacetilases de histonas

foram descritas em humanos: as classes I e II têm sido demonstradas como dependentes de zinco, e as enzimas de classe III (sirtuínas de 1 a 7) são dependentes de NAD e geralmente não são inibidas por compostos que inibem desacetilases zinco dependentes (Smith, Brachmann *et al.*, 2000; Langley, Gensert *et al.*, 2005; Neugebauer, Uchiechowska *et al.*, 2008; Marks e Xu, 2009).

Embora muitas sirtuínas catalisem uma reação de desacetilação de histonas de forma bem caracterizada, há uma série de relatos que sugerem sua atividade ADP-ribosiltransferase (figura 1). Entre os dois mecanismos pelos quais atuam as sirtuínas, as SIRT 1, 2, 3, 5 e 7 agem por desacetilação com a utilização de NAD (nicotinamida adenina dinucleotídeo). O NAD, ligado à sirtuína, reage com o grupo acetil de uma proteína alvo liberando nicotinamida, a proteína desacetilada e ainda 2 isômeros 3'-O-acetil-ADP-ribose e 2'-O- acetil-ADP-ribose. A nicotinamida é inibidora de sirtuínas podendo reverter a reação. Já as SIRT 4 e 6 são ADP-ribosiltransferases, ligam à proteína uma ADP-ribose e liberam nicotinamida. Destes dois mecanismos, o primeiro é o mais estudado (Smith, Brachmann *et al.*, 2000; Porcu e Chiarugi, 2005; Michan e Sinclair, 2007; Vakhrusheva, Braeuer *et al.*, 2008).

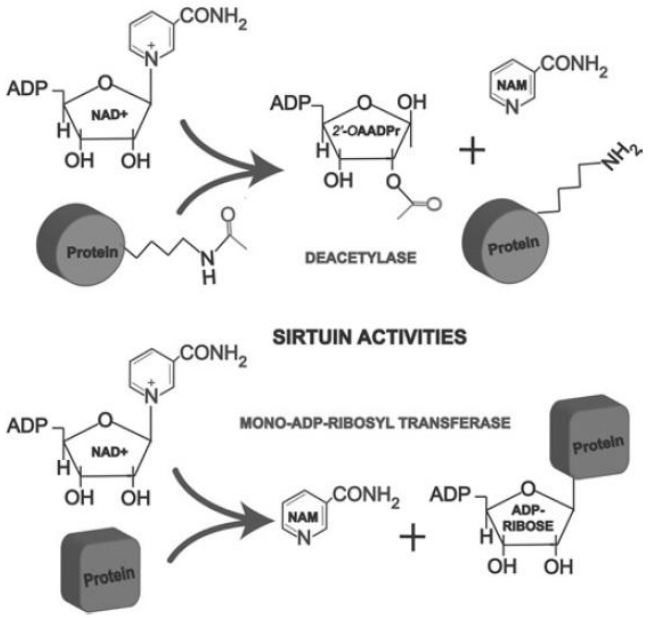


**Figura 1**. Mecanismo de ação de sirtuínas. Fonte: Michan e Sinclair, 2007

### 1.1.1.2. Substratos de sirtuínas e seus efeitos

As sirtuínas agem em diversos substratos com atividade transcricional, de apoptose e de regulação metabólica. Em geral, a diminuição da regulação transcricional pelas sirtuínas é associada com a desacetilação de histonas (Sauve, Wolberger *et al.*, 2006). Os substratos de sirtuínas não-histonas incluem vários reguladores transcricionais, tal como o fator nuclear kB (NFk-B), os fatores transcricionais da familia *forkhead box type O* (FOXO), e o proliferador e ativador de peroxisomas, PPAR-γ um coativador de PGC-1α, além de enzimas, como acetil coenzima A sintase 2 (AceCS2), glutamato desidrogenase (GDH) e proteínas estruturais, tal como a α-tubulina (Tabela 1). Deste modo, as sirtuínas são responsáveis por regular uma variedade de processos celulares e metabólicos de mamíferos (Sauve, Wolberger *et al.*, 2006; Yamamoto, Schoonjans *et al.*, 2007).

Entre as sirtuínas, a mais estudada e bem descrita sirtuína humana é a SIRT1, localizada no núcleo. Ela atua por desacetilação, tendo como alvos PCG-1α, NFk-B, $FOXO_S$, diminuindo a inflamação, a neurodegeneração, podendo ser neuroprotetora, e também está envolvida em diversos processos metabólicos, como metabolismo de lipídios por exemplo, conforme tabela 1 e figura 2.

A SIRT2 desacetila a histona H4 e a $\alpha$-tubulina, agindo como inibidora do ciclo celular e da tumorogênese (Vaquero, Scher *et al.*, 2006). Já a SIRT3, mitocondrial, atua na enzima AceCS2, facilitando o consumo de acetato e gerando energia quando o ATP está escasso (Hallows, Lee *et al.*, 2006; Hirschey, Shimazu *et al.*, 2010). A SIRT4 interage com a glutamato desidrogenase (GDH), diminuindo sua atividade. Assim ocorre a redução da produção de ATP, promovendo ativação mitocondrial e inibindo a secreção de insulina. A SIRT1 e SIRT4 apresentam efeitos antagônicos na secreção de insulina: a primeira estimula e a segunda inibe (Haigis, Mostoslavsky *et al.*, 2006).

**Tabela 1**. Características de sirtuínas de mamíferos.

| SIRT | LOCAL | ATIVIDADE | ALVOS | FUNÇÃO BIOLÓGICA |
|---|---|---|---|---|
| SIRT1 | Núcleo | Desacetilase | PGC-1α, p53, NFk-B, FOXOs | Metabolismo/inflamação/ neurodegeneração/ciclo celular |
| SIRT2 | Citoplasma | Desacetilase | H4, α-tubulina | Ciclo celular/tumorogênese |
| SIRT3 | Núcleo e mitocôndria | Desacetilase | AceCS2 | Metabolismo |
| SIRT4 | Mitocôndria | ADP-ribosil transferase | GDH | Secreção de insulina |
| SIRT5 | Mitocôndria | Desacetilase | Desconhecido | Desconhecido |
| SIRT6 | Núcleo | ADP-ribosil transferase | DNA polimerase β | Reparo do DNA |
| SIRT7 | Núcleo | Desacetilase | RNA polimerase I, p53 | Transcrição do rDNA |

Fonte: Yamamoto, Schoonjans *et al*, 2007 (adaptado).

O substrato nativo da SIRT5 permanece desconhecido (Schuetz, Min *et al.*, 2007). A SIRT6 é uma fraca desacetilase, mas dotada de robusta atividade ADP-ribosiltransferase, que está envolvida na manutenção da integridade do genoma, promovendo reparos no DNA (Mostoslavsky, Chua *et al.*, 2006). A última delas, a SIRT7, interage na RNA polimerase I ativando a transcrição de rDNA, ao passo que sua regulação negativa diminui a transcrição. Foi também relatado que esta sirtuína inibe o p53 por desacetilação. Assim, a SIRT7 inibe a proliferação e promove o controle do ciclo celular. Contudo no câncer de mama ocorre o aumento significativo na expressão da SIRT7 e também da SIRT3, bem como estes níveis estão aumentados em células senescentes, sendo pertinente a ligação entre a expressão transcricional de genes envolvidos no envelhecimento e no câncer (Ashraf, Zino *et al.*, 2006; Ford, Voit *et al.*, 2006; Vakhrusheva, Braeuer *et al.*, 2008).

A figura 2 apresenta resumidamente diversos eventos celulares e do metabolismo nos quais a SIRT1 está envolvida. Essa sirtuína é a chave reguladora da sobrevivência celular em resposta ao estresse, ou seja, promove resistência ao estresse resultando em longevidade, efeito semelhante ao observado em Sir2 de leveduras.

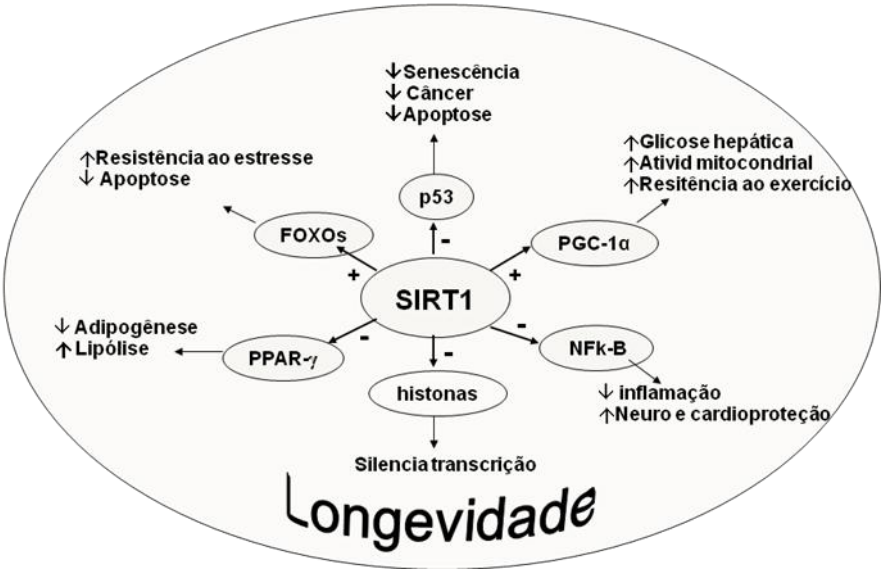


**Figura 2**. Processos celulares e metabólicos ativados (+) ou inibidos (-) por SIRT1.

A SIRT1 inibe ou ativa seus substratos por desacetilação (figura 2). O supressor tumoral p53 é inibido, aumentando a sobrevivência celular, diminuindo senescência, a perda celular no estresse e a possibilidade de câncer por inibir o ciclo celular em resposta a dano de DNA. O PPAR-$\gamma$ é inibido, mobilizando gordura das células adiposas e diminuindo adipogênese. Também inibe NFk-B diminuindo a resposta inflamatória e gerando efeito neuro e cardioprotetor. A SIRT1 age como um sensor de energia celular com PGC-1α, através das alterações nos níveis de NAD, o qual afeta sua atividade de desacetilase. Ainda, ativa o PGC-1α, promovendo ativação mitocondrial no músculo, aumentando a resistência ao exercício, e aumentando a glicose hepática. Essa sirtuína afeta fatores de transcrição da família FOXO, diminuindo a apoptose e aumentando a resistência ao estresse oxidativo (Picard, Kurtev *et al.*, 2004; Frescas, Valenti *et al.*, 2005; Nemoto, Fergusson *et al.*, 2005; Rodgers, Lerin *et al.*, 2005; Bordone, Motta *et al.*, 2006; Lagouge, Argmann *et al.*, 2006; Michan e Sinclair, 2007; Opie e Lecour, 2007; Sedding e Haendeler, 2007; Yamamoto, Schoonjans *et al.*, 2007; Vakhrusheva, Braeuer *et al.*, 2008).

Também, dados controversos sugerem que as sirtuínas podem não só prevenir, mas promover o câncer. SIRT1 pode diminuir a proliferação e ativar os

mecanismos de defesas ao estresse e reparo de DNA, permitindo assim a preservação da integridade genômica. Por outro lado em certos tipos de cânceres, SIRT1 parece favorecer o crescimento tumoral. A SIRT1 pode agir de forma diferenciada dependendo do tipo de tumor e das alterações genéticas que ocorrem durante a tumorogênese (Ford, Jiang *et al.*, 2005; Greer e Brunet, 2005; Brooks e Gu, 2009a; b).

#### 1.1.1.3. Moduladores de sirtuínas

As sirtuínas promovem longevidade em diversos organismos e podem aumentar a expectativa de vida. As rotas das sirtuínas também modulam mecanismos fundamentais nas doenças neurodegenerativas e relacionadas ao envelhecimento, incluindo agregação de proteínas, respostas ao estresse, homeostase mitocondrial e processos inflamatórios. A ativação de mecanismos moleculares que retardam o envelhecimento pode ser estratégica na prevenção e no tratamento destas doenças (Gan e Mucke, 2008; Kyrylenko e Baniahmad, 2010).

Com base nos benefícios à saúde observados pela restrição calórica em mamíferos, na qual se constatam sirtuínas aumentadas, Howitz *et al* (2003) apresentaram um estudo no qual foi realizada uma busca por pequenas moléculas, entre elas alguns polifenóis do vinho, que podem modular a atividade de sirtuínas. Inicialmente foram identificados diversos inibidores de SIRT1, porém o resultado mais notável foi o de terem sido identificados dois compostos com estruturas similares – quercetina e piceatanol – que estimularam a atividade de SIRT1.

##### 1.1.1.3.1. Ativadores de sirtuínas

A ativação das rotas das sirtuínas tem efeito antienvelhecimento e pode fornecer novas alternativas terapêuticas para prevenir ou retardar doenças a ele relacionadas. As SIRT1 e, em menor intensidade, a SIRT2 têm papéis importantes

no envelhecimento e nas doenças degenerativas (Baur, Pearson *et al.*, 2006). As sirtuínas podem bloquear diversos processos que contribuem com o dano neuronal ligado ao envelhecimento, o acúmulo de proteínas alteradas, morte celular e disfunção mitocondrial. Por aumentar a resistência ao estresse e promover processos de reparo a sirtuínas podem neutralizar os resultados do crescente dano oxidativo. Além de proteger os neurônios diretamente, os ativadores da sirtuínas também reprimem a resposta inflamatória (Gan e Mucke, 2008).

No estudo publicado por Howitz et al (2003), dois compostos polifenólicos, além do resveratrol, apresentaram importante ativação da sirtuína humana SIRT1. Quando comparados estes dois compostos, foi sugerida uma possível relação estrutura-atividade. Os anéis de *trans*-estilbeno do piceatanol se sobrepoem nos anéis A e B dos anéis do flavonoide quercetina, as hidroxilas nas posições 5, 7, 3`e 4` da quercetina podem ser alinhadas com respectivamente as hidroxilas em 3, 5, 3` e 4`do piceatanol, como pode ser observado na tabela 1 do anexo I. Quercetina e piceatanol são polifenóis, membros de um grande grupo de metabólitos secundários de plantas, que incluem flavonas, estilbenos, flavononas, isoflavonas, catequinas (flavona-3-óis), chalconas, taninos e antocianidinas. Numa segunda busca na família destes compostos, foram identificados mais 15 ativadores de SIRT1, entre eles foram encontrados alguns muito conhecidos e frequentes em plantas medicinais como quercetina, camferol, luteonina, entre outros (Howitz, Bitterman *et al.*, 2003).

O crescente interesse da comunidade científica pela molécula do resveratrol deve-se a existência de muitos estudos que demonstram a possibilidade desta molécula prevenir a progressão de várias doenças, assim como aumentar a resistência ao estresse e a expectativa de vida. O estudo desenvolvido por Jang e colaboradores em 1997, no qual o resveratrol inibiu eventos celulares associados com iniciação, promoção e progressão tumoral (Jang, Cai *et al.*, 1997), despertou

interesse da comunidade científica, e essa molécula tornou-se conhecida, desde então, por seus diversos efeitos como antioxidante, anti-inflamatória, antiviral, cardioprotetora, neuroprotetora, quimiopreventiva de câncer, além de reduzir a obesidade e prevenir o envelhecimento (Baur e Sinclair, 2006).

O resveratrol é um polifenol produzido por uma ampla variedade de plantas, muitas das quais são componentes da dieta humana, como, por exemplo, a uva e o amendoim. A casca da uva fresca contém aproximadamente 50 a 100µg de resveratrol por grama, e a concentração no vinho tinto varia de 1.5 a 3mg.L-1 (Jang, Cai *et al.*, 1997). Experimentos realizados com diferentes linhagens de células humanas demonstraram que o resveratrol modulou uma variedade de processos através da dependência da SIRT1, incluindo neuroproteção, supressão tumoral, diferenciação e inflamação (Michan e Sinclair, 2007). Foi observado o potencial neuroprotetor do resveratrol bem como da quercetina contra vários diferentes tipos de danos incluindo a doença de Parkinson e Alzheimer (Okawara, Katsuki *et al.*, 2007; Opie e Lecour, 2007). Estudo recente demonstrou que o resveratrol via SIRT1 também desempenha um papel crítico na regulação da inflamação que controla a colite e o câncer de cólon (Hofseth, Singh *et al.*, 2010). Recentemente, foi postulada a nova hipótese de que o resveratrol não ativa diretamente a SIRT1 (Tang, 2010)

#### 1.1.1.3.2. Inibidores de sirtuínas

As sirtuínas dependem de $NAD^+$ para realizarem a desacetilação e são inibidas seletivamente por nicotinamida (SIRT1 inibida com $IC_{50}$ de 40 µM e a SIRT2 com $IC_{50}$ de 10 µM) (Marcotte, Richardson *et al.*, 2004). A atividade das sirtuínas está relacionada a diversas patogenias, como câncer e o HIV, além de doenças neurológicas. Somente um número limitado de inibidores de sirtuínas é conhecido e alguns deles não são capazes de inibir os subtipos humanos (Neugebauer, Uchiechowska *et al.*, 2008; Zhang, Sang *et al.*, 2010).

A inibição das sirtuínas é uma área importante para a investigação na indústria farmacêutica, uma vez que tais compostos poderiam modular processos celulares por induzir hiperacetilação de histonas, p53 e, possivelmente outras proteínas. O primeiro inibidor sintético descoberto foi o sirtinol. Logo após, a splitomicina foi publicada como inibidor de sirtuínas de levedura, mas mostrou fraca inibição nas enzimas humanas. O primeiro inibidor das formas humanas de sirtuína foi um derivado de splitomicina com $IC_{50}$ menor do que 5μM. Mais tarde o cambinol foi descoberto a partir de um screening aleatório o qual apresentou atividade anticâncer (Marcotte, Richardson *et al.*, 2004; Neugebauer, Uchiechowska *et al.*, 2008). A investigação da inibição das sirtuínas pode também ser de grande interesse no processo de envelhecimento. Já é conhecido que a Sir2 apresenta tanto um papel de pró quanto antienvelhecimento (Longo e Kennedy, 2006). Foi descoberto que a SIRT1 tem efeitos diversos na senescência, dependendo da forma particular de sua ativação. Uma análise detalhada de sua função é importante no entendimento da atividade moduladora de SIRT1 no envelhecimento de mamíferos (Chua, Mostoslavsky *et al.*, 2005).

Entre os inibidores de SIRT2 conhecidos estão 1,4-bis[2-(4-hidroxi-feinl)-etilamina]-antraquinona (Tervo, Kyrylenko *et al.*, 2004), para-sirtinol (Mai et al, 2005), N,N`-bis(2-hidroxibenzilideno)benzeno-1,4-diamina (Kiviranta, Leppanen *et al.*, 2006), cambinol (Heltweg, Gatbonton *et al.*, 2006) e EX-527 que é também um potente inibidor de SIRT1 (Lain, Hollick *et al.*, 2008). Recentemente foi relatado que miméticos de adenosina (Trapp, Jochum *et al.*, 2006), análogos da suramina (Trapp, Meier *et al.*, 2007) e derivados de floroglucinol (Gey, Kyrylenko *et al.*, 2007) também são inibidores de SIRT2. Além disso, um inibidor de SIRT2 potente e seletivo chamado AGK2 foi identifico por Outeiro *et al*.(2007). Todos os inibidores de SIRT2, que são pequenas moléculas, conseguem inibi-la ao nível de micromolar (Outeiro,

Kontopoulos *et al.*, 2007; Brooks e Gu, 2008; Kiviranta, Salo *et al.*, 2008; Lain, Hollick *et al.*, 2008).

Sirtinol e M15, bem como splitomicina, foram identificados através de *screening* de bibliotecas como inibidores de enzimas humanas ou de levedura. No entanto, estes compostos têm limitada solubilidade em água e são menos potentes do que a nicotinamida (Marcotte, Richardson *et al.*, 2004). Liu e colaboradores (2009) observaram que a nicotinamida foi capaz de preservar os níveis de NAD em neurônios atenuando a morte celular induzida por agressões citotóxicas através da inibição da atividade da SIRT1. Esta pesquisa sugere que há um potencial benefício terapêutico de agentes que preservam os níveis de NAD celulares, como ocorre com a utilização da nicotinamida, um precursor de NAD e inibidor de SIRT1 (Marcotte, Richardson *et al.*, 2004; Liu, Gharavi *et al.*, 2009). A suramina demonstrou atividade inibitória contra SIRT1, apresentando um $IC_{50}$ de 2,6 µM (Schuetz, Min *et al.*, 2007). Trapp e colaboradores desenvolveram análogos à suramina, obtendo assim maior seletividade. Além da atividade antiproliferativa, tem sido atribuída à molécula da suramina e a seus derivados uma atividade antiviral e antitripanossomal (Trapp, Meier *et al.*, 2007; De Clercq, 2009).

Relatou-se que diversos inibidores de sirtuínas possuem atividade antitumoral, tais como nicotinamida, esplitomicina, sirtinol, cambinol, dihidrocumarina, alguns indóis e salermida (Bedalov, Gatbonton *et al.*, 2001) (Bitterman, Anderson *et al.*, 2002; Avalos, Bever *et al.*, 2005; Olaharski, Rine *et al.*, 2005; Heltweg, Gatbonton *et al.*, 2006; Ota, Tokunaga *et al.*, 2006; Lara, Mai *et al.*, 2009). Contudo o efeito antitumoral que esses compostos apresentam em comum depende, em geral, do tipo de tumor e das condições de estresse. Além disso, os seus mecanismos de ação ocorrem de forma variada ou ainda não estão completamente elucidados. Lara e colaboradores (2009) descreveram a síntese e o

mecanismo de ação de salermida, um potente inibidor de SIRT1 e SIRT2, induzindo a apoptose somente no câncer e preservando as células normais. Através de dados experimentais, estudos de *docking* e mecânica molecular foi identificado um novo inibidor de denominado β-fenilesplitomicina. Foi demonstrado que os derivados de splitomicinas são inibidores não competitivos com o NAD. A relação entre o aumento da inibição da enzima e a atividade anticâncer foi estabelecida. Dessa forma, estes inibidores são candidatos para futuras otimizações como potenciais drogas anticâncer (Neugebauer, Uchiechowska et al., 2008).

Estudos indicam que inibidores específicos da expressão de sirtuínas levam ao aumento da morte de células tumorais. Lain e colaboradores (2008) demonstraram através de testes *in vitro* que os tenovinas (1 e 6) inibem SIRT1 e SIRT2 sendo capazes de inibir o crescimento tumoral. Para tanto, preliminarmente, foi realizado screening de 30 mil pequenas moléculas com potencial de inibição. A tenovina-6 apresentou solubilidade em água sete vezes maior que a tenovina 1, o que lhe conferiu maior eficiência, sendo identificado como potente inibidor seletivo de SIRT1 e SIRT2 humanas purificadas que indiretamente ativaram o p53 em concentrações micromolares, apresentando ainda maior toxicidade às células de melanoma. Portanto este composto pode ser um atraente quimoterápico como agentes únicos ou em combinação com outros ativadores específicos de p53 (Brooks e Gu, 2008; Lain, Hollick *et al.*, 2008).

Ferramentas computacionais têm tornado possível a obtenção de informações para o desenvolvimento de inibidores de sirtuínas e seus sítios de ligação. As sirtuínas obtidas por modelagem tridimensional por homologia podem ser utilizadas como alvos eficazes nos testes para desenvolver drogas anti-tripanossomais e anti-leishmania. É possível obter informações através de estudos estruturais detalhados que comparam o acoplamento de sirtuínas humanas como SIRT1 e Sir2 de

protozoários. Estas informações são importantes no desenvolvimento de novas estratégias para o desenho de fármacos antiparasitários que sejam inibidores seletivos, com maior toxicidade em relação à proteína alvo do parasita e menor toxicidade à proteína humana (Zemzoumi, Sereno *et al.*, 1998; Vergnes, Sereno *et al.*, 2002; Vergnes, Vanhille *et al.*, 2005; Alsford, Kawahara *et al.*, 2007; Glover, Alsford *et al.*, 2007; Kiviranta, Salo *et al.*, 2008; Kaur, Shivange *et al.*, 2010).

#### 1.1.1.4. Estruturas de sirtuínas

Cristalografia de proteínas é uma ferramenta essencial para a descoberta e a investigação de interações farmacológicas ao nível molecular. Isto permite a visualização direta das estruturas tridimensionais de proteínas, incluindo enzimas, receptores e hormônios. O conhecimento crescente destas interações está sendo utilizado no processo de descoberta de novos fármacos. O fármaco desejado poderia ser um inibidor de enzima ou um agonista que mimetiza transmissores endógenos ou hormônios. Uma vez que a estrutura tridimensional de um alvo farmacologicamente relevante é conhecida, processos computacionais podem ser usados para buscar bancos de dados de compostos para identificar os que podem interagir fortemente com o alvo. Novos compostos podem ser melhorados ou aprimorados usando a estrutura tridimensional do complexo deste composto com seu alvo biológico (Bernstein, Koetzle *et al.*, 1977; Berman, Westbrook *et al.*, 2000) (Westbrook, Feng, Burkhardt *et al.*, 2003) (Westbrook, Feng, Chen *et al.*, 2003) (Westbrook, Ito *et al.*, 2005; Canduri e De Azevedo, 2008).

A elucidação de estruturas tridimensionais de várias sirtuínas abriu a possibilidade de correlacionar estudos estruturais e funcionais, que tornam possível entender fatores chave relacionados ao mecanismo de ação e inibição destas enzimas (Finnin, Donigian *et al.*, 2001; Avalos, Boeke *et al.*, 2004; Avalos, Bever *et al.*, 2005; Hoff, Avalos *et al.*, 2006). A busca no PDB (Berman, Westbrook *et al.*,

2000) usando as palavras Sir2 e “sirtuin” indicou a presença de 44 estruturas de sirtuínas, todas resolvidas por cristalografia de proteínas por difração de raios x. As tabelas 2 e 3 (anexo I), apresentam os códigos PDB (*protein data bank*) de acesso para todas as estruturas cristalográficas disponíveis até dezembro de 2010. São diversas as estruturas tridimensionais publicadas atualmente, mas nenhuma estrutura tridimensional de sirtuína 1 está disponível.

A análise das estruturas terciárias indicou um típico enovelamento do tipo *Rossmann fold* em todas as estruturas das sirtuínas, motivo estrutural típico encontrado em proteínas que se ligam a nucleotídeos tais como o $NAD^+$. As estruturas das sirtuínas apresentam uma folha $\beta$ aberta e torcida com hélices $\alpha$ em ambos lados, um arranjo estrutural construído a partir de motivos $\beta/\alpha/\beta$ que são conectados, assim como as fitas $\beta$ são paralelas (Finnin, Donigian *et al.*, 2001). As sirtuínas possuem, nas suas estruturas, um domínio catalítico conservado de 250 a 275 aminoácidos, com uma variação no tamanho das sequencias na região N e C terminal. A estrutura do domínio catalítico consiste numa conformação do tipo *Rossmann-fold* e um pequeno sítio de ligação de zinco. A interface entre o subdomínio grande e pequeno é em geral subdividida em sítios A, B e C. Esta subdivisão é baseada na interação de adenina (sítio A), sítio de ribose (sítio B) e o de nicotinamida, que são partes do cofator $NAD^+$ (sítio C). (Sauve, Wolberger *et al.*, 2006; Michan e Sinclair, 2007; Neugebauer, Uchiechowska *et al.*, 2008).

Estudos de *docking* entre SIRT2 humana e estudos experimentais de competição com o $NAD^+$ demonstram que os compostos interagem no sítio da adenina e da nicotinamida (suramina). Devido à diferença estrutural entre estes inibidores e a splitomicina, pode-se esperar que eles interajam de uma forma diferente com a sirtuína. A inclusão de 4 moléculas de água encontradas em todos os monômeros de SIRT2 e localizadas na cavidade próxima ao sítio ativo melhorou

significativamente os resultados de *docking*. As regiões polares dos inibidores conhecidos, tais como cambinol, demonstraram interação com os resíduos polares Gln167 e Asn168 e com as moléculas de água do sítio de nicotinamida (Neugebauer, Uchiechowska *et al.*, 2008). Estas interações foram identificadas através de simulações com o programa GOLD (Jones, Willett *et al.*, 1997b).

A elucidação da estrutura de Sir2 de *Thermotoga maritima* (Sir2Tm) revelou interações complementares de cadeia lateral que contribuem para compreensão da especificidade de substratos de sirtuínas. Estas interações de cadeia lateral contribuem para a ligação do peptídeo alvo (p53) através de interações de hidrogênio e interações de van der Waals (Cosgrove, Bever *et al.*, 2006).

### 1.1.2. *Virtual screening*

Para a simulação computacional da interação de proteína com ligante, um processo chamado de *docking*, há diversos programas disponíveis, que podem ser classificados pelos seus algoritmos (Tabela 4, anexo I), levando em conta diversos fatores como a flexibilidade das moléculas, a carga dos átomos e interações de van der Waals (Goodsell, Morris *et al.*, 1996). Esses programas foram desenvolvidos com o objetivo de obter um procedimento rápido capaz de identificar um novo composto, *virtual screening*, ou reproduzir uma estrutura experimental cristalográfica para validação, ou *redocking*. Previamente às simulações de docking é executada a validação, com o objetivo de verificar a capacidade do algoritmo de docking de encontrar o posicionamento de uma molécula no sítio de ligação.

Os complexos gerados a partir das simulações de *docking* são comparados com a estrutura cristalográfica, sendo assim o RMSD (desvio médio quadrático) calculado. O valor de RMSD é calculado pela seguinte equação:

$$RMSD(C,D) = \sqrt{\frac{1}{N}\sum_{i=1}^{N}[(C_{ix} - D_{ix})^2 + (C_{iy} - D_{iy})^2 + (C_{iz} - D_{iz})^2}$$

Onde C e D são os grupos de coordenadas atômicas (x, y e z) de um número determinado de átomos, para duas moléculas, C para o ligante observado na estrutura cristalográfica e D para cada estrutura do ligante obtida por *docking*. Assim é obtido o RMSD para cada estrutura resultante do *docking*. O melhor complexo binário é o que tem maior aproximação à estrutura determinada por cristalografia de raio-x, ou seja, o de menor valor de RMSD (Dias e De Azevedo, 2008). Em simulações de *docking*, os melhores resultados apresentam valores de RMSD inferiores a 2,0 Å (Tsai, Wang *et al.*, 2008).

Existem inúmeros métodos de busca do complexo de maior afinidade utilizados pela aplicação de *docking*s: geometria de distância (*Distance Geometry*) (Moré e Wu, 1999), programação evolutiva (*Evolutionary programming*) e algoritmos genéticos (*Genetic Algorithms*), simulação com recozimento (*Simulated annealing*), busca tabu (*Tabu search*) (De Azevedo e Dias, 2008; Dias e De Azevedo, 2008).

Simulações de *docking* (acoplamento) podem ser rígidas (*rigid-body docking*) – ligante e proteína – não apresentam liberdade de variar os ângulos de torção, ou flexíveis (*flexible-body docking*) – os ângulos de torção do ligante ou até a proteína podem girar – na simulação. As duas formas de simulação obtêm como resultado as coordenadas tridimensionais de um complexo da proteína com o seu possível ligante. A inclusão de flexibilidade em simulações de *docking* está associada ao aumento da demanda de CPU, pois neste método ocorre um aumento de graus de liberdade de molécula (Dias e De Azevedo, 2008; Dias, Timmers *et al.*, 2008).

O processo de acoplamento geralmente resulta em inúmeras conformações possíveis. Funções de pontuação (*scoring functions*) são capazes de classificar os resultados avaliando a afinidade de ligação intermolecular ou energia livre de ligação. Assim, pode-se obter a melhor posição após o procedimento de

acoplamento (De Azevedo e Dias, 2008). Resultados de pesquisas recentes indicam fortemente que as abordagens de acoplamento de maior sucesso são aquelas baseadas em algoritmos biologicamente inspirados (*Biologically Inspired Algorithms – BIAs*) (Thomsen e Christensen, 2006; De Azevedo, 2010), tal como a programação evolutiva (*Evolutionary Programing – EP*) (Eiben e Smith, 2003) (Fogel, Owens *et al.*, 1966) e algoritmos genéticos (*Genetic Algorithms – Gas*) (Jones, Willett *et al.*, 1995; Jones, Willett *et al.*, 1997a; Morris, Goodsell *et al.*, 1998).

MOLDOCK apresenta dois BIAs para realizar buscas em posição de simulações de encaixe. Um é o algoritmo otimizador de busca (MOLDOCK *Optimizer*), que é baseado em algoritmo evolucionário (EA). O segundo é um algoritmo de evolução diferencial guiada (GDEA) chamado MOLDOCK SE. GDEA é baseado em uma adaptação da EA chamado de evolução diferencial (ED), que fornece um método diferenciado de seleção e modificação de soluções candidatas (indivíduos). O GDEA emprega um algoritmo de predição de cavidade para limitar conformações previstas (poses) durante o processo de busca. Antes de iniciar as simulações de *docking* molecular, todos os locais potenciais de ligação podem ser identificados por meio de "*detect cavities*" opção no programa MOLDOCK. Na aplicação do GDEA para simulações moleculares de *docking*, apenas as propriedades dos ligantes são representados nos indivíduos, pois a proteína permanece fixa ao longo da simulação de *docking*.

São atribuídos à estrutura do ligante, três parâmetros principais: orientação do ligante, ângulos de torção flexíveis e conformação das coordenadas (x, y, z) do ligante. Cada um dos três parâmetros é codificado como uma posição referente ao ligante cristalográfico. Para x, y, e z é atribuído um número aleatório igualmente disperso entre um -15,0 e 15,0, que é adicionado ao centro do ligante de referência

cristalográfico. Os ângulos de torção são considerados como um ângulo aleatório que varia de -180 ° a 180 °. Um ângulo de torção é calculado a partir das coordenadas atômicas do ligante.

Simulações moleculares de *docking* utilizam uma função de energia baseada em pontuação (*scoring*) para encontrar a conformação do ligante mais energicamente favorável, quando acoplado com a proteína alvo. A pontuação de mais baixa energia indica o melhor complexo, comparado com os valores mais elevados (Thomsen e Christensen, 2006; De Azevedo, 2010). Quatro funções *scoring* foram implementadas na versão mais recente do MOLDOCK, incluindo MOLDOCK *score* (Thomsen e Christensen, 2006) e PLANTS *score* (Korb, Stutzle *et al.*, 2009). Essas duas funções oferecem versões baseada em grade (*grid*) na qual a direção da ligação de hidrogênio não é considerada. As funções de pontuação baseadas em grade (*grid*) oferecem cerca de quatro vezes maior rapidez realizando um pré-processamento dos valores de energia potencial em uma grade cúbica igualmente espaçada. A função de pontuação MOLDOCK (MOLDOCK *score*) baseia-se em funções de pontuação propostas inicialmente por Gehlhaar et al. (Gehlhaar, Verkhivker *et al.*, 1995; Gehlhaar, Bouzida *et al.*, 1997) e desenvolvido por Yang et al. (Yang, 2004; Yang e Chen, 2004). A função scoring de *docking* $E_{MOLDOCK\ SCORE}$ se define por:

$$E_{MOLDOCK\ SCORE} = E_{Intramol} + E_{intermol}$$

onde $E_{intermol}$ energia de interação molecular:

$$E_{intermol} = \sum_{i \in ligand} \sum_{j \in protein} \left[ 332 \frac{q_i q_j}{Dr_{ij}} + E_{PLP}(r_{ij}) \right]$$

Todos os átomos não-hidrogênios no ligante e proteína são considerados no somatório, e átomos como água e cofatores podem ser incluídos nesta soma. O

primeiro termo calculado corresponde às interações eletrostáticas, em que o fator 332 é usado para obter a energia em kJ / mol. D representa a constante dielétrica, que é a seguinte: $D=4r_{ij}$, onde $r_{ij}$ é a distância de duas partículas (i e j). O segundo termo ($E_{PLP}$) foi descrito em trabalho prévio (Yang, 2004; Yang e Chen, 2004; De Azevedo, 2010). Para garantir que nenhum termo de energia possa ser superior à penalidade de colisão, o termo eletrostático é limitado a um nível equivalente ou inferior à distância de 2,0Å. A energia intramolecular é dada pela seguinte equação:

$$E_{intramol} = E_{penalty} + \sum_{i \in ligand} \sum_{j \in ligand} E_{PLP}(r_{ij}) + \sum_{singlebonds} [1 - \cos(n\varphi - \varphi_0)]$$

O termo $E_{penalty}$ é uma energia de penalidade a ser adicionado ao $E_{intramol}$ quando dois átomos não ligados são mais próximos que 2 A (para átomos de não-hidrogênio). Este termo evita topologias moleculares irrealistas para os ligantes. O segundo termo é uma PLP, já mencionado. O último termo corresponde à energia de torção, que é expresso como uma função periódica. Nesse termo, A, n, e $\phi$ são empiricamente determinados (Yang, 2004; Yang e Chen, 2004).

MOLDOCK define uma esfera para limitar onde a pesquisa está focada. Se um átomo não-hidrogênio de ligante é posicionado fora dessa esfera limitante (espaço de busca), então uma constante de penalidade de 10000 é adicionado ao total de energia. Além da função de pontuação empírica descrita anteriormente, MOLDOCK também calcula a função de pontuação PLANTS (*Plants score*) (Korb, Stutzle *et al.*, 2009), que é definido como o seguinte:

$$E_{PLANTS} = -20 + E_{PENALTY} + E_{SPHERE} + E_{TORSION} + E_{PLP}$$

Onde um valor base (corte) de energia de -20 foi inicialmente necessário para o algoritmo de busca realizada pelo PLANTS (método de busca) e é incorporado na implementação de PLANTS *score* no algoritmo MOLDOCK. O valor de penalidade do ligante leva em conta os conflitos internos do ligante (Korb, Stutzle *et al.*, 2009).

$E_{TORSION}$ é a energia de torção, como descrito anteriormente. $E_{SPHERE}$ descreve uma penalidade que é calculada se a conformação do ligante (pose) está situada fora da esfera do espaço de busca.

## 1.2. OBJETIVOS

### 1.2.1. GERAL

Aplicar *virtual screening* para identificar possíveis inibidores de SIRT1.

### 1.2.2. ESPECÍFICOS

- Modelar a sirtuína 1 humana (SIRT1m).

- Realizar análise estrutural da SIRT1m.

- Construir biblioteca de pequenas moléculas com potencial inibitório de sirtuínas.

- Realizar simulações de *docking* das bibliotecas construídas com a SIRT1m.

# CAPÍTULO 2

## ARTIGO CIENTÍFICO

## Bio-inspired algorithms applied to molecular *docking* simulations

**Bio-inspired algorithms applied to molecular docking simulations**

Graziela Heberlé[a,b], Walter Filgueira de Azevedo Jr.[a,c]

[a] Faculdade de Biociências, Laboratório de Bioquímica Estrutural, Programa de Pós-Graduação em Biologia Celular e Molecular. Instituto Nacional de Ciência e Tecnologia em Tuberculose-Pontifícia Universidade Católica do Rio Grande do Sul, CEP 90619-900, Porto Alegre – RS, Brazil.

[b]Centro de Ciências Biológicas e da Saúde, Centro Universitário-UNIVATES, Rua Avelino Tallini, 171 - Bairro Universitário. Lajeado –RS, Brazil. CEP 95.900-000

[c]Programa de Pós-Graduação em Medicina e Ciências da Saúde, Pontifícia Universidade Católica do Rio Grande do Sul, Porto Alegre - RS, Brazil.

[*]Corresponding author:

Walter Filgueira de Azevedo Jr.

Av. Ipiranga, 6681, CEP 90619-900, Porto Alegre, Rio Grande do Sul, Brazil. E-mail: walter@azevedolab.net

Telephone: +55 51 3353-4529

Fax: +55 51 3320-3629

http://azevedolab.net

**Abstract**

Nature as a source of inspiration has been shown to have a great beneficial impact on the development of new computational methodologies. In this scenario, analyses of the interactions between a protein target and a ligand can be simulated by biologically inspired algorithms (BIAs). These algorithms mimic biological systems to create new paradigms for computation, such as neural networks, evolutionary computing, and swarm intelligence. This review provides a description of the main concepts behind BIAs applied to molecular docking simulations. Special attention is devoted to evolutionary algorithms, guided-directed evolutionary algorithms, and Lamarckian genetic algorithms. Recent applications of these methodologies to protein targets identified in the *Mycobacterium tuberculosis* genome are described.

**Keywords:** Bio-inspired computing, evolutionary algorithms, molecular docking, structure-based virtual screening, protein-ligand, docking, InhA, PNP, EPSP synthase.

**Introduction**

The development of biology has greatly relied on computational tools, with one of the most successful stories the application of sequence data analysis algorithms to genome projects [1-5]. This role will clearly be even more important in the coming years [6]. The relationship between biology and computing led Harold Morowitz to state, "Computers are to biology what mathematics is to physics."

This synergy between biology and computation goes even further with the use of biological models as paradigms for the development of algorithms and methodologies. These biologically inspired algorithms (BIAs) comprise a collection of computational methodologies that employ biological phenomena as a source of inspiration. This bio-inspiration may derive from different sources, such as the emergence of swarm intelligence observed in social insects (e.g., wasps, bees, ants, and termites), Darwinian evolution, and neural networks. The success of BIAs gives the status of natural science to computing, or as Denning stated [7], "We have lived for so long in the belief that computing is a science of the artificial, it may be difficult to accept that many scientists now see information processes abundantly in nature."

These ideas have evolved, and information processes are believed to be present in deep structures in many fields of research [7]. Nobel Laureate and Caltech President David Baltimore proposed:

> "Biology is today an information science. The output of the system, the mechanics of life, are encoded in a digital medium and read out by a series of reading heads. Biology is no longer solely the province of the small laboratory. Contributions come from many directions."

The integration of BIA as an important area of scientific computation takes computing closer to the natural sciences [7], which may be interpreted as a contrast to what has been so brilliantly proposed by Harold Morowitz (see above quotation). Therefore, biological systems may act as inspiration, furnishing new paradigms for computation, or, less formally, biology is to computation what a muse is to a poet.

Life has evolved on Earth for approximately 3.5 billion years. In the struggle to survive, only those species that are best adapted to their environments survive, whereas the others die. Therefore, life has faced complex problems in the course of evolution and had to evolve by selecting solutions and succeeding in the daunting task of survival. The solutions to life's challenges can be seen in a honey bee colony or in a neural network working in an orchestrated and interconnected fashion. These are elegant and creative solutions to complex problems, and not using them as a repertory of strategies to solve computational problems would be

a loss. A recent study showed that, even without being planned to follow biological inspiration, computers and biological systems may possibly evolve to improve the exchange between complexity and physical cost. This relationship results in the appearance of similar principles of efficient and modular design across numerous types of nervous and computational networks [8]. Selective pressures found in nature could be mimicked by economic and technological motivations, generating similar solutions.

To establish a productive view of biological solutions and extract relevant paradigms from biology, adopting a systematic view is necessary. In these approaches, biology can be seen as a collection of systems, in which physical modeling of these systems may furnish the raw material for the development of new algorithms. Under this view, an organism may be seen as a system, in which the organs are components of this system. A cell could be also seen as a system, in which the components are the organelles. The organelle itself can be seen as a system, in which the components are the macromolecules. These abstractions can go even further by considering biomolecular systems. Each of these biological systems can be described by a network topology that is mostly determined by each node's physical position [8].

In this scenario, BIAs can be considered a subclass of a larger set of computational methodologies called "Nature Inspired Computing" (NIC). For a detailed description of these methodologies, refer to a previous excellent review article [9]. The main goal of NIC is to obtain ideas by observing how nature behaves in various situations to solve complex problems and apply algorithms inspired by these models.

Additionally, NIC not only opens the possibility of integrating new approaches to solve computing problems but also works the other way around, in which NIC brings new methodologies to obtain deeper insights into the natural sciences and promotes an integrated view of nature. Richard Feymann predicted in the early 1960s [10]:

> "A poet once said that the whole universe is a glass of wine. We will probably never know in what sense the poet meant that, for poets do not write to be understood. But it is true that if we look at a glass of wine closely enough we see the entire universe. There are the things of physics: the twisting liquid which evaporates depending on the wind and weather, the reflections in the glass, and our imagination adds the atoms. The glass is a distillation of the earth's rocks, and in its composition we see the secrets of the universe's age, and the evolution of stars. What strange array of chemicals is in the wine? How did they come to be? There are ferments, the enzymes, the substrates, and the

products. There in wine is found the great generalization: all life is fermentation. Nobody can discover the chemistry of wine without discovering, as did Louis Pasteur, the cause of much disease. How vivid is the claret, pressing its existence into the consciousness that watches it! If our small minds, for some convenience, divide this glass of wine, this universe, into parts - physics, biology, geology, astronomy, psychology, and so on – remember that nature does not know it! So let us put it all back together, not forgetting ultimately what it is for. Let it give us one more final pleasure: drink it and forget it all!"

Considering this prophetic view of integration of natural sciences, in which computing can also be considered natural science, one example should be highlighted. Two of the most successful theories of the last 150 years, quantum theory and Darwinian evolution, are now being combined to provide deeper insights into the nature of quantum phenomena. This integration of Darwinian evolution and quantum theory is called quantum Darwinism. The foundation of nearly every theoretical quantum-to-classical transition lies in the notion of decoherence. At the atomic and molecular levels, numerous possible quantum states collapse into a single state as a result of interactions with the surroundings. To quantum Darwinists, decoherence is a natural selection process, and the final, stable state is called a pointer state. Although pointer states are quantum states, they are fit enough to be transmitted through the surroundings without collapsing and can then build copies of themselves that can be observed in the macroscopic world. This process leads to environment-induced superselection or *einselection*, a quantum process related to selective information loss [11]. Quantum Darwinism was first proposed by Wojciech Zurek [11], and numerous studies have supported these ideas [12-14]. Most recently, a team of researchers from Arizona State University performed experiments using scanning gate microscopy to image scar structures in an open quantum dot [15]. Their results strongly indicated the existence of periodic scar offspring states that evolve and finally contribute to a stable state, which is a similar derivation of the pointer state predicted by quantum Darwinism.

Today, BIAs are successfully applied to computer simulations in chemistry, physics, engineering, drug discovery, and design [16]. Biologically inspired algorithms comprise a class of stochastic optimization and adaptation methodologies, designed for global optimization. One of the most promising BIAs is the evolutionary algorithm (EA). The great majority of EAs extracts inspiration from the process of genetic evolution. In Darwinian evolution, species selection is based on their capacity of survival of the fittest in an ecosystem. Under this view, classes of EAs, known as genetic algorithms (GAs), genetic programming (GP), and

evolutionary programming (EP), have been developed. All classes of EAs share a large number of characteristics [16].

These methodologies are all population-based stochastic search algorithms and employ the survival-of-the-fittest criteria. These algorithms begin by creating an initial population of possible solutions, and it evolves iteratively from generation to generation toward the finest solution. In consecutive iterations of the algorithm, fitness-based choices occur within the population of solutions. Superior solutions are preferentially chosen for survival in the next generation of solutions, with a multiplicity introduced to the chosen solutions in an effort to reveal even better solutions over subsequent generations, with the goal of searching for a global optimum [16, 17].

Here, the focus is on EAs, more specifically the application of EAs to molecular docking simulations. We do not intend to be complete in our description of EAs. Our main goal is to illustrate the basic concepts of EAs and their use in simulating molecular docking of complexes involving a protein target and a ligand (small molecule). Additionally, we discuss the applications of EAs to protein targets identified in *Mycobacterium tuberculosis*.

*Molecular docking*

Molecular docking is a simulation process that predicts the conformation of a receptor-ligand complex, in which the receptor can be either a protein or a nucleic acid, and the ligand is a small molecule. Visualizing this simulation as analogous to the key-and-lock problem is possible, in which the lock is the receptor and the key is the ligand. The goal here is to adjust the position of the key in the lock. A computer simulation can generate many possible positions for the key in the lock. Therefore, a criterion is necessary that will allow comparisons of all possible positions of the key, and then a selection can be made for the best position.

Drugs are usually discovered by trial and error by means of high-throughput screening approaches that use *in vitro* experiments to evaluate the activity of a large number of compounds against a known target. This procedure is very costly and time-consuming. If the crystallographic structure of the protein target is available, then molecular docking simulations can be a helpful computational approach in the drug-discovery process. This computer simulation process allows for faster and cheaper identification of promising drug candidates using structure-based virtual screening [18-25]. Subsequently, *in vitro* tests can be performed to further evaluate the drug candidates found by the virtual screening process [26]. Virtual screening is founded on the

principle that computationally obtaining the three-dimensional structures of protein and ligand complexes is feasible. With regard to BIAs, molecular docking simulation is a computational problem that may benefit from such methodologies. In molecular docking simulations, the main goal is to find the fittest solution (pose) using a fitness function (scoring function). Biological systems evolved to find the fittest solution to complex biological problems. Therefore, BIAs showed promising results in molecular docking simulations. Among these techniques, one of the most promising involves EAs.

The main docking programs currently in use are DOCK [27], AUTODOCK [28, 29], GOLD [30, 31], FLEXX [32, 33], ZDOCK [34], M-ZDOCK [35], MS-DOCK [36], SURFLEX [37], MCDOCK [38], GLIDE [39-43], GEMDOCK [44-45], and MOLDOCK [24-26]. These programs were developed with the goal of obtaining a rapid procedure capable of identifying a novel lead compound (in virtual screening) or replicating an experimental crystallographic structure (for validation with experimental data) that is as highly accurate as possible. Docking programs can search for the best fit between two or more molecules by considering several parameters obtained from receptor and ligand atomic coordinates, such as geometrical complementarity, atomic VDW radius, charge, torsion angles, intermolecular hydrogen bonds, and hydrophobic contacts. As a result, docking applications return the predicted orientations (poses) of a ligand in the target's binding site. The posing process usually returns numerous possible conformations and several positions for a key. Scoring functions, which are able to evaluate intermolecular binding affinity or binding free energy, are employed to optimize and rank the results to obtain the best orientation after the docking procedure and selecting the best key position [46].

Docking applications can be classified according to their search algorithms, which are defined by a set of rules and parameters applied to predict the conformations. When we consider the flexibility of the ligand or the receptor, docking algorithms can be separated into two major groups: rigid-body and flexible docking. The rigid-body docking procedure does not take into account the flexibility of either the ligand or receptor, which limits the specificity and accuracy of the results when considering the fundamental geometric complementarities between two molecules. Flexible docking methods can take into account numerous potential conformations of a ligand, receptor, or both molecules at the same time. The inclusion of flexibility in docking simulations is associated with increased CPU demand because variables are added to the conformational space to be scanned [47-50].

In molecular docking applications, the best binary complex is the one closer to the structure determined by x-ray crystallography. Therefore, we must establish a methodology that assesses the distance from the computer-generated solution (pose) to the crystallographic structure. This distance can be calculated using the root-mean-square deviation (RMSD), which is a measure of the differences between values predicted by a model and the values actually observed from the object being modeled or estimated (protein-ligand complex). The RMSD is calculated between two sets of atomic coordinates, in this case, one for the crystallographic structure ($x_{xtal}$, $y_{xtal}$, $z_{xatl}$; the object being modeled) and another for the atomic coordinates obtained from the docking simulations ($x_{dock}$, $y_{dock}$, $z_{dock}$; predicted model). A summation is then taken over all N atoms being compared, using the following equation:

$$\mathrm{RMSD} = \sqrt{\frac{1}{N}\sum_{i=1}^{N}(x_{xtal,i} - x_{dock,i})^2 + (y_{xtal,i} - y_{dock,i})^2 + (z_{xtal,i} - z_{dock,i})^2} \ .$$

In docking simulations, we expect that the best results generate RMSD values less than 2.0 Å compared with crystallographic structures [39]. This procedure of obtaining the crystallographic position of the ligand is often called “re-docking,” which is essentially a validation procedure that determines whether the molecular docking algorithm is able to recover the crystallographic position using computer simulation. In this review, all RMSD calculations were calculated for non-hydrogen atoms.

Molecular docking simulations of the crystallographic structure solved at high-resolution for mycolic acid cyclopropane synthase in complex with *S*-adenosyl-L-homocysteine (Protein Data Bank [PDB] accession no. 1KPI) [51] is presented here to illustrate the application of RMSD to the analysis of the docking results. Application of the default MOLDOCK protocol generated the structure shown in Fig. (**1**), with an RMSD of 0.8 Å. Clearly, the default protocol worked for this complex.

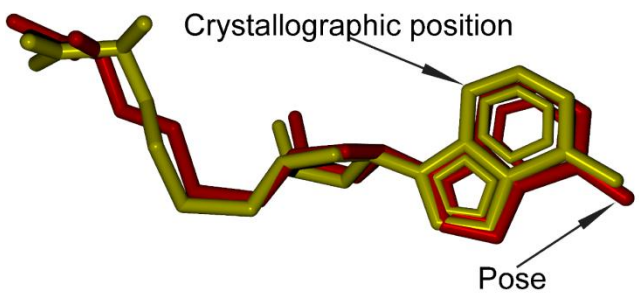


**Fig. (1).** Pose and crystallographic structure of *S*-adenosyl-L-homocysteine in the active site of mycolic acid cyclopropane synthase (PDB accession no. 1KPI).

In addition to re-docking, a procedure called “cross-docking” can also be used to further validate a docking protocol. Considering that several crystallographic structures are available for the same protein, cross-docking can be applied. This procedure involves docking a number of ligands found in a variety of crystal structures of a protein identical to a single rigid protein crystallographic conformation [52]. When a protein target presents major conformational changes upon ligand binding, a significant difference is expected between the crystallographic and docked structures.

Docking applications frequently employ one or more of the following algorithms: Monte Carlo (MC) [38], fast shape matching (SM) [53], incremental construction (IC) [32, 33], distance geometry (DG) [54], simulated annealing (SA) [55, 56], and tabu search (TS) [57]. All of these computational methodologies have been recently reviewed [47]. Although intense research has been conducted on the application of the aforementioned algorithms to the problem of molecular docking simulations, recent results strongly indicate that the most successful approaches are those based on BIAs [24, 26], such as EP [58, 59] and GAs [60-62]. The remainder of this review focuses on these methodologies.

*Evolutionary algorithms*

Evolutionary algorithms consist of a collection of computational methodologies derived from the ideas of Darwin’s theory of evolution. The main goal of these algorithms is to locate the most favorable solution for complex problems [63]. Evolutionary algorithms can also be classified as heuristic algorithms. These algorithms are likely to locate the best solution or one of the best solutions, but they can also be trapped in the local optimal solutions, incapable of locating the global best result. We can confirm that in EAs, the evolutionary course is simplified and consequently does not have much in common with biological evolution. Nevertheless, biological inspiration remained at the core of this approach and is therefore considered a BIA. Evolutionary algorithms are composed of a population of individuals (candidate solutions) submitted to random variation by means of variation operators, such as mutation and recombination [24]. The individual being altered is often referred to as the parent, and the resulting solution after variation is called the offspring. Occasionally, more than one parent is employed to make the offspring by a recombination of solutions, which is referred to as crossover.

The basic ideas behind the evolutionary process are shown in Fig. (**2**). First, a population is created with different individuals, which is called *initialization*. All members of this population are evaluated using a

fitness function, which is also referred to as a scoring function. Second, the individuals with the highest scores (best fitness function) are selected, which is called *selection* (Fig. (**2A**)). Third, *recombination* (Fig. (**2B**)) occurs, followed by *mutation* (Fig. (**2C**)). At this stage, we have new individuals in the population, and the fitness function is calculated for these new individuals, which is called *evaluation* (Fig. (**2D**)). At this point, one cycle is completed (i.e., one iteration). This cycle is repeated until a convergence criterion is met, which could be a fixed number of iterations, a cut-off value for the fitness function, or a variation value.

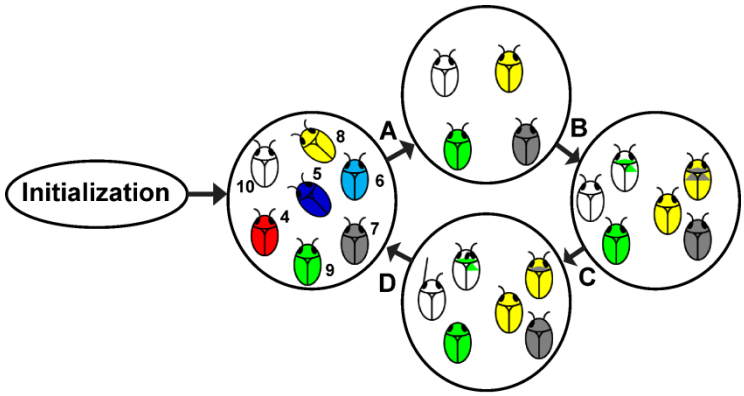


**Fig. (2).** Evolutionary process. Initially a population with different individuals is generated (*initialization*). *Selection* (A) is then carried out, and the individuals with the highest scores are chosen. In the next step, *recombination* (B) is performed followed by a step in which *mutation* (C) takes place. Finally, the fitness function is calculated for these new individuals (D).

Evolutionary algorithms may be classified into three major groups [64]: GAs, EP, and evolution strategies (ESs). Genetic algorithms were the first to be proposed and successfully applied to molecular docking simulations [29, 60]. All of these methodologies have common features, but also substantial differences. The most striking feature common to all of these methodologies is the fundamental concept of creating a population of candidate solutions to the optimization problem (*initialization*). The members of the population are evaluated by applying a scoring function that measures the excellence of these solutions. The population adapts over time and may evolve toward better solutions (*selection*). This method of generating new solutions is usually referred to as “breeding,” in which new solutions are the “offspring” generated from the “parents” of the preceding iteration. At this point, one clarification must be made regarding how all EAs will be described here. The algorithms discussed here are iterative; that is, we begin from few candidate solutions and then continue further in cycles according to an algorithm that we hope moves toward a better solution. A cycle is

known as an iteration. All EAs described here are employed to address the problem of finding the global minimum energy.

*Genetic algorithms*

Possibly the most studied of the three groups is the GA [63]. The significant biological inspiration behind a GA is to follow the course of evolution when choosing the path to arrive at an optimum configuration of a given complex system. For example, in an interacting many-body system, equilibrium is reached by stirring the system to the configuration that is at the global minimum on its potential energy surface [34]. As shown in Fig. (**3**), which describes a rugged-potential energy surface, finding the global minimum may involve extreme computing to perform a complete search for the global minimum. Therefore, application of BIAs to evaluate the landscape may lessen CPU demand.

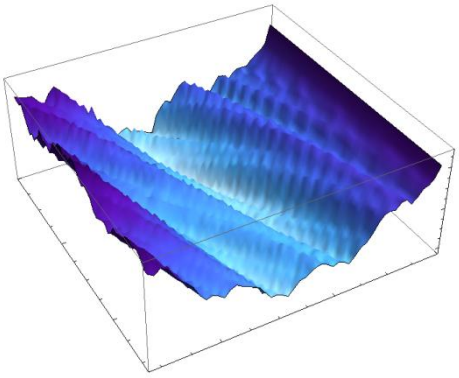

**Fig. (3).** Potential energy surface. The potential energy is a function of two independent variables. The rugged character of the surface is clear, indicating several local minima.

A number of steps are implicated in a GA. In the first step, generating an initial population of configurations is indispensable, which is called the initial "gene pool" of *N* possible solutions. In the application of GAs to molecular docking, this population corresponds to a set of randomly generated conformations of the ligand to be docked in the protein target. Here, this member of the gene pool (population) is known as a "chromosome," which is frequently stored as a function of 0 and 1. The chromosomes code for the values of the torsion angles of the rotatable bonds in the ligand. Fig. (**4**) illustrates an example of the torsion angles identified in the cyclin-dependent kinase CDK2 inhibitor flavopiridol [65-66]. This molecule exhibits two torsion angles, labeled $\phi_1$ and $\phi_2$. The initial gene pool is most directly generated by randomly setting the bits to 0 or 1 in the chromosomes. After decoding each chromosome and assigning the torsion angles to the proper values in the ligand, the fitness of each member of the population can be determined. This fitness function may be an internal potential energy function. Then we must select some members of the gene pool to be parents for

reproduction. The operator that can mix the genes of the two parents is called a crossover, which reflects how genetic attributes are passed on. To create a true offspring, each of the parent chromosomes is cut into segments that are exchanged and joined to generate the new chromosomes of the offspring. Another operator, called the mutation operator, performs mutations on selected chromosomes. Subsequently, a certain percentage of bits in the chromosome is permitted to mutate. This completes one cycle (iteration) of the GA. The new gene pool then becomes the current population ready for a new cycle [24]. The GA repeatedly applies this sequence for a predetermined number of iterations or until it converges.

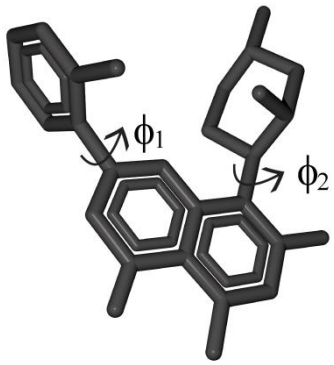


**Fig. (4).** Torsion angles of the rotatable bonds in the structure to be docked.

*Evolutionary programming*

The major difference between the previously described GAs and EP is that the latter does not employ the crossover operator. It employs solely the mutation operator to create new individuals from parents. Additionally, individuals in EP are often represented by means of a sequence of real numbers stored in a vector as an alternative to employing a binary function of 0 and 1.

*Evolutionary strategies*

Evolutionary strategies are very similar to EP but are different in two important respects. First, all individuals are evaluated by direct ranking. Second, the crossover operators introduced in the GAs are now included in the ES algorithm.

*MOLDOCK algorithm*

GEMDOCK [44, 45] and MOLDOCK [24, 26] are the most recently developed programs for docking simulations based on EAs. This review focuses on the implementation of EAs in the MOLDOCK program, which seems to be one of the most successful molecular docking simulation programs. Recent evaluation of

MOLDOCK strongly indicates that it is capable of finding the right position of a ligand. Furthermore, MOLDOCK exhibits better overall performance compared with SURFLEX, FLEXX, and GOLD [24,26].

In the implementation of EAs in MOLDOCK, computational approximations of an evolution course, called genetic operators, are applied to simulate the permanence of the most positive features. In a sample space, where there is a problem or a search routine and many different possible solutions (candidates), each option is ranked based on a set of parameters (scoring function or fitness function), and only the best ranked solutions are kept for the next iteration. This cycle is repeated until an optimal solution can be found. In the molecular docking simulations, the optimal solution is the one with the best scoring function, which should be the closest to the crystallographic structure.

MOLDOCK presents two BIAs to perform positional searches in docking simulations. One is called the optimizer search algorithm (MOLDOCK Optimizer), which is based on an EA [67,68]. The second is a guided differential evolution algorithm (GDEA) called MOLDOCK SE. GDEA is based on an EA adjustment called differential evolution (DE), which provides a distinct method for selecting and modifying candidate solutions (individuals).

The main innovative inspiration of DE is to generate offspring from a weighted difference of parent solutions. The DE works as the following. In the first step, all individuals are initialized and evaluated according to the score function. Afterward, the following process will be performed if the termination condition is not met. For each individual in the population, an offspring is created by adding a weighted difference of the parent solutions, which are randomly chosen from the population. The offspring then replaces the parent, if and only if it is fitter. Otherwise, the parent survives and is passed on to the next generation (iteration of the algorithm). The termination condition is reached when the number of fitness (energy) evaluations performed exceeds the maximum number of evaluations allowed (max evaluations parameter setting). Additionally, early termination is allowed if the variance of the population is below a certain threshold (0.01 here).

Furthermore, GDEA employs a cavity prediction algorithm to limit predicted conformations (poses) during the search procedure. Before beginning the molecular docking simulations, all potential binding sites can be identified using the “detect cavities” option in the MOLDOCK program. More specifically, if a candidate solution is found outside the cavity, then it is translated so that a randomly chosen ligand atom will be located within the region spanned by the cavity. Fig. (**5**) shows the cavities predicted by MOLDOCK for the structure of

5-enolpyruvylshikimate-3-phosphate synthase (EPSPS) in complex with shikimate-3-phosphate (S3P; PDB accession no. 2O0D) [69]. Clearly, this approach is only employed if a cavity has been found. If no cavities are found, then the search process does not restrict the candidate solutions.

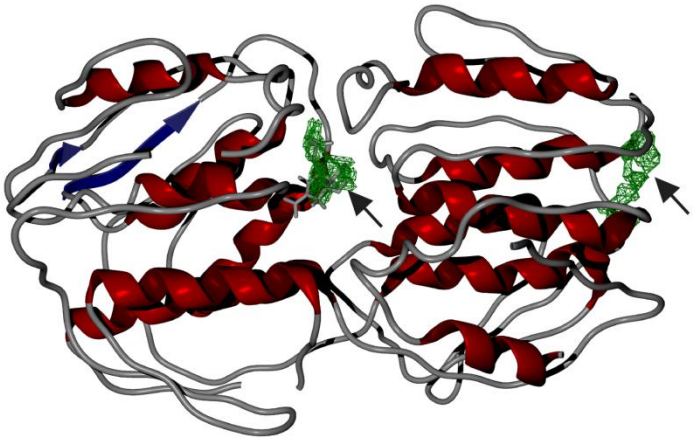

**Fig. (5).** Cavities predicted by MOLDOCK for the structure of EPSPS in complex with shikimate-3-phosphate (PDB accession no. 2O0D).

In the application of GDEA to molecular docking simulations, only the ligand properties are represented in the individuals because the protein remains inflexible throughout the docking simulation. As a result, a candidate solution is determined by a vector of real-valued numbers representing the ligand position, orientation, and conformation as Cartesian coordinates for the ligand translation, four variables specifying the ligand orientation (encoded as a rotation vector and a rotation angle), and one angle for each flexible torsion angle in the ligand (if present). For each individual in the initial population, each of the three translational parameters (encoded as a position relative to the crystallographic native ligand) for *x*, *y*, and *z* is assigned an equally dispersed random number between -15.0 and 15.0 Å, which is added to the center of the crystallographic reference ligand. Initializing the orientation is performed using Shoemake's methodology [70]. This algorithm is employed to create uniform random quaternions and convert these quaternions to their rotation axis/rotation angle representation. The flexible torsion angles (if present) are given a random angle ranging from -180° to +180°. A torsion angle is calculated from the atomic coordinates of the ligand.

Molecular docking simulations usually use an energy-based scoring function to find the energetically most promising ligand conformation when bound to the protein target. The idea is that lower energy scores indicate better protein-ligand binding compared with higher energy values. As a result, molecular docking can be formulated as an optimization problem, in which the task is to find the ligand-binding mode with the lowest

energy. Because precise methods of calculating ligand-binding energy are usually highly CPU-demanding tasks, the application of fast empirical scoring functions should be preferred in molecular docking simulations. The empirical scoring function implemented in MOLDOCK is derived from piecewise linear potential (PLP) scoring functions [24, 26, 44, 45]. The scoring function used by MOLDOCK improves these scoring functions with a new hydrogen bonding term and new charge schemes [24, 26]. Four scoring functions were implemented in the latest version of MOLDOCK, including MOLDOCK score [26] and PLANTS score [71]. These two functions offer grid-based versions, in which hydrogen bond directionality is not considered. The grid-based scoring functions offer approximately four-fold greater speed by performing a precalculation of potential-energy values on an equally spaced cubic grid.

The MOLDOCK scoring function (MOLDOCK score) is based on the PLP scoring functions initially proposed by Gehlhaar et al. [72, 73] and further developed by Yang et al. [44, 45]. The docking scoring function $E_{MOLDOCK\ SCORE}$ is defined as the following:

$$E_{\text{MOLDOCK SCORE}} = E_{\text{Intramol}} + E_{\text{intermol}}$$

where $E_{intermol}$ is the intermolecular interaction energy:

$$E_{\text{intermol}} = \sum_{i \in \text{ligand}} \sum_{j \in \text{protein}} \left[ 332 \frac{q_i q_j}{D r_{ij}} + E_{\text{PLP}}(r_{ij}) \right]$$

All non-hydrogen atoms in the ligand and protein are taken in the summation. Water and co-factor non-hydrogen atoms can be included in this summation, if present. The first term accounts for electrostatic interactions, in which the factor 332 is used to obtain energy in kJ/mol. *D* represents the dielectric constant, which is the following: $D = 4r_{ij}$. The second term ($E_{PLP}$) is a PLP, described elsewhere [44, 45]. To ensure that no energy term can be superior to the clash penalty, the electrostatic term is cut off at a level equivalent to the distance of 2.0 Å for distances less than 2.0 Å.

Intramolecular energy is given by the following equation:

$$E_{\text{intramol}} = E_{\text{penalty}} + \sum_{i \in \text{ligand}} \sum_{j \in \text{ligand}} E_{\text{PLP}}(r_{ij}) + \sum_{\text{singlebonds}} A\left[1 - \cos\left(n\varphi - \varphi_0\right)\right]$$

The term $E_{penalty}$ is a penalty energy to be added to $E_{intramol}$ when two non-bonded atoms are closer than 2 Å (for non-hydrogen atoms). This term avoids unrealistic molecular topologies for the ligands. The second term is a PLP, already mentioned [44-45]. The last term accounts for torsion energy, which is expressed as a periodic function. In this term, $A$, $n$, and $\phi_o$ are empirically determined [44, 45].

MOLDOCK defines a limiting sphere where the search is focused. If a ligand non-hydrogen atom is positioned outside this limiting sphere (the search space sphere), then a constant penalty of 10000 is added to the total energy (implemented for the grid-based version of the MOLDOCK score). Fig. (**6**) shows the search space sphere defined for molecular docking simulations of the EPSPS structure in complex with S3P (PDB accession no. 2O0D) [69]. This search sphere is centered at $x$ = 1.62 Å, $y$ = 30.87 Å, and $z$ = 18.30 Å, with a radius of 15 Å. During docking simulations, if a non-hydrogen atom is found outside this sphere, then the position for the ligand is discarded.

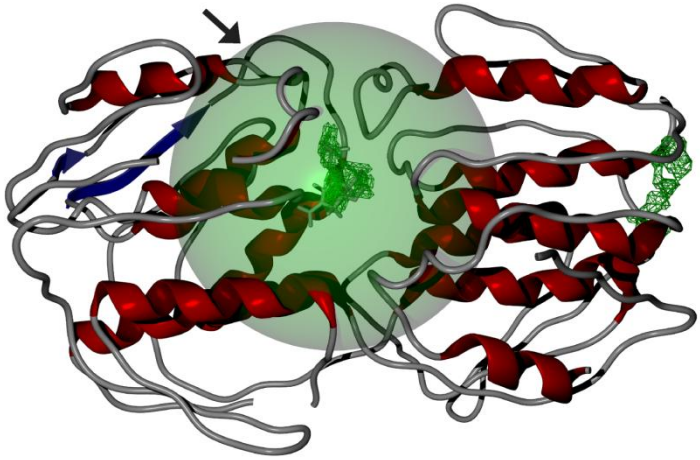

**Fig. (6).** Search space sphere defined for molecular docking simulations of EPSPS structure in complex with shikimate-3-phosphate (PDB accession no. 2O0D).

In addition to the previously described empirical scoring function, MOLDOCK can also calculate the PLANTS scoring function (PLANTS score) [71], which is defined as the following:

$$E_{PLANTS} = -20 + E_{PENALTY} + E_{SPHERE} + E_{TORSION} + E_{PLP}$$

where the -20 energy offset was initially required for the PLANTS search algorithm and is incorporated in the implementation of PLANTS scores in the MOLDOCK algorithm. The ligand clash penalty takes into account internal ligand clashes [71]. $E_{TORSION}$ is the torsion energy, as previously described. $E_{SPHERE}$ describes a penalty that is calculated if a ligand conformation (pose) is located outside the search space sphere, as shown in Fig.

(**6**). $E_{PLP}$ is the previously mentioned piecewise linear potential, which takes into account protein-ligand interactions.

Both empirical scoring functions were able to locate the crystallographic position for the ligands present in the test sets [24, 26, 71]. Testing both when performing molecular docking simulations for new protein-ligand complexes is recommended. Several studies reported successful applications of MOLDOCK [74-95] (Table 1).

Table 1. Virtual screening and molecular docking projects based on MOLDOCK.

| **Targets** | **PDB access codes** | **References** |
|---|---|---|
| Phosphohistidine phosphatase | 2HW4 | [74] |
| NAD(P)H:quinone oxidoreductase-1 | 1H69 | [75, 76] |
| Angiotensin-I-converting enzyme | 1UZF | [77] |
| Kynureninase | 2HZP | [78] |
| Chk2 Kinase | 2CN5 | [79] |
| DNA gyrase | Modeled structure | [80] |
| EGFR tyrosine kinase | 1XKK | [81] |
| CD4 enzyme in the bound state with gp120 and 17b | 1G9N | [82] |
| Dihydrofolate reductase-thymidylate synthase | 1J3I, 1J3K | [83] |
| RNA Polymerase | Modeled structure | [84] |
| Acetohydroxyacid synthase | 1N0H, 1Z8N, 1YI0 | [85] |
| HIV-1 reverse transcriptase | 1REV | [86] |
| Transcriptional activator protein LASR | 2UV0 | [87] |
| Androgen receptor ligand binding domain | 1T7T | [88] |
| Glucocorticoid receptor | 1P93 | [88] |
| Renilla luciferase (RLUC) | IZ7A, 2PSD, 2PSF, 2PSJ and modeled structure | [89] |
| Triosephosphate isomerase (TIM) | 1AG1 | [90] |
| Rhodesain | 2P7U | [90] |
| Farnesyl Diphosphate Synthase | 2P1C | [90] |
| Trypanothione reductase (TR) | TVE2 | [90] |
| Tyrosine kinase | 1M52 | [91] |
| Angiotensin-converting enzyme | 1O8A | [92] |
| Thermolysin | 2TMN, 3TMN, 1TLP, 1GXW | [93] |
| HIV-1 reverse transcriptase | 1REV | [94] |
| Purine nucleoside phosphorylase | 3IOM | [95] |

*AUTODOCK algorithm*

Several computational methodologies have been developed to improve the effectiveness of GAs [28, 29, 56, 60]. Standard GAs consider the genome a fixed-length bit string and make use of binary crossover and binary mutation to produce new individuals in the population, as previously described in this review. Nevertheless, the exploratory performance of the GA is poor and can be enhanced by introducing the local search (LS) computational approach of Solis and Wets [96]. This computational method has the advantage of not needing gradient information about the local energy landscape, which is expected to improve the torsional space search. Furthermore, the LS method has an adaptive character, in which it changes the step size depending on the recent history of energies. The integration of LS into the GA method forms a new type of GA, called Lamarckian GA (LGA) [60]. The LS method is a stochastic heuristic for continuous parameter spaces and introduces a probabilistic element. Its main goal is the local optimization of functions that do not present gradient information [97].

The application of LGA to molecular docking simulations showed better overall performance compared with GA alone [60]. Consequently, the addition of these new GA-based docking methods improves molecular docking simulations and allows tasks with more degrees of freedom to be tackled. Lamarckian genetic algorithms have been implemented in the AUTODOCK program since version 3, and this BIA has also been successfully applied to several protein targets [98-120].

The next sections describe the application of BIAs to important protein targets identified in *Mycobacterium tuberculosis*, for which crystallographic structures are available. The complete genome sequence of *Mycobacterium tuberculosis* has given the scientific community a databank with which to explore singular features of this pathogen [121]. Metabolic pathway enzymes can be evaluated as possible targets for drug development. Molecular docking simulations for three important protein targets are described here: purine nucleoside phosphorylase (PNP), EPSPS, and enoyl-[acyl-carrier-protein] reductase (InhA). The application of GDEA is described for PNP. The application of EA is described for EPSPS. The application of LGA is described for InhA. All of these BIAs were able to successfully predict the correct ligand-binding mode.

*Purine nucleoside phosphorylase*

PNP **(**EC 2.4.2.1) catalyzes the reversible phosphorolysis of *N*-ribosidic bonds of both purine nucleosides and deoxynucleosides, with the exception of adenosine, to generate purine base and ribose (or

deoxyribose) 1-phosphate. This enzyme has been intensively studied, mostly for its importance for immune suppression. Additionally, PNP inhibitors can also be employed to prevent cleavage of anticancer and antiviral drugs because many of these drugs imitate natural purine nucleosides and can thereby be cleaved by PNP prior to accomplishing their therapeutic function [122-123]. Furthermore, the purine recycling and salvaging pathways represent essential cellular processes that are critical for the life of many organisms [122-139].

*Mycobacterium. tuberculosis* purine metabolism has been implicated in bacterial latency and is the source of interest in MtPNP studies. Our group recently published results related to the application of GDEAs to docking simulations of ligands against the structure of MtPNP [95]. This study validated a docking protocol using MOLDOCK that used the default protocol of GDEA implemented in the MOLDOCK program. The following were the default parameters: population size = 50, max number of iterations = 1500, grid resolution = 0.3 Å. All docking simulations were performed with center coordinates of $x$ = 50.57, $y$ = -49.23, and $z$ = 24.07 Å and a docking sphere with a radius of 15 Å. The cavity search algorithm was set to identify up to 10 cavities in the structure. Fig. (**7**) shows the docking sphere and cavities used in the re-docking simulations. The crystallographic structure for the complex of MtPNP and 2dGuo is a dimer in the asymmetric crystallographic unit, but the canonical trimeric structure can be generated in the crystallographic packing. Fig. (**8**) shows the canonical trimer observed in all MtPNPs. The active site of trimeric PNPs resides at the interface between monomers, and they are all equivalent to each other. Therefore, molecular docking simulations could focus on any of these binding pockets.

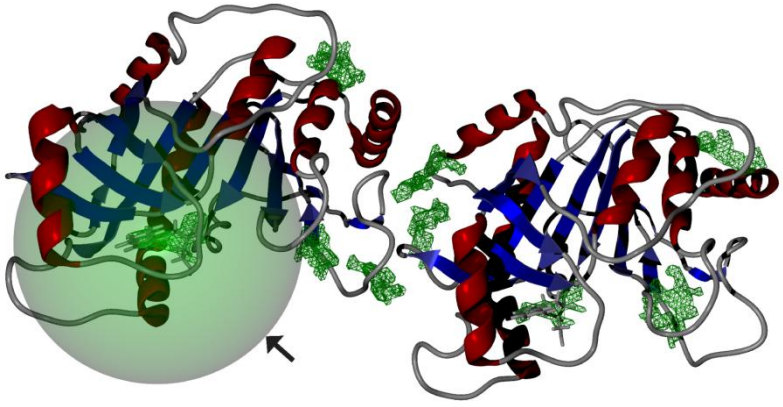

**Fig. (7).** Docking sphere and cavities used in the re-docking simulations for the MtPNP and 2dGuo complex.

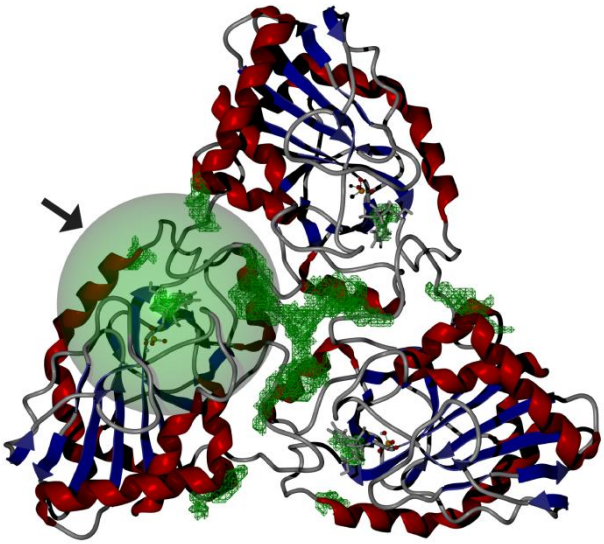

**Fig. (8).** Canonical trimer observed in all MtPNP crystallographic structures.

The application of GDEA implemented in the MOLDOCK program to the structure of MtPNP in complex with 2dGuo (PDB accession no. 3IOM) was able to accurately predict its positioning in the active site of MtPNP. Fig. (**9**) shows the superposition of the best docked structure and crystallographic structure, with an RMSD of superposition of non-hydrogen atoms of 0.5 Å. Furthermore, this study reported that the application of the same docking protocol to two other solved structures of MtPNPs (PDB accession no. 1G2O and 1I80) [140] generated an RMSD of 0.4 Å. Fig. (**10**) and Fig. (**11**) show these docked structures. Altogether, these strongly indicated that the GDEA implemented in MOLDOCK can be employed against any of these MtPNP structures.

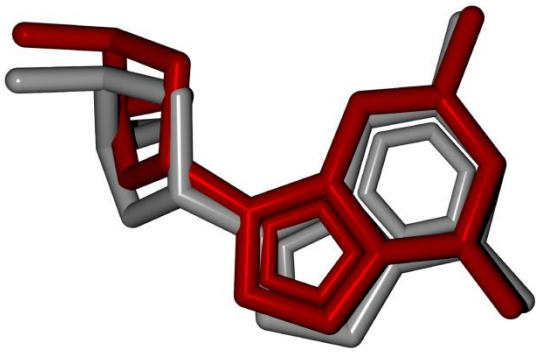

**Fig. (9).** Superposition of the best docked structure and crystallographic structure for the MtPNP and 2dGuo complex (PDB accession no. 3IOM).

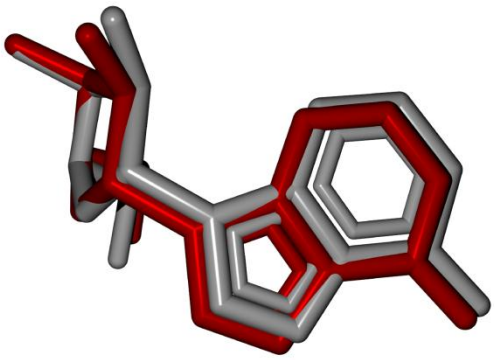

**Fig. (10).** Superposition of the best docked structure and crystallographic structure for the MtPNP and 1,4-dideoxy-4-aza-1-(*S*)-(9-deazahypoxanthin-9-yl)-D-ribitol complex (PDB accession no. 1G2O).

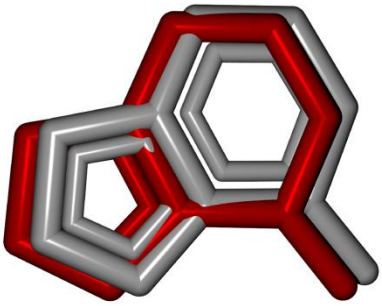

**Fig. (11).** Superposition of the best docked structure and crystallographic structure for the MtPNP and 9-deazaahypoxanthine complex (PDB accession no. 1I80).

*5-Enolpyruvylshikimate-3-phosphate synthase*

Enzymes of the shikimate pathway are attractive targets for the discovery and development of antibacterial drugs and herbicides [141] because this pathway is essential for bacteria and plants, whereas it is not present in mammals [142-154]. Therefore, in bacterial diseases, inhibition of any of the shikimate pathway enzymes is unlikely to produce toxic side effects in the host. Additionally, the value of the shikimate pathway can be indicated by the finding that deletion of the *aroA* gene, which codes EPSPS (EC 2.5.1.19), attenuates the virulence of the *Streptomyces pneumoniae* and *Bordetella bronchiseptica* strains [146, 148]. The shikimate route is composed of seven enzymatic steps, and the EPSPS enzyme is the sixth step.

The crystallographic structure of EPSPS from *Mycobacterium tuberculosis* in complex with S3Ps is available (PDB accession no. 2O0D) [69]. A re-docking simulation of MtEPSPS in complex with S3P generated an RMSD of 1.2 Å. In this simulation, all co-factors present in the crystallographic structure were retained during the search, and the search sphere was limited to 10 Å. The re-docking simulation was able to identify the

crystallographic position of the ligand, nevertheless with a higher RMSD compared with simulations of PNP ligands. Fig. (**12**) shows the crystallographic and docked structures obtained for the complex involving MtEPSPS and S3P.

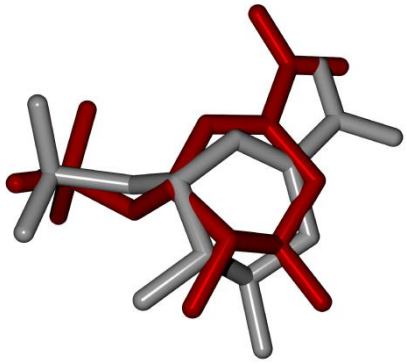

**Fig. (12).** Crystallographic and docked structures obtained for the MtEPSPS and S3P complex (PDB accession no. 2O0D).

*Enoyl-[acyl-carrier-protein] reductase*

InhA (EC 1.3.1.9) has been shown in several genetic and structural studies to be the primary target for the antitubercular drug isoniazid (INH) and a first-line antibiotic for tuberculosis therapy. INH has been used as a primary drug against tuberculosis for more than 50 years. To inhibit InhA, INH is activated by the catalase/peroxidase KatG and the isoniazid-activated intermediate forms an isonicotinyl-NAD adduct (INH-NAD) through the addition of either an isonicotinic acyl anion to NAD or an isonicotinic acyl radical to an NAD radical [155]. The INH-NAD adduct is able bind to the InhA active site with an equilibrium dissociation constant of 0.4 nM. Crystallographic studies focused on the wildtype form of InhA and on the I21V, I47T, and S94A mutant InhA enzymes were able to identify the precise intermolecular interactions between the adduct and enzyme active site. Fig. (**13**) shows the crystallographic structure of MtInhA in complex with the adduct (PDB accession no. 2IDZ) [155, 156].

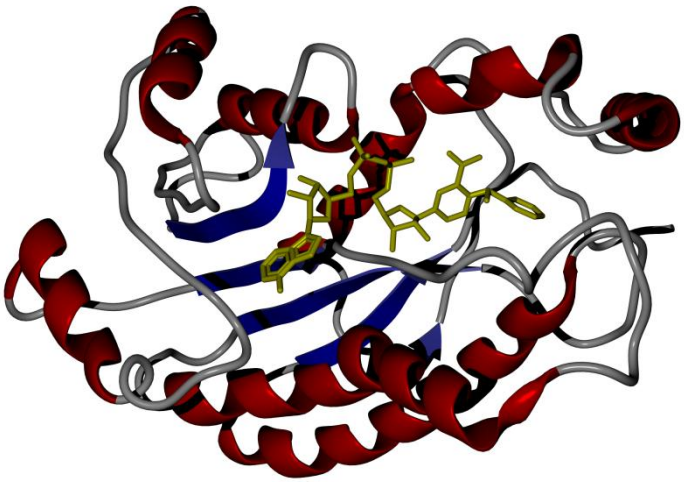

**Fig. (13).** Crystallographic structure of MtInhA in complex with adduct (PDB accession no. 2IDZ).

Because of the importance of InhA as a target for the development of antitubercular drugs, several crystallographic and molecular docking studies have been performed [155-157, 107]. Most recently, molecular docking simulations using LGA [60] implemented in the AUTODOCK 3.05 program successfully predicted ligand-binding modes of a series of isoniazide derivatives [107]. This important study indicated that intermolecular hydrogen bond interactions play an important role in adduct binding in InhA, especially the hydrogen bonds of the pyrophosphate part. Fig. (**14**) shows the main intermolecular hydrogen bonds identified in a complex involving InhA and the isoniazide adduct (PDB accession no. 2IDZ). The main residues involved in these interactions are Gly 14, Asp 64, Ile 95, Lys 165, Ile 194, and Thr 196. Molecular docking simulations using LGA were able to confirm the importance of these for substrate binding [107].

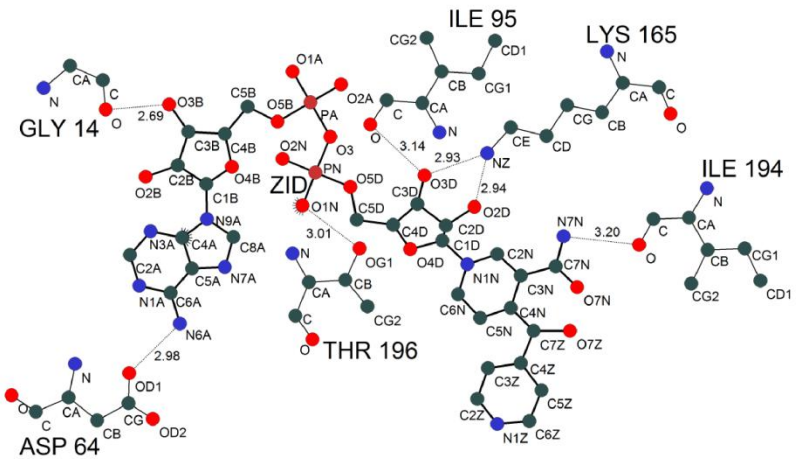


**Fig. (14).** Intermolecular hydrogen bonds identified in the structure of InhA and isoniazide adduct (PDB accession no. 2IDZ).

**Final remarks**

A binding mode is considered properly identified if the RMSD (to the crystallographic binary complex) is less than 2.0 Å [39]. Molecular docking simulations based on BIAs have been shown to be able to generate poses with an RMSD below 2.0 Å [74-95, 98-120]. Among the BIAs applied to molecular docking simulations, two promising algorithms are EA and GDEA implemented in the MOLDOCK program [26]. This program has been intensively applied to a variety of protein targets, with overall performance better than other methodologies implemented in molecular docking programs [26, 74-95]. AUTODOCK has also been successfully applied to a variety of protein targets, among them protein targets identified in *Mycobacterium tuberculosis*, such as InhA [107, 157]. One of the major drawbacks of AUTODOCK is its relative slowness compared with more advanced algorithms, such as those implemented in the MOLDOCK program. Furthermore, recent LGA developments have shown promising results by integrating gradient-based methods for local optimization of binary complexes to GAs. These results showed that the novel methodology is obviously better than other LGAs that employ a stochastic optimization algorithm [97].

MOLDOCK combines four scoring functions (MOLDOCK score, MOLDOCK score GRID, PLANTS, PLANTS GRID) with two search algorithms (MOLDOCK optimizer and MOLDOCK SE), resulting in eight possible docking protocols [26]. This flexibility of protocols for docking simulation and affinity prediction opens the possibility of testing different scenarios, which may improve the chances of success in protein-ligand simulations. Nevertheless, drawbacks exist in docking and affinity prediction, and extra computational tools may enhance computer simulation. For example, the application of additional computational analysis using polynomial empirical scoring functions implemented in the POLSCORE program [158] was able to provide more reliable information in the prediction of PNP inhibition [95]. This work clearly indicated that the application of POLSCORE to rank molecular docking results, obtained with MOLDOCK, was able to remove false positives and recognize PNP inhibitors, such as DADME-IMMH presenting the highest p$K_d$ in a dataset of 581 molecules, with better overall performance compared with native implementation of EAs available in MOLDOCK [95].

Compared with the standard MOLDOCK scoring functions (MOLDOCK score, MOLDOCK score GRID, PLANTS, PLANTS GRID), the new ranking criterion that employs a polynomial empirical scoring function implemented in the POLSCORE program considerably improved the selection of correct docking solutions,

which opens the possibility of scanning vast small-molecule libraries by employing a more reliable scoring function to predict binding affinity.

**Acknowledgments**

This manuscript has been edited by native English-speaking experts of BioMed Proofreading for which we would like to thank them. This work was supported by grants from CNPq and the Instituto Nacional de Ciência e Tecnologia do Conselho Nacional de Desenvolvimento Científico e Tecnológico-Ministério de Ciência e Tecnologia (INCT-Tuberculose, CNPq-MCT, Brazil). WFA is senior researcher for CNPq (Brazil).

**Abbreviations**

ACO = Ant colony optimization

BIA = Bio-inspired algorithm

CDK2 = Cyclin-dependent kinase 2

DE = Differential evolution

DG = Distance geometry

EA = Evolutionary algorithm

EP = Evolutionary programming

EPSPS = 5-Enolpyruvylshikimate 3-Phosphate Synthase

ES = Evolution strategies

GA = Genetic algorithms

GDEA = Guided differential evolution algorithm

IC = Incremental construction

InhA = Enoyl-[acyl-carrier-protein] reductase

$K_d$ = dissociation constant

LGA = Lamarckian genetic algorithm.

LS = Local search

MC = Monte Carlo

Mt = *Mycobacterium tuberculosis*

NIC = Nature inspired computing

NN = Neural networks

PDB = Protein data bank

p$K_d$ = - log $K_d$

PLP = Piecewise linear potential

PNP = Purine nucleoside phosphorylase

PSO = Particle swarm optimization

RLUC = Renilla luciferase

RMSD = Root mean square deviation

SA = Simulated annealing

SM = shape matching (SM)

S3P = Shikimate-3-phosphate

TIM = Triosephosphate isomerase

TR = trypanothione reductase

TS = Tabu search

VDW = van der Waals

**References**

[1] Watson, J.D. The human genome project: past, present, and future. *Science*, **1990**, *248*, 44-9.

[2] Swinbanks D. Fifth-generation project. Genome use for computer. *Nature*, **1990**, *345*, 466-7.

[3] Pearson, M.L.; Söll, D. The Human Genome Project: a paradigm for information management in the life sciences. *FASEB J*. **1991**, *5*, 35-9.

[4] Böhm, K. High performance computing for the human genome project. *Comput. Methods Programs Biomed*., **1995**, *46*, 107-12.

[5] Hormozdiari, F.; Alkan, C.; Eichler, E.E.; Sahinalp, S.C. Combinatorial algorithms for structural variation detection in high-throughput sequenced genomes. *Genome Res*., **2009**, *19*, 1270-8.

[6] Brent, R.; Bruck, J. 2020 computing: can computers help to explain biology? *Nature*., **2006**, *440*, 416-7.

[7] Denning, J.P. Computing is a natural science. Commun. ACM., **2007**, 50, 13-18.

[8] Bassett, D.S.; Greenfield, D.L.; Meyer-Lindenberg, A.; Weinberger, D.R.; Moore, S.W.; Bullmore, E.T. *PLoS Comput Biol.* 2010, 6, e1000748.

[9] Nunes de Castro, L. Fundamentals of natural computing: an overview. *Phys. Life Rev*., **2007**, *4*, 1–36.

[10] Feymann, R.P.; Leighton, R.B.; Sands, M. *The Feynman Lectures on Physics Vol. I*, Addison-Wesley Publishing Co: Reading, 1977.

[11] Zurek, W.H.; Decoherence, einselection, and the quantum origins of the classical. *Rev. Mod. Phys*., **2003**, *3*, 715-75.

[12] Zwolak, M.; Quan, H.T.; Zurek, W.H.. Quantum darwinism in a mixed environment. *Phys. Rev. Lett*., **2009**, *103*, 110402;

[13] Blume-Kohout, R.; Zurek, W.H. Quantum Darwinism in quantum Brownian motion. *Phys. Rev. Lett*., **2008**, *101*, 240405.

[14] Brunner, R.; Akis, R.; Ferry, D.K.; Kuchar, F.; Meisels, R. Coupling-induced bipartite pointer states in arrays of electron billiards: quantum Darwinism in action? *Phys. Rev. Lett*., **2008**, *101*, 024102.

[15] Burke, A.M.; Akis, R.; Day, T.E.; Speyer, G.; Ferry, D.K.; Bennett, B.R. Periodic Scarred States in Open Quantum Dots as Evidence of Quantum Darwinism. *Phys. Rev. Lett*., **2010**, *104*, 176801**.**

[16] Tang, W.J.; Wu, Q.H. Biologically inspired optimization: a review. *Trans. Inst. Meas. Control*., **2009**, *31*, 495–515.

[17] Salomon, R. Evolutionary algorithms and gradient search: similarities and differences. *IEEE Trans. Evol. Comput*., **1998**, *2*, 45-55.

[18] De Azevedo Jr., W.F. Structure-based virtual screening. *Curr. Drug Targets*, **2010**, *11*, 261-3.

[19] Bellows, M.L.; Floudas, C.A. Computational methods for de novo protein design and its applications to the human immunodeficiency virus 1, purine nucleoside phosphorylase, ubiquitin specific protease 7, and histone demethylases. *Curr. Drug Targets*, **2010**, *11*, 264-78.

[20] Rizzolio, F.; Tuccinardi, T.; Caligiuri, I.; Lucchetti, C.; Giordano, A. CDK inhibitors: from the bench to clinical trials. *Curr. Drug Targets*, **2010**, *11*, 279-90.

[21] Krystof, V.; Uldrijan, S. Cyclin-dependent kinase inhibitors as anticancer drugs. *Curr. Drug Targets*, **2010**, *11*, 291-302.

[22] Hernandes, M.Z.; Cavalcanti, S.M.; Moreira, D.R.; de Azevedo Junior, W.F.; Leite, A.C. Halogen atoms in the modern medicinal chemistry: hints for the drug design. *Curr. Drug Targets*, **2010**, *11*, 303-14.

[23] Mitrasinovic, P.M. Advances in the structure-based design of the influenza A neuraminidase inhibitors. *Curr. Drug Targets*, **2010**, *11*, 315-26.

[24] De Azevedo Jr., W.F. MolDock Applied to Structure-Based Virtual Screening. *Curr. Drug Targets*, **2010**, *11*, 327-34.

[25] Kim. D.; Lee, Y.H.; Hwang, H.Y.; Kim, K.K.; Park, H.J. Z-DNA binding proteins as targets for structure-based virtual screening. *Curr. Drug Targets*, **2010**, *11*, 335-44.

[26] Thomsen, R.; Christensen, M.H. MolDock: a new technique for high-accuracy molecular docking. *J. Med. Chem*., **2006**, *49*, 3315-21.

[27] Ewing, T.J.; Makino, S.; Skillman, A.G.; Kuntz, I.D. DOCK 4.0: search strategies for automated molecular docking of flexible molecule databases. *J. Comput. Aided Mol. Des*., **2001**, *15*, 411-28.

[28] Rosenfeld, R.J.; Goodsell, D.S.; Musah, R.A.; Morris, G.M.; Goodin, D.B.; Olson, A.J. Automated docking of ligands to an artificial active site: augmenting crystallographic analysis with computer modeling. *J. Comput. Aided Mol. Des*.; **2003**, *17*, 525-36.

[29] Goodsell, D.S.; Morris, G.M.; Olson, A.J. Automated docking of flexible ligands: applications of AutoDock. *J. Mol. Recognit*.; **1996**, *9*, 1-5.

[30] Verdonk, M.L.; Cole, J.C.; Hartshorn, M.J.; Murray, C.W.; Taylor, R.D. Improved protein-ligand docking using GOLD. *Proteins*, **2003**, *52*, 609-23.

[31] Joy, S.; Nair, P.S.; Hariharan, R.; Pillai, M.R. Detailed comparison of the protein-ligand docking efficiencies of GOLD, a commercial package and ArgusLab, a licensable freeware. *In Silico Biol*., **2006**, *6*, 601-5.

[32] Rarey, M.; Kramer, B.; Lengauer, T.; Klebe, G. A fast flexible docking method using an incremental construction algorithm. *J. Mol. Biol*., **1996**, *261*, 470-89.

[33] Kramer, B.; Rarey, M.; Lengauer, T. Evaluation of the FLEXX incremental construction algorithm for protein-ligand docking. *Proteins*, **1999**, *37*, 228-41.

[34] Chen, R.; Li, L.; Weng, Z. ZDOCK: an initial-stage protein-docking algorithm. *Proteins,* **2003**, *52*, 80-7.

[35] Pierce, B.; Tong, W.; Weng,, Z. M-ZDOCK: a grid-based approach for Cn symmetric multimer docking. *Bioinformatics*, **2005**, *21*, 1472-8.

[36] Sauton, N.; Lagorce, D.; Villoutreix, B.O.; Miteva, M.A. MS-DOCK: accurate multiple conformation generator and rigid docking protocol for multi-step virtual ligand screening. BMC Bioinformatics, **2008**, *9*, 184-96.

[37] Jain, A.N. Surflex: fully automatic flexible molecular docking using a molecular similarity-based search engine. *J. Med. Chem*., **2003**, *46*, 499-511.

[38] Liu, M.; Wang, S. MCDOCK: a Monte Carlo simulation approach to the molecular docking problem. *J. Comput. Aided Mol. Des*., **1999**, *13*, 435-51.

[39] Friesner, R.A.; Banks, J.L.; Murphy, R.B.; Halgren, T.A.; Klicic, J.J.; Mainz, D.T.; Repasky, M.P.; Knoll, E.H.; Shaw, D.E.; Shelley, M.; Perry, J.K.; Francis, P.; Shenkin, P. S. Glide: A New Approach for Rapid, Accurate Docking and Scoring. 1. Method and Assessment of Docking Accuracy. *J. Med. Chem*., **2004**, *47*, 1739–49.

[40] Halgren, T.A.; Murphy, R.B.; Friesner, R.A.; Beard, H.S.; Frye, L.L.; Pollard, W.T.; Banks, J.L. Glide: A New Approach for Rapid, Accurate Docking and Scoring. 2. Enrichment Factors in Database Screening. *J. Med. Chem*., **2004**, *47*, 1750–9.

[41] Kirkpatrick, P. Virtual screening: Gliding to success. *Nat. Rev. Drug Discov*., **2004**, *3*, 299-9.

[42] Krovat, E.M.; Steindl, T.; Langer, T., Recent Advances in Docking and Scoring. *Current Computer-Aided Drug Design*, **2005**, *1*, 93–102.

[43] Friesner, R.A.; Murphy, R.B.; Repasky, M.P.; Frye, L.L.; Greenwood, J.R.; Halgren, T.A.; Sanschagrin, P.C.; Mainz, D.T. Extra Precision Glide: Docking and Scoring Incorporating a Model of Hydrophobic Enclosure for Protein-Ligand Complexes. *J. Med. Chem*., **2006**, *49*, 6177–96.

[44] Yang, J.M. Development and evaluation of a generic evolutionary method for protein-ligand docking. *J. Comput. Chem*., **2004**, *25*, 843-57.

[45] Yang, J.M.; Chen, C.C. GEMDOCK: a generic evolutionary method for molecular docking. *Proteins*. **2004**, *55*, 288-304.

[46] De Azevedo Jr., W.F.; Dias, R. Computational methods for calculation ligand-binding affinity. *Curr. Drug Targets*, **2008**, *9*, 1031-9.

[47] Dias, R.; De Azevedo Jr., W.F. Molecular docking algorithms. *Curr. Drug Targets*, **2008**, *9*, 1040-7.

[48] Dias, R., Timmers, L.F.S.M.; Caceres, R.A.; De Azevedo Jr., W.F. Evaluation of molecular docking using polynomial empirical scoring functions. *Curr. Drug Targets*, **2008**, *9*, 1062-70.

[49] Canduri, F.; De Azevedo Jr., W.F. Protein crystallography in drug discovery. *Curr. Drug Targets*, **2008**, *9*, 1048-53.

[50] De Azevedo Jr., W.F, Dias, R. Experimental approaches to evaluate the thermodynamics of protein-drug interactions. *Curr. Drug Targets*, **2008**, *9*, 1071-76.

[51] Huang, C.-C.; Smith, C.V.; Glickman, M.S.; Jacobs Jr., W.R.; Sacchettini, J.C. Crystal structures of mycolic acid cyclopropane synthases from Mycobacterium tuberculosis. *J.Biol..Chem.* **2002**, *277*, 11559-69.

[52] Thilagavathi, R.; Mancera, R.L. Ligand-protein cross-docking with water molecules. *J. Chem. Inf. Model*., **2010**, *50*, 415-21.

[53] Kuntz, I.D.; Blaney, J.M.; Oatley, S.J.; Langridge, R.; Ferrin, T.E. A geometric approach to macromolecule-ligand interactions. *J. Mol. Biol.*, **1982**, *161*, 269-88.

[54] Moré, J.J.; Wu, Z. Distance geometry optimization for protein structures *J. Global Optim.*, **1999**, *15*, 219-34.

[55] Kirkpatrick, S.; Gelatt, C.D.; Vecchi, M.P. Optimization by simulated annealing. *Science*, **1983**, *220*, 671-80.

[56] Goodsell, D.S.; Olson, A.J. Automated docking of substrates to proteins by simulated annealing. *Proteins-Struct. Funct. Genet.*, **1990**, *8*, 195-202.

[57] Baxter, C.A.; Murray, C.W.; Clark, D.E.; Westhead, D.R.; Eldridge, M.D. *Proteins*, **1998**, 33, 367-382.

[58] Eiben, A.E.; Smith, J.E. *Introduction to Evolutionary Computing.* Springer-Verlag: New York, 2003.

[59] Fogel, L.J.; Owens, A.J.; Walsh, M.J. *Artificial Intelligence through Simulated Evolution*. John Wiley: New York, 1966.

[60] Morris, G.M.; Goodsell, D.S.; Halliday, R.S.; Huey, R.; Hart, W.E.; Belew, R.K.; Olson, A.J. Automated docking using a Lamarckian genetic algorithm and an empirical binding free energy function. *J. Comput. Chem.*, **1998**, *19*, 1639-62.

[61] Jones, G.; Willett, P.; Glen, R.C. A genetic algorithm for flexible molecular overlay and pharmacophore elucidation. J. Comput. Aided Mol. Des. **1995**, *9*, 532-49.

[62] Jones, G.; Willett, P.; Glen, R.C.; Leach, A.R.; Taylor, R. Development and validation of a genetic algorithm for flexible docking. *J. Mol. Biol.*, **1997**, *267*, 727-48.

[63] Goldberg, D.E. *Genetic Algorithms in Search, Optimization, and Machine Learning*. Addilson-Wiley: New York, 1989.

[64] Leach, A.R. *Molecular Modelling. Principles and Applications*, 2nd ed. Pearson Prentice Hall: Essex, 2001.

[65] De Azevedo Jr., W.F.; Mueller-Dieckmann, H.J.; Schulze-Gahmen, U.; Worland, P.J.; Sausville, E.; Kim, S.H. Structural basis for specificity and potency of a flavonoid inhibitor of human CDK2, a cell cycle kinase. *Proc. Natl. Acad. Sci. USA.*, **1996**, *93*, 2735-40.

[66] De Azevedo Jr., W.F.; Leclerc, S.; Meijer, L.; Havlicek, L.; Strnad, M.; Kim, S.H. Inhibition of cyclin-dependent kinases by purine analogues: crystal structure of human cdk2 complexed with roscovitine. *Eur. J. Biochem.,* **1997**, *243*, 518-26.

[67] Michalewicz, Z. *Genetic Algorithms + Data Structures* ) *Evolution Programs*. Springer-Verlag: Berlin, 1992.

[68] Michalewicz, Z.; Fogel, D.B. *How to Solve It: Modern Heuristics*. Springer-Verlag: Berlin, 2000.

[69] Arcuri H.A.; Zafalon G.F.D.; Marucci, E.A.; Bonalumi, C.E.; da Silveira, N.J.F.; Machado, J.M.;, De Azevedo Jr., W.F.; Palma, M.S. SKPDB: a structural database of shikimate pathway enzymes. BMC Bioinformatics, **2010**, *11*, 2.

[70] Shoemake K. In Graphics Gems III; Kirk D. Ed. Boston: AP Professional (Academic Press) 1992; pp 124–32.

[71] Korb, O.; Stutzle, T.; Exner, T.E. Empirical Scoring Functions for Advanced Protein-Ligand Docking with PLANTS. *J. Chem. Inf. Model.*, **2009**, *49*, 84-96.

[72] Gehlhaar, D.K.; Verkhivker, G.; Rejto, P.A.; Fogel, D.B.; Fogel, L.J.; Freer, S.T. Docking Conformationally Flexible Small Molecules into a Protein Binding Site through Evolutionary Programming. *Proceedings of the Fourth International Conference on Evolutionary Programming* **1995**, 615-627.

[73] Gehlhaar, D.K.; Bouzida, D.; Rejto, P.A. Fully Automated and Rapid Flexible Docking of Inhibitors Covalently Bound to Serine Proteases. *Proceedings of the Seventh International Conference on Evolutionary Programming* **1998**, 449-461.

[74] Busam, R.D.; Thorsell, A.G.; Flores, A.; Hammarström, M.; Persson, C.; Hallberg, B.M. First structure of a eukaryotic phosphohistidine phosphatase. *J. Biol. Chem.* **2006**, *281*, 33830-4.

[75] Criddle D.N.; Gillies, S.; Baumgartner-Wilson, H.K.; Jaffar, M.; Chinje, E.C.; Passmore, S.; Chvanov, M.; Barrow, S.; Gerasimenko, O.V.; Tepikin, A.V.; Sutton, R.; Petersen, O.H. Menadione-induced reactive oxygen species generation via redox cycling promotes apoptosis of murine pancreatic acinar cells. *J. Biol. Chem*., **2006**, *281*, 40485-92.

[76] Volpato, M.; Abou-Zeid, N.; Tanner, R.W.; Glassbrook, L.T.; Taylor, J.; Stratford, I.; Loadman, P.M.; Jaffar, M.; Phillips, R.M. Chemical synthesis and biological evaluation of a NAD(P)H:quinone oxidoreductase-1 targeted tripartite quinone drug delivery system. *Mol. Cancer Ther*., **2007**, *6*, 3122-30.

[77] Pripp, A.H. Docking and virtual screening of ACE inhibitory dipeptides. *Eur. Food Res. Technol*., **2007**, *225*, 589–92.

[78] Lima, S.; Khristoforov, R.; Momany, C.; Phillips, R.S. Crystal structure of Homo sapiens kynureninase. *Biochemistry*, **2007**, *46*, 2735-44.

[79] Jobson, A.G.; Cardellina, J.H. 2nd; Scudiero, D.; Kondapaka, S.; Zhang, H.; Kim, H.; Shoemaker, R.; Pommier, Y. Identification of a Bis-guanylhydrazone [4,4'-Diacetyldiphenylurea-bis(guanylhydrazone); NSC 109555] as a novel chemotype for inhibition of Chk2 kinase. *Mol. Pharmacol.,* **2007**, *72*, 876-84.

[80] da Cunha, E.F.; Ramalho, T.C.; Reynolds, R.C. Binding mode analysis of 2,4-diamino-5-methyl-5-deaza-6-substituted pteridines with Mycobacterium tuberculosis and human dihydrofolate reductases. *J. Biomol. Struct. Dyn.,* **2008**, *25*, 377-85.

[81] Abouzid, K.; Shouman, S. Design, synthesis and in vitro antitumor activity of 4-aminoquinoline and 4-aminoquinazoline derivatives targeting EGFR tyrosine kinase*. Bioorg. Med. Chem*., **2008**, *16*, 7543-51.

[82] Pinheiro, J.R.; Bitencourt, M.; da Cunha, E.F.; Ramalho, T.C.; Freitas, M.P. Novel anti-HIV cyclotriazadisulfonamide derivatives as modeled by ligand- and receptor-based approaches. *Bioorg. Med. Chem*., **2008**, *16*, 1683-90.

[83] Fogel, G.B.; Cheung, M.; Pittman, E.; Hecht, D. In silico screening against wild-type and mutant Plasmodium falciparum dihydrofolate reductase. *J. Mol. Graph. Model*., **2008**, *26*, 1145-52.

[84] Josa, D.; da Cunha, E.F.; Ramalho, T.C.; Souza, T.C.; Caetano, M.S. Homology modeling of wild-type, D516V, and H526L Mycobacterium tuberculosis RNA polymerase and their molecular docking study with inhibitors. *J. Biomol. Struct. Dyn*., **2008**, *25*, 373-6.

[85] Kalme, S.; Pham, C.N.; Gedi, V.; Le, D.T.; Choi, J.D.; Kim, S.K.; Yoona, M.Y. Inhibitors of Bacillus anthracis acetohydroxyacid synthase. *Enzyme Microb. Tech.,* **2008***, 43,* 270–5.

[86] Sapre, N.S.;Gupta, S.; Sapre, N. Assessing ligand efficiencies using template-based molecular docking and Tabu-clustering on tetrahydroimidazo-[4,5,1-jk][1,4]-benzodiazepin-2(1H)-one and -thione (TIBO) derivatives as HIV-1RT inhibitors. *J. Chem. Sci.,* **2008***, 120,* 395–404.

[87] Skindersoe, M.E.; Alhede, M.; Phipps, R.; Yang, L.; Jensen, P.O.; Rasmussen, T.B.; Bjarnsholt, T.; Tolker-Nielsen, T.; Høiby, N.; Givskov, M. Effects of antibiotics on quorum sensing in Pseudomonas aeruginosa. *Antimicrob. Agents Chemother*., **2008**, *52*, 3648-63.

[88] Yemelyanov, A.; Czwornog, J.; Gera, L.; Joshi, S.; Chatterton, R.T. Jr.; Budunova, I. Novel steroid receptor phyto-modulator compound a inhibits growth and survival of prostate cancer cells. Cancer Res., **2008**, *68*, 4763-73.

[89] Woo, J.; Howell, M.H.; von Arnim, A.G. Structure-function studies on the active site of the coelenterazine-dependent luciferase from Renilla. *Protein Sci*., **2008**, *17*, 725-35.

[90] Ogungbe, I.V.; Setzer, W.N. Comparative molecular docking of antitrypanosomal natural products into multiple Trypanosoma brucei drug targets. *Molecules***, 2009**, *14*, 1513-36.

[91] Honda, T.; Terao, T.; Aono, H.; Ban, M. Synthesis of novel 1,4-benzoxazin-3-one derivatives as inhibitors against tyrosine kinases. *Bioorg. Med. Chem*., **2009**, *17*, 699-708.

[92] Pina, A.S.; Roque, A.C. Studies on the molecular recognition between bioactive peptides and angiotensin-converting enzyme. *J. Mol. Recognit*., **2009**, *22*, 162-8.

[93] Khan, M.T.; Fuskevåg, O.M.; Sylte, I. Discovery of potent thermolysin inhibitors using structure based virtual screening and binding assays. *J. Med. Chem*., **2009**, *52*, 48-61.

[94] Sapre, N.S.; Gupta, S.; Pancholi, N.; Sapre, N. A group center overlap based approach for "3D QSAR" studies on TIBO derivatives. *J. Comput. Chem*., **2009**, *30*, 922-33.

[95] Ducati, R.G.; Basso, L.A.; Santos, D.S.; de Azevedo Junior, W.F. Crystallographic and docking studies of purine nucleoside phosphorylase from *Mycobacterium tuberculosis*. *Bioorg. Med. Chem*., **2010**, *18*, 4769-74.

[96] Solis, F.; Wets, R.-B. Minimization by Random Search Techniques. *Math. Oper. Res*., **1981**, *2*, 19-30.

[97] Fuhrmann, J.; Rurainski, A.; Lenhof, H.P.; Neumann, D. A new Lamarckian genetic algorithm for flexible ligand-receptor docking. *J. Comput. Chem*. **2010**, *31*, 1911-8.

[98] Li, C.; Xu, L.; Wolan, D.W.; Wilson, I.A.; Olson, A.J. Virtual screening of human 5- aminoimidazole-4-carboxamide ribonucleotide transformylase against the NCI diversity set by use of AutoDock to identify novel nonfolate inhibitors. *J. Med. Chem*., **2004**, *47*, 6681-90.

[99] Rogers, J.P.; Beuscher, A.Et.; Flajolet, M.; McAvoy, T.; Nairn, A.C.; Olson, A.J.; Greengard, P. Discovery of protein phosphatase 2C inhibitors by virtual screening. *J. Med. Chem*., **2006**, *49*, 1658-67.

[100] Chang, M.W.; Lindstrom, W.; Olson, A.J.; Belew, R.K. Analysis of HIV wild-type and mutant structures via in silico docking against diverse ligand libraries. *J. Chem. Inf. Model*., **2007**, *47*, 1258-62.

[101] Kovac, A.; Konc, J.; Vehar, B.; Bostock, J.M.; Chopra, I.; Janezic, D.; Gobec, S. Discovery of new inhibitors of D-alanine:D-alanine ligase by structure-based virtual screening. *J. Med. Chem.*, **2008**, *51*, 7442-8.

[102] Cosconati, S.; Hong, J.A.; Novellino, E.; Carroll, K.S.; Goodsell, D.S.; Olson, A.J. Structure-based virtual screening and biological evaluation of Mycobacterium uberculosis adenosine 5'-phosphosulfate reductase inhibitors. *J. Med. Chem*., **2008**, *51*, 6627-30.

[103] Jiang, H.; Bower, K.E.; Beuscher, A.Et.; Zhou, B.; Bobkov, A.A.; Olson, A.J.; Vogt, P.K. Stabilizers of the Max homodimer identified in virtual ligand screening inhibit Myc function. *Mol. Pharmacol*., **2009**, *76*, 491-502.

[104] Utsintong, M.; Talley, T.T.; Taylor, P.W.; Olson, A.J.; Vajragupta, O. Virtual screening against alpha-cobratoxin. *J. Biomol. Screen*., **2009**, *14*, 1109-18.

[105] Cosconati, S.; Marinelli, L.; Trotta, R.; Virno, A.; Mayol, L.; Novellino, E.; Olson, A.J.; Randazzo, A. Tandem application of virtual screening and NMR experiments in the discovery of brand new DNA quadruplex groove binders. *J. Am. Chem. Soc*., **2009**, *131*, 16336-7.

[106] Cosconati, S.; Marinelli, L.; La Motta, C.; Sartini, S.; Da Settimo, F.; Olson, A.J.; Novellino, E. Pursuing aldose reductase inhibitors through in situ cross-docking and similarity-based virtual screening. *J. Med. Chem*., **2009**, *52*, 5578-81.

[107] Punkvang, A.; Saparpakorn, P.; Hannongbua, S.; Wolschann, P.; Pungpo, P. *Molecules*., **2010**, *15*, 2791-813.

[108] Jayakanthan, M.; Chandrasekar, S.; Muthukumaran, J.; Mathur, P.P. Analysis of CYP3A4-HIV-1 protease drugs interactions by computational methods for Highly Active Antiretroviral Therapy in HIV/AIDS. *J. Mol. Graph. Model*., **2010**, *28*, 455-63.

[109] Ali, H.I.; Fujita, T.; Akaho, E.; Nagamatsu, T. A comparative study of AutoDock and PMF scoring performances, and SAR of 2-substituted pyrazolotriazolopyrimidines and 4-substituted pyrazolopyrimidines as potent xanthine oxidase inhibitors. *J. Comput. Aided Mol. Des.,* **2010**, *24*, 57-75.

[110] Reszka P, Schulz R, Methling K, Lalk M, Bednarski PJ. Synthesis, enzymatic evaluation, and docking studies of fluorogenic caspase 8 tetrapeptide substrates. *ChemMedChem*., **2010**, *5*, 103-17.

[111] Kamel, M.M.; Ali, H.I.; Anwar, M.M.; Mohamed, N.A.; Soliman, A.M. Synthesis, antitumor activity and molecular docking study of novel sulfonamide-Schiff's bases, thiazolidinones, benzothiazinones and their C-nucleoside derivatives. *Eur. J. Med. Chem*., **2010**, *45*, 572-80.

[112] Issaraseriruk, N.; Shitangkoon, A.; Aree, T. Molecular docking study for the prediction of enantiodifferentiation of chiral styrene oxides by octakis(2,3-di-O-acetyl-6-O-tert-butyldimethylsilyl)-gamma-cyclodextrin. *J. Mol. Graph. Model*., **2010**, *28*, 506-12.

[113] Garg, A.; Tewari, R.; Raghava, G.P. KiDoQ: using docking based energy scores to develop ligand based model for predicting antibacterials*. BMC Bioinformatics*., **2010**, *11*, 125.

[114] Azizian, H.; Bahrami, H.; Pasalar, P.; Amanlou, M. Molecular modeling of Helicobacter pylori arginase and the inhibitor coordination interactions. *J. Mol. Graph. Mode*l., **2010**, *28*, 626-35.

[115] Musmuca, I.; Caroli, A.; Mai, A.; Kaushik-Basu, N.; Arora, P.; Ragno, R. Combining 3-D quantitative structure-activity relationship with ligand based and structure based alignment procedures for in silico screening of new hepatitis C virus NS5B polymerase inhibitors. *J. Chem. Inf. Model*., **2010**, *50*, 662-76.

[116] Comes Franchini, M.; Bonini, B.F.; Camaggi, C.M.; Gentili, D.; Pession, A.; Rani, M.; Strocchi, E. Design and synthesis of novel 3,4-disubstituted pyrazoles for nanomedicine applications against malignant gliomas. *Eur. J. Med. Chem*., **2010***, 45*, 2024-33.

[117] Ramisetty, S.R.; Baranger, A.M. Cooperative binding of a quinoline derivative to an RNA stem loop containing a dangling end. *Bioorg. Med. Chem. Lett*., **2010**, *20*, 3134-7.

[118] Neuhaus, F.C. Role of Arg301 in substrate orientation and catalysis in subsite 2 of D-alanine:D-alanine (D-lactate) ligase from Leuconostoc mesenteroides: a molecular docking study. *J. Mol. Graph. Model*., **2010**, *28*, 728-34.

[119] Lu, S.Y.; Jiang, Y.J.; Lv, J.; Wu, T.X.; Yu, Q.S.; Zhu, W.L. Molecular docking and molecular dynamics simulation studies of GPR40 receptor-agonist interactions. *J. Mol. Graph Model*., **2010**, *28*, 766-74.

[120] Zaheer-ul-Haq.; Halim, S.A.; Uddin, R.; Madura, J.D. Benchmarking docking and scoring protocol for the identification of potential acetylcholinesterase inhibitors. *J. Mol. Graph. Model*., **2010**, *28*, 870-82.

[121] Cole, S.T.; Brosch, R.; Parkhill, J.; Garnier, T.; Churcher, C.; Harris, D.; Gordon, S.V.; Eiglmeier, K.; Gas, S.; Barry, C.E. 3rd.; Tekaia, F.; Badcock, K.; Basham, D.; Brown, D.; Chillingworth, T.; Connor, R.; Davies, R.; Devlin, K.; Feltwell, T.; Gentles, S.; Hamlin, N.; Holroyd, S.; Hornsby, T.; Jagels, K.; Krogh, A.; McLean, J.; Moule, S.; Murphy, L.; Oliver, K.; Osborne, J.; Quail, M.A.; Rajandream, M.A.; Rogers, J.; Rutter, S.; Seeger, K.; Skelton, J.; Squares, R.; Squares, S.; Sulston, J.E.; Taylor, K.; Whitehead, S.; Barrell, B.G. Deciphering the biology of Mycobacterium tuberculosis from the complete genome sequence. *Nature*., **1998**, *393*, 537-44.

[122] De Azevedo Jr., W.F.; Canduri, F.; Santos, D.M.; Silva, R.G.; de Oliveira, J.S.; de Carvalho, L.P.; Basso, L.A.; Mendes, M.A.; Palma, M.S.; Santos, D.S. Crystal structure of human purine nucleoside phosphorylase at 2.3 A resolution. *Biochem. Biophys. Res. Commun*., **2003**, *308*, 545-52.

[123] Santos, D.M.; Canduri, F.; Pereira, J.H.; Vinicius Bertacine Dias, M.; Silva, R.G.; Mendes, M.A.; Palma, M.S.; Basso, L.A.; De Azevedo Jr., W.F.; Santos, D.S. Crystal structure of human purine nucleoside phosphorylase complexed with acyclovir. *Biochem. Biophys. Res. Commun*., **2003**; *308*, 553-9.

[124] De Azevedo Jr., W.F.; Canduri, F.; Dos Santos, D.M.; Pereira, J.H.; Dias, M.V.; Silva, R.G.; Mendes, M.A.; Basso, L.A.; Palma, M.S.; Santos, D.S. Structural basis for inhibition of human PNP by immucillin-H. *Biochem. Biophys. Res. Commun*., **2003**, *309*, 917-22.

[125] De Azevedo Jr., W.F.; Santos, G.C.; Santos, D.M.; Olivieri, J.R.; Canduri, F.; Silva, R.G.; Basso, L.A.; Renard, G.; Fonseca, I.O.; Mendes, M.A.; Palma, M.S.; Santos, D.S. Docking and small angle X-ray scattering studies of purine nucleoside phosphorylase. *Biochem. Biophys. Res. Commun.*, **2003**, *309*, 923-928.

[126] De Azevedo Jr., W.F.; Canduri, F.; dos Santos, D.M.; Pereira, J. H., Silva, R.G.; Mendes, M.A.; Basso, L.A.; Palma, M.S.; Santos, D.S. Crystal structure of human PNP complexed with guanine. *Biochem. Biophys. Res. Commun.,* **2003**, *312*, 767-72.

[127] Canduri, F.; dos Santos, D.M.; Silva RG.; Mendes, M.A.; Basso, L.A.; Palma, M.S.; De Azevedo, W.F.; Santos, D.S. Structures of human Purine Nucleoside Phosphorylase complexed with Inosine and ddI. *Biochem. Biophys. Res. Commun*., **2004**, *313*, 907-14.

[128] Da Silveira, N.J.F.; Uchoa, H.B.; Canduri, F.; Pereira, J.H.; Camara Jr. J.C; Basso, L.A.; Palma, M.S.; Santos, D.S.; de Azevedo Jr., W.F. Structural Bioinformatics Study of PNP from *Schistosoma mansoni*.. *Biochem. Biophys. Res. Commun.,* **2004**, *322*, 100-4.

[129] Nolasco, D.O.; Canduri, F.; Pereira, J.H.; Cortinoz, J.R.; Palma, M.S.; Oliveira, J.S.; Basso, L.A.; de Azevedo, W,F. Jr.; Santos, D.S. Crystallographic structure of PNP from *Mycobacterium tuberculosis* at 1.9 A resolution. *Biochem. Biophys. Res. Commun*., **2004**, *324*, 789-94.

[130] Canduri, F.; Fadel, V.; Dias, M.V.B.; Basso, L.A.; Palma, M.S.; Santos, D.S.; de Azevedo, W.F. Jr. Crystal structure of human PNP complexed with hypoxanthine and sulfate ion. *Biochem. Biophys. Res. Commun*., **2005**, *326*, 335-8.

[131] Canduri, F.; Fadel, V.; Basso, L.A.; Palma, M.S.; Santos, D.S.; De Azevedo Jr., W.F. New catalytic mechanism for human purine nucleoside phosphorylase. .*Biochem. Biophys. Res. Commun*., **2005**, *327*, 646-9.

[132] Canduri, F.; Silva, R.G.; dos Santos, D.M.; Palma, M.S.; Basso, L.A.; Santos, D.S.; de Azevedo, W.F. Jr. Structure of human PNP complexed with ligands. *Acta Crystallogr. D Biol. Crystallogr*., **2005**, *61*, 856-62.

[133] Silva, R.G.; Pereira, J.H.; Canduri, F.; De Azevedo Jr., W.F.; Basso, L.A.; Santos, D.S. Kinetics and crystal structure of human purine nucleoside phosphorylase in complex with 7-methyl-6-thio-guanosine. *Arch. Biochem. Biophys*. **2005**, *442*, 49-58.

[134] De Azevedo Jr., W.F.; Canduri, F.; Basso, L.A.; Palma, M.S.; Santos, D.S. Determining the Structural Basis for Specificity of Ligands Using Crystallographic Screening. *Cell Biochem. Biophys*., **2006**, *44*, 405-11.

[135] Timmers, L.F.S.M.; Caceres, R.A.; Vivan,, A.L.; Gava, L.M.; Dias, R.; Ducati, R.G.; Basso, L.A.; Santos, D.S.; de Azevedo, W.F. Jr. Structural studies of human purine nucleoside phosphorylase: towards a new specific empirical scoring function. *Arch. Biochem. Biophys*., **2008**, *479*, 28-38.

[136] Caceres, R.A.; Saraiva Timmers, L.F.; Dias, R.; Basso, L.A.; Santos, D.S.; De Azevedo Jr., W.F. Molecular modeling and dynamics simulations of PNP from *Streptococcus agalactiae*. Bioorg. Med. Chem., **2008**, *16*, 4984-93.

[137] Timmers, L.F.S.M.; Caceres, R.A.; Basso, L.A.; Santos, D.S.; De Azevedo Jr., W.F. Structural Bioinformatics Study of PNP from *Listeria monocytogenes*. *Prot. Pept. Lett*., **2008**, *15*, 843-9.

[138] Pauli, I.; Timmers, L.F.S.M.; Caceres, R.A.; Basso, L.A.; Santos, D.S.; De Azevedo Jr., W.F. Molecular modeling and dynamics studies of Purine Nucleoside Phosphorylase from *Bacteroides fragilis. J. Mol. Model*., **2009**, *15*, 913-922.

[139] Timmers, L.F.S.M.; Caceres, R.A, Dias, R.; Basso, L.A.; Santos, D.S.; De Azevedo Jr., W.F. Molecular modeling, dynamics and docking studies of Purine Nucleoside Phosphorylase from *Streptococcus pyogenes. Biophys. Chem*., **2009**, *142*, 7-16.

[140] Shi, W.; Basso, L.A.; Santos, D.S.; Tyler, P.C.; Furneaux, R.H.; Blanchard, J.S.; Almo, S.C.; Schramm, V.L. Structures of purine nucleoside phosphorylase from Mycobacterium tuberculosis in complexes with immucillin-H and its pieces. *Biochemistry*., **2001**, *40*, 8204-15.

[141] De Azevedo Jr., W.F.; Canduri, F.; Simões de Oliveira, J.; Basso, L.A.; Palma, M.S.; Pereira, J.H.; Santos, D.S. Molecular model of shikimate kinase from *Mycobacterium tuberculosis*. *Biochem. Biophys. Res. Commun.,* **2002**, *295*, 142-8.

[142] Pereira, J.H.; Canduri, F.; de Oliveira, J.S.; Silveira, N.J.F.; Basso, L.A.; Palma, M.S.; De Azevedo, W.F.; Santos, D.S. Structural Bioinformatics Study of EPSP synthase from *Mycobacterium tuberculosis*. *Biochem. Biophys. Res. Commun.*, **2003**, *312*, 608-14.

[143] Pereira, J.H.; de Oliveira, J.S.; Canduri, F.; Dias, M.V.B.; Palma, M.S.; Basso, L.A.; Santos, D.S.; de Azevedo, W.F. Structure of shikimate kinase from *Mycobacterium tuberculosis* reveals the binding of shikimic acid. *Acta Crystallogr. D Biol. Crystallogr*., **2004**, *60*, 2310-9.

[144] Arcuri, H.A.; Canduri, F.; Pereira, J.H.; da Silveira, N.J.F.; Camara Jr., J.C.; de Oliveira, J.S.; Basso, L.A.; Palma, M.S.; Santos, D.S.; de Azevedo Jr., W.F. Molecular models for shikimate pathway enzymes of *Xylella fastidiosa*. *Biochem. Biophys. Res. Commun.,***2004**, *320*, 979-91.

[145] Borges, J.C.; Pereira, J.H.; Vasconcelos, I.B.; dos Santos, G.C.; Olivieri, J.R.; Ramos, C.H.I.;, Palma, M.S.; Basso, L.A.; Santos, D.S.; de Azevedo Jr., W.F. Phosphate closes the solution structure of the 5-enolpyruvylshikimate-3-phosphate synthase (EPSPS) from *Mycobacterium tuberculosis*. Arch. Biochem. Biophys., **2006**, *452*, 156-64.

[146] Pereira, J.H, Vasconcelos, I.B.; Oliveira, J.S.; Caceres, R.A.; de Azevedo Jr., W.F.; Basso, L.A.; Santos, D.S. Shikimate kinase: A potential target for development of novel antitubercular agents. *Curr. Drug Targets,* **2007**, *8*, 459-68.

[147] Dias, M.V.B.; Faim, L.M.; Vasconcelos, I.B.; Oliveira, J.S.; Basso, L.A.; Santos, D.S.; de Azevedo Jr., W.F. Effects of magnesium and chloride ions and shikimate on the structure of shikimate kinase from *Mycobacterium tuberculosis*. *Acta Crystallograph. Sect. F Struct. Biol. Cryst. Commun*., **2007**, *63*, 1-6.

[148] Dias, M.V.B.; Ely, F.; Palma, M.S.; De Azevedo Jr., W.F.; Basso L.A.; Santos, D.S. Chorismate synthase: An attractive target for drug development against orphan diseases. *Curr. Drug Targets*., **2007**, *8*, 437-44.

[149] Pauli, I.; Caceres, R.A.; De Azevedo Jr., W.F. Molecular modeling and dynamics studies of shikimate kinase from *Bacillus anthracis*. *Bioorg. Med. Chem*., **2008**, *16*, 8098-108.

[150] Arcuri, H.A.; Borges, J.C.; Fonseca, I.O.; Pereira, J.H.; Neto, J.R.; Basso, L.A.; Santos, D.S.; de Azevedo, W.F.Jr. Structural studies of shikimate 5-dehydrogenase from *Mycobacterium tuberculosis. Proteins*, **2008**, *72*, 720-30.

[151] Dias, M.V.; Borges, J.C.; Ely, F.; Pereira, J.H.; Canduri, F.; Ramos, C.H.; Frazzon, J.; Palma, M.S.; Basso, L.A.; Santos, D.S.; de Azevedo, W.F.Jr. Structure of chorismate synthase from *Mycobacterium tuberculosis*. *J. Struct. Biol*., **2006**, *154*, 130-43.

[152] Marques, M.R.; Vaso, A.; Neto, J.R.; Fossey, M.A.; Oliveira, J.S.; Basso, L.A.; dos Santos, D.S.; de Azevedo Jr., W.F.; Palma, M.S. Dynamics of glyphosate-induced conformational changes of *Mycobacterium tuberculosis* 5-enolpyruvylshikimate-3-phosphate synthase (EC 2.5.1.19) determined by hydrogen-deuterium exchange and electrospray mass spectrometry. *Biochemistry*., **2008**, *47*, 7509-22.

[153] Marques, M.R.; Pereira, J.H.; Oliveira, J.S.; Basso, L.A.; Santos, D.S.; de Azevedo Jr., W.F.; Palma, M.S. The inhibition of 5-enolpyruvylshikimate-3-phosphate synthase as a model for development of novel antimicrobials. *Curr. Drug Targets*, **2007**, *8*, 445-457.

[154] Barcellos, G.B.; Caceres, R.A.; De Azevedo Jr., W.F. Structural studies of shikimate dehydrogenase from *Bacillus anthracis* complexed with cofactor NADP. J. Mol. Model., **2009**, *15*, 147-55.

[155] Dias, M.V.; Vasconcelos, I.B.; Prado, A.M.; Fadel, V.; Basso, L.A.; de Azevedo, W.F. Jr.; Santos, D.S. Crystallographic studies on the binding of isonicotinyl-NAD adduct to wild-type and isoniazid resistant 2-trans-enoyl-ACP (CoA) reductase from *Mycobacterium tuberculosis. J. Struct. Biol*., **2007**, *159*, 369-380.

[156] Oliveira, J.S.; Pereira, J.H.; Canduri, F.; Rodrigues, N.C.; de Souza, O.N.; de Azevedo Jr., W.F.; Basso, L.A.; Santos, D.S. Crystallographic and pre-steady-state kinetics studies on binding of NADH to wild-type and isoniazid-resistant enoyl-ACP(CoA) reductase enzymes from *Mycobacterium tuberculosis*. *J. Mol. Biol*., **2006**, *359*, 646-66.

[157] Stigliani, J.L.; Arnaud, P.; Delaine, T.; Bernardes-Génisson, V.; Meunier, B.; Bernadou, J. Binding of the tautomeric forms of isoniazid-NAD adducts to the active site of the Mycobacterium tuberculosis enoyl-ACP reductase (InhA): a theoretical approach. *J. Mol. Graph. Model*., **2008**, *27*, 536-45.

[158] De Azevedo, W.F. Jr., Dias, R. Evaluation of ligand-binding affinity using polynomial empirical scoring functions. *Bioorg. Med. Chem*., **200**8, **16**, 9378-83.

**Figure Legends**

**Fig. (1).** Pose and crystallographic structure of *S*-adenosyl-L-homocysteine in the active site of mycolic acid cyclopropane synthase (PDB accession no. 1KPI).

**Fig. (2).** Evolutionary process. Initially a population with different individuals is generated (*initialization*). *Selection* (A) is then carried out, and the individuals with the highest scores are chosen. In the next step, *recombination* (B) is performed followed by a step in which *mutation* (C) takes place. Finally, the fitness function is calculated for these new individuals (D).

**Fig. (3).** Potential energy surface. The potential energy is a function of two independent variables. The rugged character of the surface is clear, indicating several local minima.

**Fig. (4).** Torsion angles of the rotatable bonds in the structure to be docked.

**Fig. (5).** Cavities predicted by MOLDOCK for the structure of EPSPS in complex with shikimate-3-phosphate (PDB accession no. 2O0D).

**Fig. (6).** Search space sphere defined for molecular docking simulations of EPSPS structure in complex with shikimate-3-phosphate (PDB accession no. 2O0D).

**Fig. (7).** Docking sphere and cavities used in the re-docking simulations for the MtPNP and 2dGuo complex.

**Fig. (8).** Canonical trimer observed in all MtPNP crystallographic structures.

**Fig. (9).** Superposition of the best docked structure and crystallographic structure for the MtPNP and 2dGuo complex (PDB accession no. 3IOM).

**Fig. (10).** Superposition of the best docked structure and crystallographic structure for the MtPNP and 1,4-dideoxy-4-aza-1-(*S*)-(9-deazahypoxanthin-9-yl)-D-ribitol complex (PDB accession no. 1G2O).

**Fig. (11).** Superposition of the best docked structure and crystallographic structure for the MtPNP and 9-deazaahypoxanthine complex (PDB accession no. 1I80).

**Fig. (12).** Crystallographic and docked structures obtained for the MtEPSPS and S3P complex (PDB accession no. 2O0D).

**Fig. (13).** Crystallographic structure of MtInhA in complex with adduct (PDB accession no. 2IDZ).

**Fig. (14).** Intermolecular hydrogen bonds identified in the structure of InhA and isoniazide adduct (PDB accession no. 2IDZ).

# CAPÍTULO 3

## ARTIGO CIENTÍFICO

## *In silico* study of SIRT1 inhibitors

**_In silico_ study of SIRT1 inhibitors**

Graziela Heberlé[a,b], Walter Filgueira de Azevedo Jr.[a,c]

[a] *Faculdade de Biociências, Laboratório de Bioquímica Estrutural, Programa de Pós-Graduação em Biologia Celular e Molecular. Instituto Nacional de Ciência e Tecnologia em Tuberculose-Pontifícia Universidade Católica do Rio Grande do Sul, CEP 90619-900, Porto Alegre – RS, Brazil.*

[b]*Centro de Ciências Biológicas e da Saúde, Centro Universitário-UNIVATES, Rua Avelino Tallini, 171 - Bairro Universitário. Lajeado –RS, Brazil. CEP 95.900-000*

[c]*Programa de Pós-Graduação em Medicina e Ciências da Saúde, Pontifícia Universidade Católica do Rio Grande do Sul, Porto Alegre - RS, Brazil.*

E-mail: walter@azevedolab.net .

[*]Corresponding author:

Walter Filgueira de Azevedo Jr.

*Address:* Faculdade de Biociências, Instituto Nacional de Ciência e Tecnologia em Tuberculose-CNPq, Laboratório de Bioquímica Estrutural, Pontifícia Universidade Católica do Rio Grande do Sul - PUCRS, 90619-900. Porto Alegre, Brazil.

*Telephone:+*55 51 3353-4529. *Fax:+*55 51 3320-3629. *E-mail:* walter@azevedolab.net

**ABSTRACT**

Sirtuins compose an important family of proteins, nicotine adenine dinucleotide (NAD) deacetylases that regulate gene silencing, transcriptional repression, recombination, the cell apoptosis division cycle, chromosomal stability, and cellular responses to DNA-damaging agents. These proteins are emerging as molecular targets for pharmaceutical development of drugs for treating human diseases. On the basis of the structural importance of these proteins, in this work we carried out the molecular homology modeling of human SIRT1, using *Thermotoga maritima* Sir2 crystallographic structure as template. Furthermore, we also performed a virtual screening procedure for SIRT1 model against two databases. One based on a nicotinamide derivatives and the other composed of molecules from Sigma-Aldrich vendor. Based on the virtual screening results we used the lowest free binding energy (Plant Score) molecules to select the bet hits. We employed a Similarity Ensemble Approach Tool (SEA) for assessing the structure and pharmacological activity relationships. Our results indicate two nicotinamide analogues, that presented high affinity against SIRT1, which suggest new of SIRT1 inhibitors. In addition, among the bests docking results, (2R,3S,4R,5R)-2-(hydroxymethyl)-5-(6-(phenylamino)-9H-purin-9-yl)-tetrahydrofuran-3,4-diol shows a high number of pharmacological activity references. Our results suggest new compounds for development of SIRT1 inhibitors or activators.

**KEYWORDS**

Sirtuin; SIRT1; virtual screening; modeling; nicotinamide; pharmacological activity.

**GRAPHICAL ABSTRACT**

Three dimensional model of SIRT1

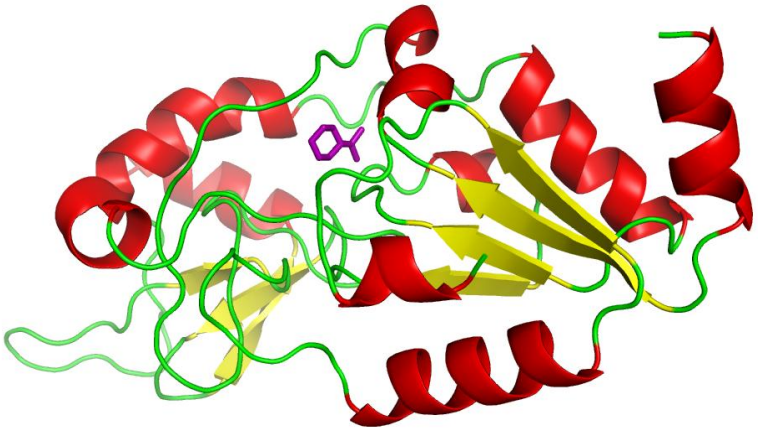

**INTRODUCTION**

Sirtuins (nicotine adenine dinucleotide deacetylases) catalyze reactions of deacetylation and mono-ADP-ribosyl-transferase. In eukaryotes, sirtuins work as regulators of gene silencing, transcriptional repression, recombination, the cell apoptosis division cycle, chromosomal stability, and cellular responses to DNA-damaging agents. Therefore it has been observed that Sirtuins have been implicated in regulating the molecular mechanisms of aging [1-5]. The first discovered sirtuins, yeast Sir2 or SIRT1 in human, are actually well established as key enzymes that affect life spam in a large variety of organism models [6].

These proteins were classified in four different phylogenetic groups, based on their sequence similarity. SIRT1, SIRT2 and SIRT3 form the class I; SIRT4 forms the class II; SIRT5 forms the class III; SIRT6 and SIRT7 form the class IV. The biological function classification is based on the subcellular localization of mammalian sirtuins. SIRT1, SIRT6 and SIRT7 are predominantly found in the nucleus, while SIRT2 is found frequently in the cytoplasm, although SIRT1 and SIRT2 have also been observed as nucleocytoplasmic enzymes.[7-9] SIRT3, SIRT4 and SIRT5 have been described as mitochondrial sirtuins. [6, 10]

Sirtuins deacetylase enzymatic activity affects the conformational state and the activities of the substrate–proteins [11]. The most common reaction catalyzed by sirtuin enzymes is that of NAD+ dependent protein deacetylation, which consumes a mole equivalent of NAD+ per acetyl group removed [12]. The reaction affects an acetyl group transfer to ADPR to form a novel compound called 2'-O-acetyl-ADPR. Sirtuins also catalyze other reactions, such as protein ADP-ribosyl-transfer, NAD+ hydrolysis and many, if not all, seem to catalyze acetyl lysine-dependent nicotinamide base-exchange into NAD+. Active site residues enforce a destabilization of the NAD+ on the active site which facilitates nicotinamide bond cleavage and down-stream reaction of NAD+ with acetyl lysine substrate.[13].

In the last years, inhibition and activation of the Sir2 proteins have presented relation with many forms of pathogenesis [14]. SIRT1 modulation has demonstrated neuroprotective action, which could play a key role in neurodegeneration. These findings suggest that novel therapeutic strategies directed to increase the supply of NAD and/or Sir2 activation may be effective for treatment of diseases characterized by axonopathy and neurodegeneration [15-17]. SIRT1 has been target of studies aimed in cancer since it interacts with p53, a tumor suppressor that plays a critical role in the prevention of human cancer and in tumor response [18-24]. Furthermore, SIRT1 demonstrated to react in tests related to Tat, a key enzyme that mediates HIV transcription [25-30].

Several studies have been carried out focused on sirtuin inhibitors. Many works demonstrated that such inhibitors are able to induce tumor cells apoptosis [31-33]. For neuronal diseases, tests using nicotinamide, a known sirtuin inhibitor, enhances neuronal cell survival during acute anoxic injury. [34] In addition, it has also been observed that nicotinamide restores cognition in Alzheimer's disease patients [35]. Furthermore, a recent study shows that SIRT1 inhibition by nicotinamide prevents NAD+ depletion and protects neurons against excitotoxicity and cerebral ischemia [17]. Therefore, nicotinamide has been considered a strong sirtuin inhibitor [36].

These proteins are conserved, from bacteria to humans. For bacteria and yeast organisms, only one sirtuin is expressed (Sir2), although complex eukaryotes have expression of many sirtuins. Mammalian sirtuin family is composed by seven homolog members (SIRT1-7) of Sir2. Each sirtuin is formed by a conserved catalytic domain shaped by 275 amino acids and also by an additional N- and/or C-terminal sequence of variable size [1, 10, 12, 37]. Tertiary structures revealed by X-ray crystallography of several Sir2 proteins have been published in the past few years, however no 3D structure has been obtained for Sirt1[38-39]. Previously reported crystallographic structure showed that Sir2 protein is present a large catalytic domain characterized by a Rossmann-fold and a smaller zinc binding domain. The interface between the large and the small subdomain is commonly subdivided into A, B, and C pockets. This division is based on the interaction of adenine (A), ribose (B) and nicotinamide (C), which are parts of the NAD+ cofactor [37].

Based on sirtuin family structural sequence similarity and inhibition capacity of nicotinamide ($IC_{50}$ range of μM), we have applied a molecular homology modeling procedure in order to obtain the three dimensional model of SIRT1 and also a virtual screening was carried on SIRT1 using two dataset, one formed by 477 nicotinamide derivative molecules and the second composed of 15181 molecules from Sigma-Aldrich vendor. The results and perspectives for a new lead discovery are discussed in this article.

## MATERIALS AND METHODS

### Molecular Modeling

The homology modeling is a technique used in order to obtain the three dimensional structure of a protein. This methodology is applied when experimental determined structure is not available. It is based on the assumption that both proteins present a higher relationship if they have at least an identity of 30% between their sequences [40-42]. There are several criteria that can be used to select a template. One of them is the identity. We selected a template that shows identity greater than 30 %, and also presents a ligand in the binding pocket, in order to facilitate docking simulations, since we expect that potential ligand-binding modifications were captured in the complexed structures.

The homology modeling program, MODELLER 9v7, was used to model the structure of SIRT1 (EC 3.5.1.-) using Sir2 from *Thermotoga maritima* complexed with nicotinamide and acetylated p53 peptide as template [38]. The complete amino acid sequence of SIRT1 was obtained from the NCBI protein database (SWISSPROT Accession Number Q96EB6). We used the atomic coordinates of Sir2 (PDB access code: 1YC5), which presents 38% identity with human sirtuin 1 (SIRT1). The sequence used for model construction was selected based on the high degree of primary sequence identity.

The first step in modeling procedure is the alignment of the sequence to be modeled (target) with related known three-dimensional structure (template). This alignment was the input to the program and the output was the three dimensional model for the target sequence containing all main-chain and side-chain non-hydrogen atoms [43]. Five models were generated and the best structure was selected using MODELLER objective function [44].

**Redocking and virtual screening**

Molecular docking is a simulation process to predict the conformation of a receptor-ligand complex, where the receptor can be a protein and the ligand a small molecule. It can also be defined as a simulation process where a ligand position is estimated in a predicted or pre-defined binding site in the receptor molecule [45].

It was applied the flexible docking protocol available in the program MolDock [45]. This program implements evolutionary algorithms, which are classified as a group of computational techniques based on the concepts of Darwin's theory of evolution that are designed to find the best possible solution to optimization problems [46].

In order to validate the docking protocol we performed the redocking against the nicotinamide-binding pocket (also known as C pocket) using the crystallographic structure of Sir2-nicotinamide complex (1YC5). We applied the Plant Score Grid scoring function to select the best poses. All redocking simulations were performed with MolDock with center at coordinates at x = 1.61, y = 22.21 and z = 8.45 Å, and docking sphere with radius of 10 Å.

It has been proposed that nicotinamide is an important template for inhibition of sirtuins, demonstrating inhibition against SIRT1 and Sir2 [47]. Based on this observation, we employed the nicotinamide core as template to carry out a search in the ZINC database in order to build a small-molecule database/library. A total of 477 molecules were retrieved and used to build this database [48-49].

The best poses, with lowest energy, were selected by the Plant Score function, which is a sum of a subset of the interaction terms (all terms are given the same weight) [50]. A total of 10 poses were selected with a cutoff in the PLANTS score of -70. The same protocol employed in redocking procedure was applied for the virtual screening against the nicotinamide and sigma databases.

**RESULTS AND DISCUSSION**

**Molecular modeling**

The elucidation of three dimensional structures of several sirtuins have provided the possibility to establish relationships between structure and activity studies, which enables us to understand key features of action and inhibition mechanisms among sirtuins. [38-39, 51-52].

Sir2 from *Thermotoga maritima* (PDB: 1YC5) has been used as template for the homology modeling of SIRT1 due to present 38% of sequential identity. For modeling only the conserved core was built. The alignment was obtained from ClustalW2 tool [53] (figure 1). As expected, the SIRT1 model presented a canonical fold of sirtuins family.

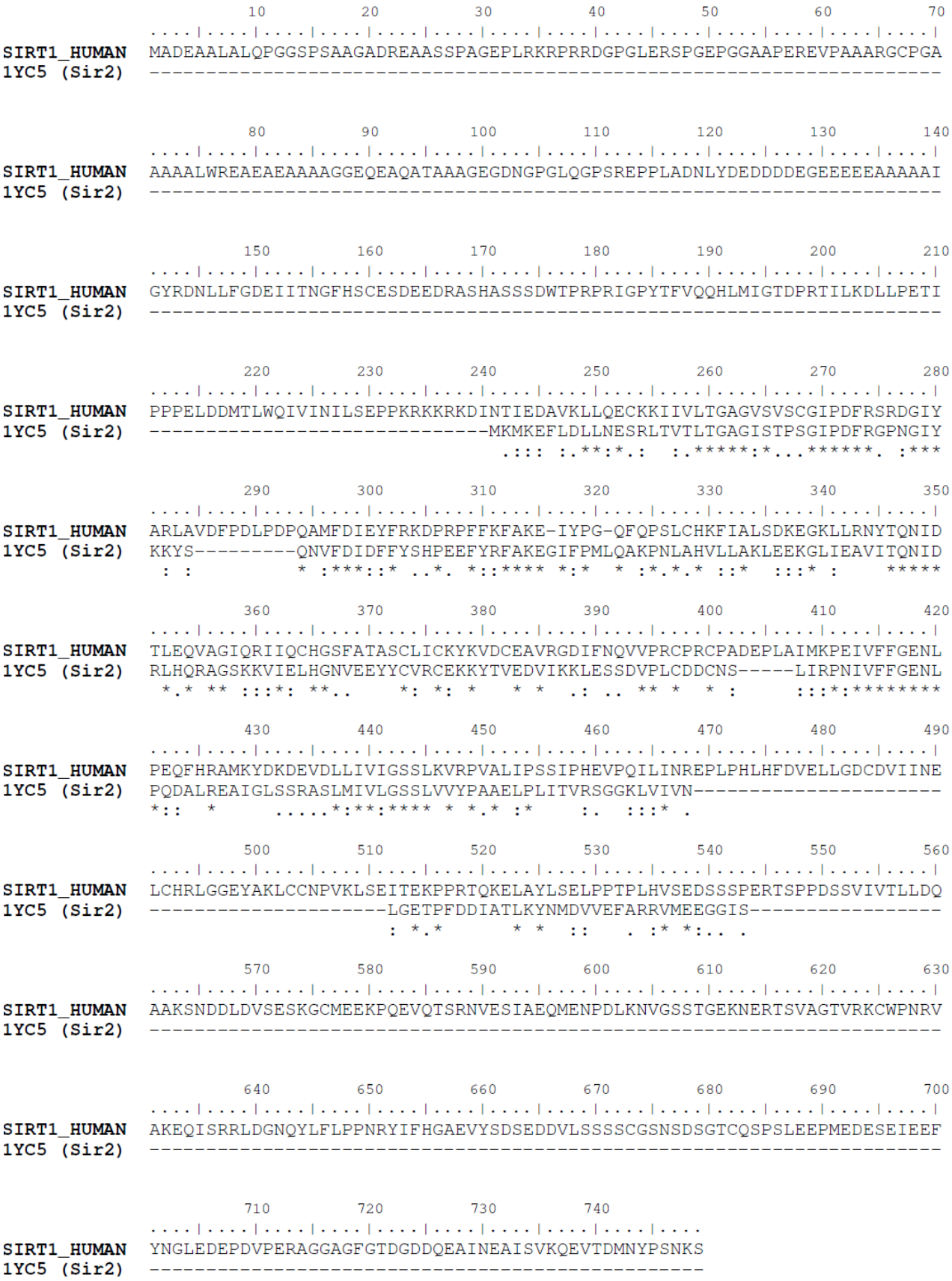


**Figure 1**. Sequence alignment between SIRT1(Q96EB6) and Sir 2 from *Thermotoga maritima* (Q9WYW0).

The superposition of SIRT1 model (SIRT1m), when compared with the crystallographic structure of Sir2 from *Thermotoga maritima* (PDB: 1YC5), is demonstrated in figure 2, in which is observed a high similarity. The SIRT1 structure presents a bilobe conformation with a larger domain formed by a modified Rossmann fold observed in several NAD(H) and NADP(H) binding enzymes, and a smaller domain. Both lobes are linked by four polypeptide chains.

In the interface between both domains there is a large cleft formed by the crossing of these four polypeptide chains, two loops of the larger domain and one loop from the smaller domain. The larger lobe is formed by four β sheets (β1-3 and β7), this central β sheet is surrounded by six helices (α1, α2, α4, α5 , α7 and 8). Between both lobes there's a cavity where NAD binds. The smaller domain contains a parallel beta sheet, formed by three beta strands (β4, β5 and β6) and two alpha helices (α3 and α6).

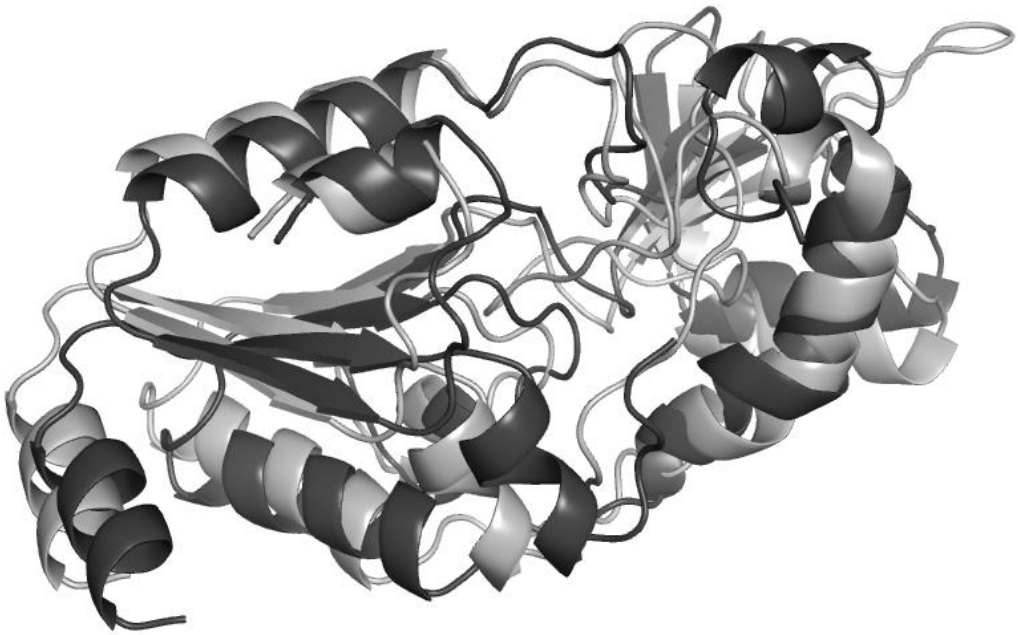

**Figure 2**. Superposition between the homology model structure of SIRT1 (light gray) and crystal structure, used as template (dark gray).

**Virtual Screening (nicotinamide derivatives)**

The use of MolDock for Sir2 structure of *Thermotoga maritima* (template) in complex with nicotinamide was able to predict correctly the binding position of nicotinamide into the site of template. Figure 3 demonstrates the superposition of the best docked structures. The smaller RMSD of superposition is 0.73 Å. In order to check the prediction capability of the present docking protocol, a blind redocking using a radius of 32 Å has been carried out. Analysis of the results indicated the same nicotinamide-binding pocket identified in

the redocking simulation using a radius of 10 Å. Similar flexible docking protocols have been adopted in virtual screening procedures against Sir2 from *Leishmania* [54]. Since the docking protocol has demonstrated to be able to reproduce the crystal structure complex, it has been applied to scan both databases (nicotinamide and sigma).

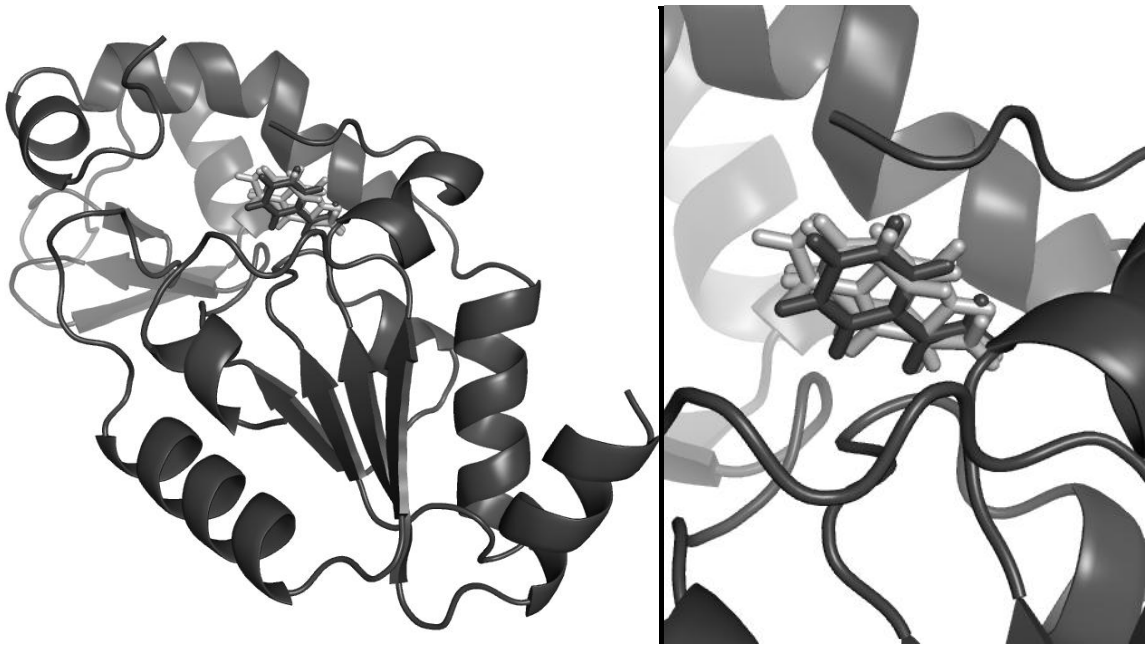


**Figure 3**. Superposition between the best results of validation docking procedure. a: three-dimensional structure of template docked with three ligands that presented lower RMSD value (light gray) and crystal structure ligand (dark gray). b. Details of binding site.

Nicotinamide has several structural properties that make it a promising molecule for structure-based virtual screening procedures. These properties are composed by: ClogP = -0.4, molecular weight of 122.1246 g/mol, rotable bonds number = 1, polar surface area = 56 $Å^2$, number of hydrogen bond donors = 1 and hydrogen bonds acceptors = 2. The properties mentioned satisfy the rules of Lipinski and Veber [55-56]. The knowledge about template conservation, allied to fragment based virtual screening procedure, has guided the search for structural properties in the construction of libraries of small molecules [57]. This knowledge is inserted in the rule of three, that establishes: a molecule to be introduced in a virtual screening library must have a molecular weight $\leq$ 300, ClogP $\leq$ 3, number of rotable bonds $\leq$ 3, number of hydrogen bond donor and acceptors $\leq$ 3 and polar area surface $\leq$ 60 $Å^2$. This information indicates that the rule of three may be useful for the construction of fragment libraries in order to discover new efficient inhibitors [58]. Through analysis of the nicotinamide structure it's possible to observe that it fulfils these requirements.

It has been showed that nicotinamide is a molecule that inhibits the deacetylation activity of SIRT1 through the interaction with a reaction intermediate [36]. The catalyzed deacetylation results in the production of 2'- e 3'-*O*-acetyl-ADP-ribose and a deacetyl lisine. If nicotinamide binds to the enzyme when it contains the intermediate O-alkyl-amidate, it can react as the intermediate in an event known as nicotinamide exchange, in which $NAD^+$ and N6-acetyl-lysine are formed [4, 52, 59-60].

**Table 1** shows best results of virtual screening. Docking simulations of these molecules against active site of SIRT1 had identified ZINC00070123 (6-(3-nitrophenyl)pyrrolo[3,4-b]pyridine-5,7-dione) as better ligand (lowest score: -74.99) among all 477 tested. Figure 4 shows ZINC00070123 docked against SIRT1.

**Table 1**. Results of virtual screening of nicotinamide database against SIRT1 model, showing the best 10 docked structures and its respective properties.

| ZINC Code<br>Molecular structure | Molecular weight (g/mol) | Plant Score | Activity(e-value /MaxTC)* |
|---|---|---|---|
| ZINC00070123 | ***$C_{13}H_7N_3O_4$*** | -74.9929 | Immunosuppressant (2.05e-03/0.53) |
| 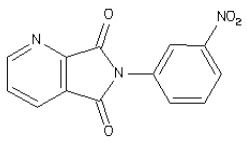 | 269.2167 | | Insulin Promoter(2.83e-01/0.33) |
| ZINC00004778 | ***$C_{15}H_{16}N_4O$*** | -74.8476 | Antiviral (AIDS) (9.42e-5/1.00) |
| 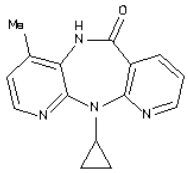 | 266.297860 | | |
| ZINC00099922 | $C_{15}H_{12}N_2O_3$ | -72.9831 | Antiviral (AIDS) (1.02e-2/0.43) |
| 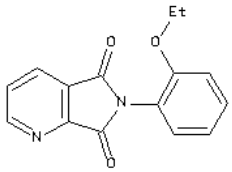 | 268.2726 | | Immunomodulator (1.01e-1/0.33)<br>Immunosuppressant (2.69e+0/0.42)<br>Antiinflammatory (3.16e+0/0.40) |
| ZINC00088263 | $C_{19}H_{15}N_3O_2$ | -70.7709 | Stimulant, Central (1.70e+0/0.33) |
| 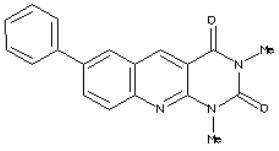 | 317.3481 | | AMPA Receptor Antagonist (9.94e+0/0.33) |

* Information from ZINC website

Analysis of ligand placement of ZINC00070123 docked in the protein (figure 5), with better Plant Score value, indicated the presence of intermolecular hydrogen bond interactions with main chain atoms of Ala 20, Phe 31, Leu 201, Leu 202, Val 203 and side chain atoms of Gln 103, Ser 199, Asn 104 (figure 5 and table 2).

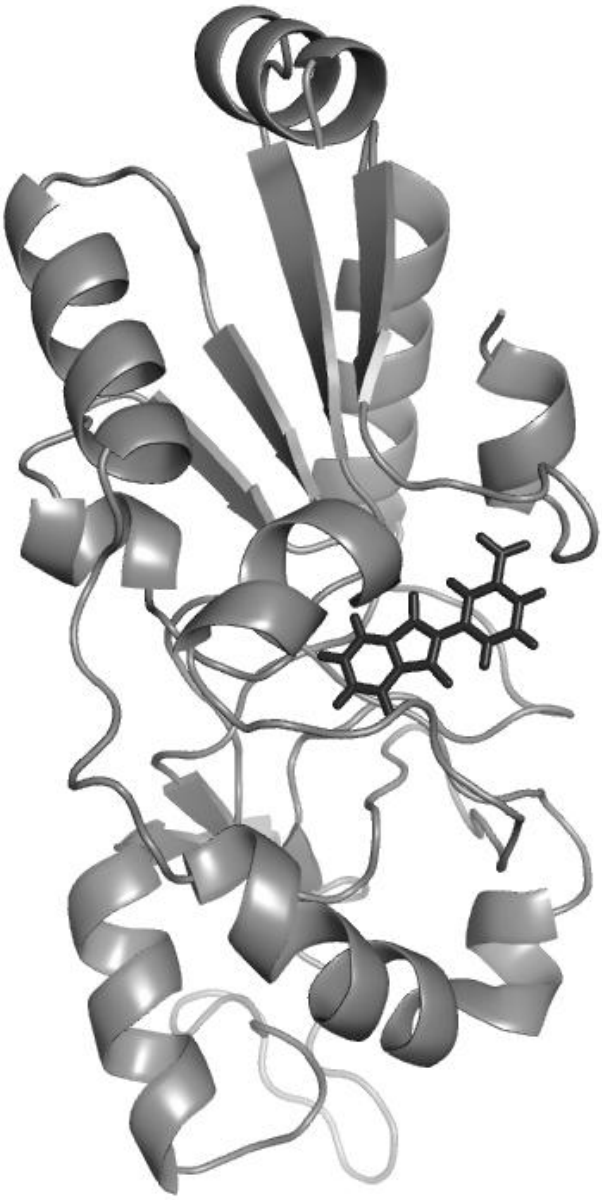

**Figure 4**. Docking of ZINC00070123 (light gray) against SIRT1m (dark gray).

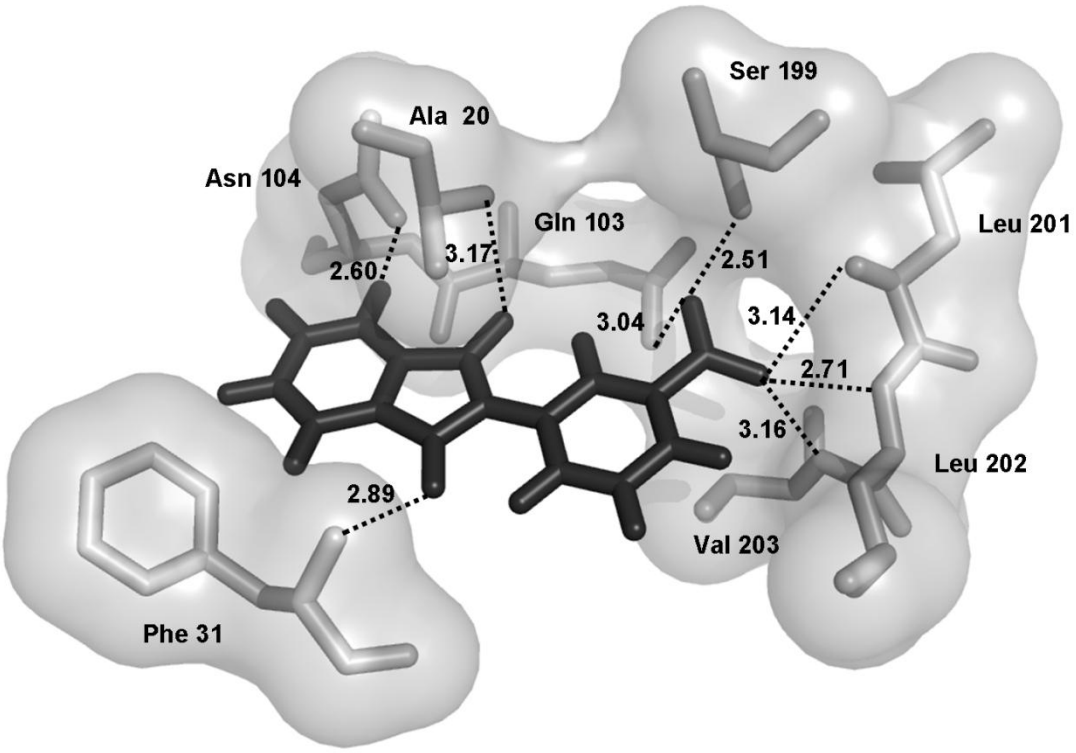


**Figure 5**. Representation of intermolecular hydrogen bonds between ZINC00070123 (dark gray) and SIRT1 (light gray).

**Table 2**. Hydrogen bonds between ZINC00070123 and SIRT1.

| Protein | | | Ligand | | Distance(Å) |
|---|---|---|---|---|---|
| Aminoacid | Number | Atom | Atom | Number | |
| GLN | 103 | NE2 | O1 | 8 | 3.04 |
| SER | 199 | OG | O1 | 8 | 2.51 |
| LEU | 201 | N | O2 | 9 | 3.14 |
| LYS | 202 | N | O2 | 9 | 2.71 |
| VAL | 203 | N | O2 | 9 | 3.16 |
| PHE | 31 | N | O3 | 12 | 2.89 |
| ASN | 104 | OD1 | N3 | 17 | 2.61 |
| ALA | 20 | N | O4 | 20 | 3.17 |

Analysis of ZINC00004778 (11-cyclopropyl-5,11-dihydro-4-methyl-6H-dipyrido [3,2-b:2',3'-e][1,4] diazepin-6-one) position in the docked complex (figure 6), with the second best Plant Score value, presented intermolecular hydrogen bond interactions with the main chain of Phe 31 and with the side chain of Asn 104 (figure 7 and table 3).

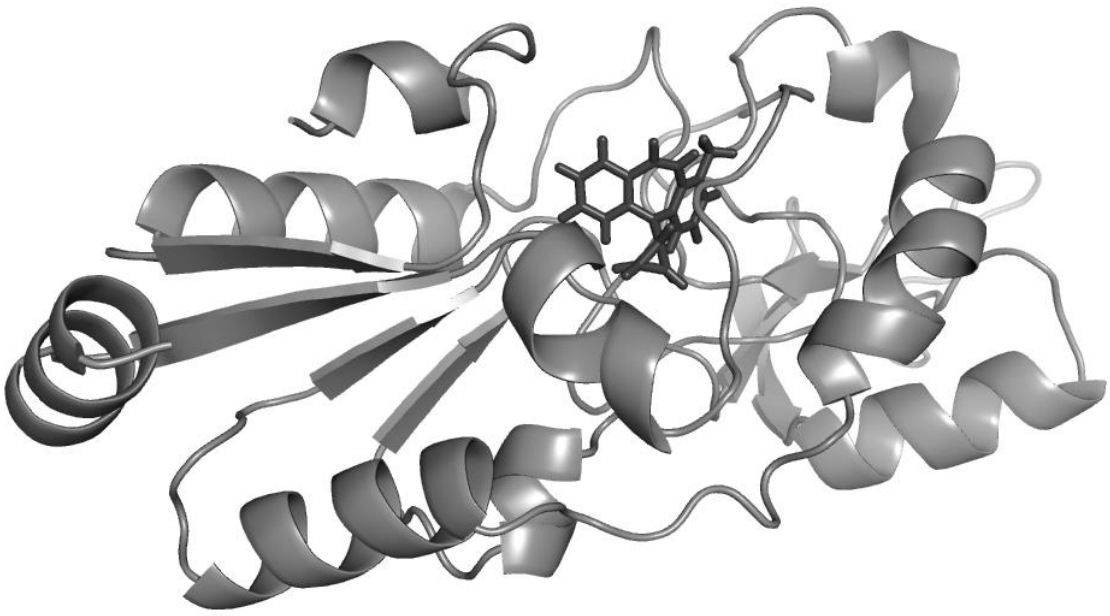

**Figure 6**. Docking of ZINC00004778 ligand (light gray) against SIRT1m (dark gray).

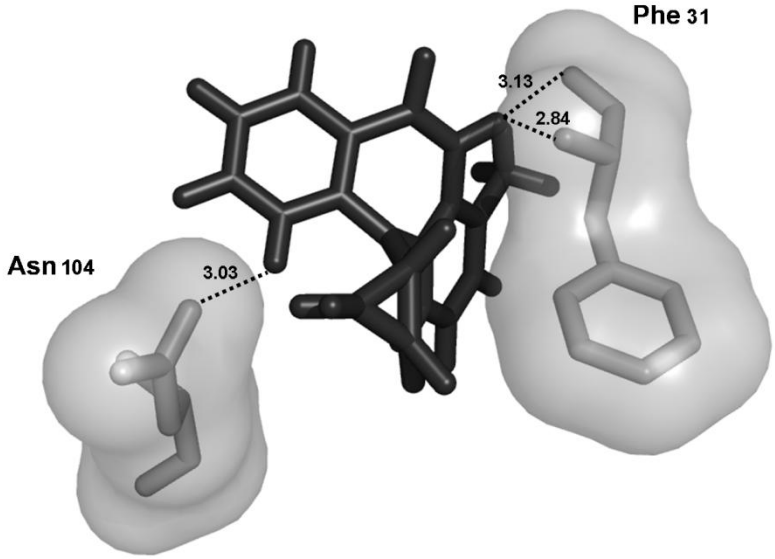


**Figure 7**. Representation of intermolecular hydrogen bonds between ZINC00004778 ligand (dark grey) and SIRT1m (light grey).

**Table 3**. Hydrogen bonds between ZINC00004778 and SIRT1m.

| Protein | | | Ligand | | Distance(Å) |
|---|---|---|---|---|---|
| Aminoacid | Number | Atom | Atom | Number | |
| PHE | 31 | N | N2 | 8 | 2.84 |
| PHE | 31 | O | N2 | 8 | 3.13 |
| ASN | 104 | OD1 | N3 | 15 | 3.03 |

It has been observed that in both better dockings the hydrogen bonds between ligands and protein (SIRT1m) occur with amide cores of ligands, possibly between its nitrogen or oxygen atoms. These results suggest that amide core must play an important role in the interaction between SIRT1m and its ligands. Furthermore, the top ranking score ligands present some common structural features in the intermolecular interactions between ligand and protein. The most striking feature is the participation of Phe 31 and Asn 104 in intermolecular hydrogen bonds, which indicates the importance of these interactions for ligand binding have not been observed in previously published VS studies. This difference may be due differences in VS strategies and also differences in small-molecule libraries, employed in VS approaches.

Sirtuins have been related to rheumatoid arthritis, diabetes, heart diseases, neuroprotection, aging, and cancer, and they are presently under examination as novel possible targets for drug discovery and development. In order to establish a relationship between structure and activity of the best results obtained by virtual screening, it has been employed a method in which groups and link compounds basing on its chemical similarities in a quantitative manner, using a set of approximation tools, Similarity Ensemble Approach (SEA). For this, a search was carried out for each one of the compounds that presented the lowest energy [61].

For identification of activities related to the best results of *virtual screening*, the parameter employed was the *e-value,* that represents the random probability of observing information. In other words, the smaller is the *e-value*, the deeper will be the relationship between the compound and reference's activity. To keep a higher reliability in the results, we selected for discussion the activities under a cut off *e-value* of $10^{-10}$, since it represents similarity in the structure-activity relation in a statistically satisfying way[61-62].

Based on results of SEA search for potential inhibitors, that relate structures with their activities, it was not possible to establish a clear relationship with activities played by SIRT1 inhibitors, despite their similarity with nicotinamide. This result implies the necessity for experimental tests of activity of the better docked molecules in order to effectively confirm the hypothesis these molecules may be SIRT1 inhibitors. Finally, it is

worth mention the interesting result obtained for ZINC00088263. SEA results (Table 1) indicate activities as CNS stimulant and AMPA receptor antagonist for this molecule. Both activities related to neuroprotection. Furthermore, recent study indicated the involvement of SIRT1 in modulation of synaptic plasticity and memory formation, which demonstrated its value as a potential therapeutic target for the treatment of central nervous system disorders [61]. Especially interesting is the result obtained for the best score ligand (ZINC00070123) and also for the molecule ZINC99922. Both have been predicted to present antiinflamatory and immunosupression activities. It has been reported the potential relationship of SIRT1 inhibition to RA, and a recent study indicated that therapeutic administration of SIRT1 inhibitors might selectively induce apoptosis at sites of inflammation in RA. Our results indicates that both molecules inhibits SIRT1, and therefore it is tempting to speculate that both may also be used a potential antiinflamattory agents.

**Virtual Screening (sigma database)**

The docking simulations of sigma database against SIRT1 active site shows ZINC02548278 (Methyl (3*S*)-(+)-3-(methyl-1*H*-indol-3-yl)-3-phenylpropanoate) as best ligand (lower score: -83.0287) between 15181 tested. **Figure 8** illustrates the complex between best ligand and SIRT1. Table 4 shows the best results of present virtual screening procedure.

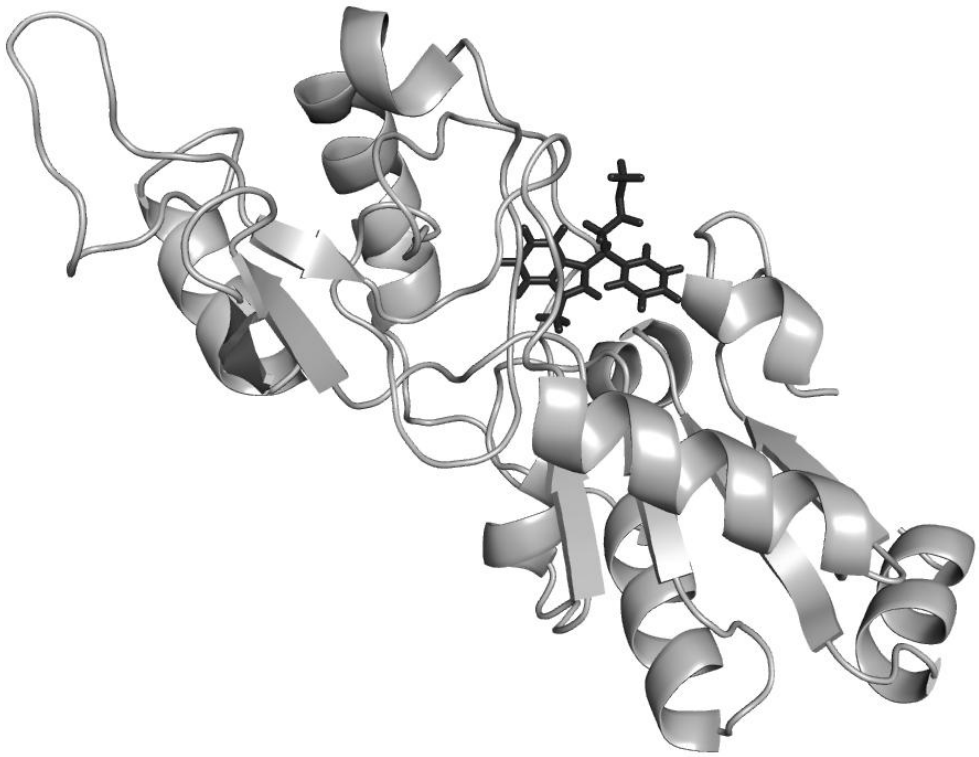

**Figure 8**. Docking of ZINC02548278 (light gray) against SIRT1m (dark gray).

**Table 4**. Results of virtual screening of Sigma database molecules against SIRT1 model, showing the best 4 docked structures and its respective properties.

| ZINC Code<br>Molecular structure | Formula and molecular weight (g/mol) | Plant Score | Activity(e-value /MaxTC)* |
|---|---|---|---|
| ZINC02548278<br> 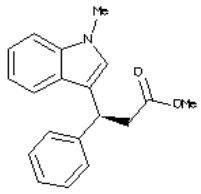 | C19H19NO2<br>293.3597 | -83.0287 | TNF Inhibitor (8.11e-3/0.37) |
| ZINC12957072<br> 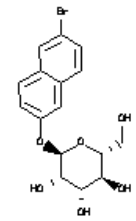 | C16H17BrO6<br>385.207 | -79.1266 | Antidiabetic (3.32e-17/0.47) |
| ZINC04078894<br> 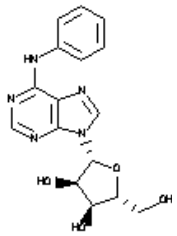 | C16H17N5O4<br>343.33728 | -78.9504 | Antiviral (2.74e-29/0.59)<br>Antitrypanosomal (1.21e-19/0.45<br>Viral Hepatitis, Agent for (3.60e-15/0.45);<br>Immunomodulator (6.56e-13/0.38)<br>Neuronal Injury Inhibitor (3.85e-10/0.60) |

* information from ZINC website.

Analysis of the ligand ZINC02548278 (methyl (3R)-(-)-3-(methyl -1H-indol-3-YL)-3-phenylpropanoate) docked in SIRT1, which obtained the best value of Plant Score, presented one hydrogen bond interaction with the main chain of Phe 31 (**figure 9**). In addition, using the program LIGPLOT [63], it has been found 35 van der Waals interactions. These results suggest that high number of van der Waals interactions may have contributed to obtain this high affinity value, indicated by Plant Score, through virtual screening approach.

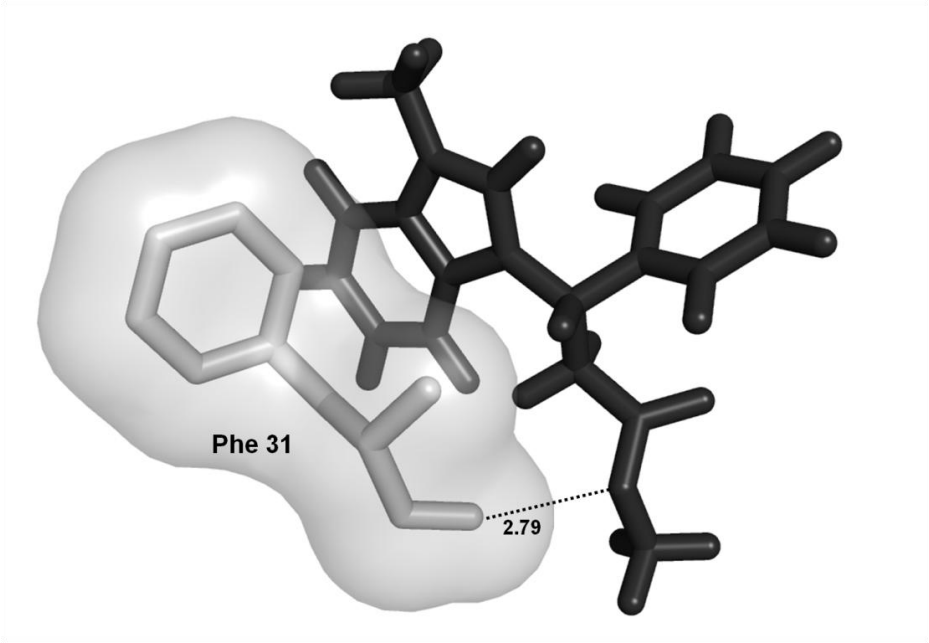


**Figure 9**. Representation of intermolecular hydrogen bonds between ZINC02548278 (dark gray) and SIRT1.

According to SEA prediction, ZINC02548278 compound (illustrated in table 4) presented relation with 5-HT4 serotonin receptor agonist activity. However, through the search for experimental data in previous works, it was not possible to establish any relation between 5-HT4 serotonin receptor agonist activity and SIRT1 inhibition [64]. For the other molecules that presented a cutoff value of -78 for Plant Score and $10^{-10}$ *e-value*, it has been found activity references related with inhibition of SIRT1 that agree with results of the search performed through the SEA approximation tool.

Previous work reported antiviral and antitrypanosomal activities for ZINC04078894, one of highest plant scores identified in the docking simulations. This information coincides with reported suramin activity, a molecule known as a SIRT1 no selective inhibitor, that has been identified as an antiviral [65]. Antitrypanosomal activity has also been reported for suramin molecule, once more confirming the SEA search results [66]. Through the identification of antitrypanosomal molecules, such as ZINC04078894, it is possible to acquire information for development of more selective inhibitors through detailed structural studies, comparing docking of human and trypanosomal sirtuins. Therefore, this information is useful for drug development strategies in order to design new selective inhibitors which present higher toxicity against parasite target sirtuin, and lower against human sirtuin [67].

## CONCLUSION

It was possible to model human SIRT1 from Sir2 of *Thermotoga maritima* (PDB: 1YC5) since it demonstrates 38% of sequential identity. SIRT1 structure obtained by homology modeling presented the canonical folding of sirtuin family, as described in previous study [67]. The present model has been used for virtual screening procedure against a molecule database based on nicotinamide scaffold and also against the sigma database. The docking protocol discussed in the present work was able to reproduce the crystal structure of sirtuins, and results obtained by the present virtual screening procedure are promising for development of new lead compounds for sirtuins inhibition, indicating new potential inhibitors for SIRT1. Nevertheless caution should be exercised when selecting SIRT1 inhibitors, since such inhibitors may have undesired side effects, in view of the fact that direct inhibition of SIRT1 may affect brain activity and also inhibition of plasticity and memory in a direct manner [61]. Furthermore, VS results were able to identify two potential anti-inflamatory agents, based on the SEA prediction results. In addition, analysis of the SEA results for the molecule ZINC04078894 indicated antiviral and antitrypanosomal activities, both related to sirtuin inhibition.

## CONFLICT OF INTEREST

The authors declare no conflicts of interests.


## ACKNOWLEDGEMENTS

This work was supported by grants from CNPq and Instituto Nacional de Ciência e Tecnologia do Conselho Nacional de Desenvolvimento Científico e Tecnológico-Ministério de Ciência e Tecnologia (INCT-Tuberculose, CNPq-MCT, Brazil). WFA is senior researcher for CNPq (Brazil).


## REFERENCES


[1] Sedding, D.; Haendeler, J., Do we age on Sirt1 expression? *Circ Res,* **2007**, *100*, (10), 1396-1398.

[2] North, B.J.; Marshall, B.L.; Borra, M.T.; Denu, J.M.; Verdin, E., The human Sir2 ortholog, SIRT2, is an NAD+-dependent tubulin deacetylase. *Mol Cell,* **2003**, *11*, (2), 437-444.

[3] North, B.J.; Verdin, E., Sirtuins: Sir2-related NAD-dependent protein deacetylases. *Genome Biol,* **2004**, *5*, (5), 224.

[4] Sauve, A.A.; Celic, I.; Avalos, J.; Deng, H.; Boeke, J.D.; Schramm, V.L., Chemistry of gene silencing: the mechanism of NAD+-dependent deacetylation reactions. *Biochemistry,* **2001**, *40*, (51), 15456-15463.

[5] Grubisha, O.; Rafty, L.A.; Takanishi, C.L.; Xu, X.; Tong, L.; Perraud, A.L.; Scharenberg, A.M.; Denu, J.M., Metabolite of SIR2 reaction modulates TRPM2 ion channel. *J Biol Chem,* **2006**, *281*, (20), 14057-14065.

[6] Yamamoto, H.; Schoonjans, K.; Auwerx, J., Sirtuin functions in health and disease. *Mol Endocrinol,* **2007**, *21*, (8), 1745-1755.

[7] North, B.J.; Verdin, E., Interphase nucleo-cytoplasmic shuttling and localization of SIRT2 during mitosis. *PLoS One,* **2007**, *2*, (8), e784.

[8] Tanno, M.; Sakamoto, J.; Miura, T.; Shimamoto, K.; Horio, Y., Nucleocytoplasmic shuttling of the NAD+-dependent histone deacetylase SIRT1. *J Biol Chem,* **2007**, *282*, (9), 6823-6832.

[9] Cohen, H.Y.; Lavu, S.; Bitterman, K.J.; Hekking, B.; Imahiyerobo, T.A.; Miller, C.; Frye, R.; Ploegh, H.; Kessler, B.M.; Sinclair, D.A., Acetylation of the C terminus of Ku70 by CBP and PCAF controls Bax-mediated apoptosis. *Mol Cell,* **2004**, *13*, (5), 627-638.

[10] Michan, S.; Sinclair, D., Sirtuins in mammals: insights into their biological function. *Biochem J,* **2007**, *404*, (1), 1-13.

[11] Grozinger, C.M.; Schreiber, S.L., Deacetylase enzymes: biological functions and the use of small-molecule inhibitors. *Chem Biol,* **2002**, *9*, (1), 3-16.

[12] Sauve, A.A.; Wolberger, C.; Schramm, V.L.; Boeke, J.D., The biochemistry of sirtuins. *Annu Rev Biochem,* **2006**, *75*, 435-465.

[13] Sauve, A.A., Sirtuin chemical mechanisms. *Biochim Biophys Acta,* **2010**.

[14] Haigis, M.C.; Sinclair, D.A., Mammalian sirtuins: biological insights and disease relevance. *Annu Rev Pathol,* **2010**, *5*, 253-295.

[15] Araki, T.; Sasaki, Y.; Milbrandt, J., Increased nuclear NAD biosynthesis and SIRT1 activation prevent axonal degeneration. *Science,* **2004**, *305*, (5686), 1010-1013.

[16] Sasaki, Y.; Vohra, B.P.; Baloh, R.H.; Milbrandt, J., Transgenic mice expressing the Nmnat1 protein manifest robust delay in axonal degeneration in vivo. *J Neurosci,* **2009**, *29*, (20), 6526-6534.

[17] Liu, D.; Gharavi, R.; Pitta, M.; Gleichmann, M.; Mattson, M.P., Nicotinamide prevents NAD+ depletion and protects neurons against excitotoxicity and cerebral ischemia: NAD+ consumption by SIRT1 may endanger energetically compromised neurons. *Neuromolecular Med,* **2009**, *11*, (1), 28-42.

[18] Puca, R.; Nardinocchi, L.; Sacchi, A.; Rechavi, G.; Givol, D.; D'Orazi, G., HIPK2 modulates p53 activity towards pro-apoptotic transcription. *Mol Cancer,* **2009**, *8*, 85.

[19] Liu, T.; Liu, P.Y.; Marshall, G.M., The critical role of the class III histone deacetylase SIRT1 in cancer. *Cancer Res,* **2009**, *69*, (5), 1702-1705.

[20] Jung-Hynes, B.; Nihal, M.; Zhong, W.; Ahmad, N., Role of sirtuin histone deacetylase SIRT1 in prostate cancer. A target for prostate cancer management via its inhibition? *J Biol Chem,* **2009**, *284*, (6), 3823-3832.

[21] Kim, E.J.; Um, S.J., SIRT1: roles in aging and cancer. *BMB Rep,* **2008**, *41*, (11), 751-756.

[22] Brooks, C.L.; Gu, W., How does SIRT1 affect metabolism, senescence and cancer? *Nat Rev Cancer,* **2009**, *9*, (2), 123-128.

[23] Deng, C.X., SIRT1, is it a tumor promoter or tumor suppressor? *Int J Biol Sci,* **2009**, *5*, (2), 147-152.

[24] Lim, C.S., SIRT1: tumor promoter or tumor suppressor? *Med Hypotheses,* **2006**, *67*, (2), 341-344.

[25] Kwon, H.S.; Ott, M., The ups and downs of SIRT1. *Trends Biochem Sci,* **2008**, *33*, (11), 517-525.

[26] Kwon, H.S.; Brent, M.M.; Getachew, R.; Jayakumar, P.; Chen, L.F.; Schnolzer, M.; McBurney, M.W.; Marmorstein, R.; Greene, W.C.; Ott, M., Human immunodeficiency virus type 1 Tat protein inhibits the SIRT1 deacetylase and induces T cell hyperactivation. *Cell Host Microbe,* **2008**, *3*, (3), 158-167.

[27] Zhang, H.S.; Wu, M.R., SIRT1 regulates Tat-induced HIV-1 transactivation through activating AMP-activated protein kinase. *Virus Res,* **2009**, *146*, (1-2), 51-57.

[28] Zhang, H.S.; Zhou, Y.; Wu, M.R.; Zhou, H.S.; Xu, F., Resveratrol inhibited Tat-induced HIV-1 LTR transactivation via NAD(+)-dependent SIRT1 activity. *Life Sci,* **2009**, *85*, (13-14), 484-489.

[29] Blazek, D.; Peterlin, B.M., Tat-SIRT1 tango. *Mol Cell,* **2008**, *29*, (5), 539-540.

[30] Pagans, S.; Pedal, A.; North, B.J.; Kaehlcke, K.; Marshall, B.L.; Dorr, A.; Hetzer-Egger, C.; Henklein, P.; Frye, R.; McBurney, M.W.; Hruby, H.; Jung, M.; Verdin, E.; Ott, M., SIRT1 regulates HIV transcription via Tat deacetylation. *PLoS Biol,* **2005**, *3*, (2), e41.

[31] Glaser, K.B.; Li, J.; Pease, L.J.; Staver, M.J.; Marcotte, P.A.; Guo, J.; Frey, R.R.; Garland, R.B.; Heyman, H.R.; Wada, C.K.; Vasudevan, A.; Michaelides, M.R.; Davidsen, S.K.; Curtin, M.L., Differential protein acetylation induced by novel histone deacetylase inhibitors. *Biochem Biophys Res Commun,* **2004**, *325*, (3), 683-690.

[32] Lara, E.; Mai, A.; Calvanese, V.; Altucci, L.; Lopez-Nieva, P.; Martinez-Chantar, M.L.; Varela-Rey, M.; Rotili, D.; Nebbioso, A.; Ropero, S.; Montoya, G.; Oyarzabal, J.; Velasco, S.; Serrano, M.; Witt, M.; Villar-Garea, A.; Imhof, A.; Mato, J.M.; Esteller, M.; Fraga, M.F., Salermide, a Sirtuin inhibitor with a strong cancer-specific proapoptotic effect. *Oncogene,* **2009**, *28*, (6), 781-791.

[33] Grozinger, C.M.; Chao, E.D.; Blackwell, H.E.; Moazed, D.; Schreiber, S.L., Identification of a class of small molecule inhibitors of the sirtuin family of NAD-dependent deacetylases by phenotypic screening. *J Biol Chem,* **2001**, *276*, (42), 38837-38843.

[34] Chong, Z.Z.; Lin, S.H.; Li, F.; Maiese, K., The sirtuin inhibitor nicotinamide enhances neuronal cell survival during acute anoxic injury through AKT, BAD, PARP, and mitochondrial associated "anti-apoptotic" pathways. *Curr Neurovasc Res,* **2005**, *2*, (4), 271-285.

[35] Green, K.N.; Steffan, J.S.; Martinez-Coria, H.; Sun, X.; Schreiber, S.S.; Thompson, L.M.; LaFerla, F.M., Nicotinamide restores cognition in Alzheimer's disease transgenic mice via a mechanism involving sirtuin inhibition and selective reduction of Thr231-phosphotau. *J Neurosci,* **2008**, *28*, (45), 11500-11510.

[36] Bitterman, K.J.; Anderson, R.M.; Cohen, H.Y.; Latorre-Esteves, M.; Sinclair, D.A., Inhibition of silencing and accelerated aging by nicotinamide, a putative negative regulator of yeast sir2 and human SIRT1. *J Biol Chem,* **2002**, *277*, (47), 45099-45107.

[37] Neugebauer, R.C.; Uchiechowska, U.; Meier, R.; Hruby, H.; Valkov, V.; Verdin, E.; Sippl, W.; Jung, M., Structure-activity studies on splitomicin derivatives as sirtuin inhibitors and computational prediction of binding mode. *J Med Chem,* **2008**, *51*, (5), 1203-1213.

[38] Avalos, J.L.; Bever, K.M.; Wolberger, C., Mechanism of sirtuin inhibition by nicotinamide: altering the NAD(+) cosubstrate specificity of a Sir2 enzyme. *Mol Cell,* **2005**, *17*, (6), 855-868.

[39] Finnin, M.S.; Donigian, J.R.; Pavletich, N.P., Structure of the histone deacetylase SIRT2. *Nat Struct Biol,* **2001**, *8*, (7), 621-625.

[40] Kroemer, R.T.; Doughty, S.W.; Robinson, A.J.; Richards, W.G., Prediction of the three-dimensional structure of human interleukin-7 by homology modeling. *Protein Eng,* **1996**, *9*, (6), 493-498.

[41] Baker, D.; Sali, A., Protein structure prediction and structural genomics. *Science,* **2001**, *294*, (5540), 93-96.

[42] Sanchez, R.; Sali, A., Comparative protein structure modeling. Introduction and practical examples with modeller. *Methods Mol Biol,* **2000**, *143*, 97-129.

[43] Canduri, F.; Uchoa, H.B.; de Azevedo, W.F., Jr., Molecular models of cyclin-dependent kinase 1 complexed with inhibitors. *Biochem Biophys Res Commun,* **2004**, *324*, (2), 661-666.

[44] Sali, A.; Blundell, T.L., Comparative protein modelling by satisfaction of spatial restraints. *J Mol Biol,* **1993**, *234*, (3), 779-815.

[45] Thomsen, R.; Christensen, M.H., MolDock: a new technique for high-accuracy molecular docking. *J Med Chem,* **2006**, *49*, (11), 3315-3321.

[46] de Azevedo, W.F., Jr., MolDock Applied to Structure-Based Virtual Screening. *Curr Drug Targets,* **2009**.

[47] Marcotte, P.A.; Richardson, P.L.; Guo, J.; Barrett, L.W.; Xu, N.; Gunasekera, A.; Glaser, K.B., Fluorescence assay of SIRT protein deacetylases using an acetylated peptide substrate and a secondary trypsin reaction. *Anal Biochem,* **2004**, *332*, (1), 90-99.

[48] Irwin, J.J.; Shoichet, B.K., ZINC--a free database of commercially available compounds for virtual screening. *J Chem Inf Model,* **2005**, *45*, (1), 177-182.

[49] Timmers, L.F.; Pauli, I.; Caceres, R.A.; de Azevedo, W.F., Jr., Drug-binding databases. *Curr Drug Targets,* **2008**, *9*, (12), 1092-1099.

[50] Korb, O.; Stutzle, T.; Exner, T.E., Empirical scoring functions for advanced protein-ligand docking with PLANTS. *J Chem Inf Model,* **2009**, *49*, (1), 84-96.

[51] Hoff, K.G.; Avalos, J.L.; Sens, K.; Wolberger, C., Insights into the sirtuin mechanism from ternary complexes containing NAD+ and acetylated peptide. *Structure,* **2006**, *14*, (8), 1231-1240.

[52] Avalos, J.L.; Boeke, J.D.; Wolberger, C., Structural basis for the mechanism and regulation of Sir2 enzymes. *Mol Cell,* **2004**, *13*, (5), 639-648.

[53] Larkin, M.A.; Blackshields, G.; Brown, N.P.; Chenna, R.; McGettigan, P.A.; McWilliam, H.; Valentin, F.; Wallace, I.M.; Wilm, A.; Lopez, R.; Thompson, J.D.; Gibson, T.J.; Higgins, D.G., Clustal W and Clustal X version 2.0. *Bioinformatics,* **2007**, *23*, (21), 2947-2948.

[54] Kadam, R.U.; Tavares, J.; Kiran, V.M.; Cordeiro, A.; Ouaissi, A.; Roy, N., Structure function analysis of Leishmania sirtuin: an ensemble of in silico and biochemical studies. *Chem Biol Drug Des,* **2008**, *71*, (5), 501-506.

[55] Lipinski, C.A.; Lombardo, F.; Dominy, B.W.; Feeney, P.J., Experimental and computational approaches to estimate solubility and permeability in drug discovery and development settings. *Adv Drug Deliv Rev,* **2001**, *46*, (1-3), 3-26.

[56] Veber, D.F.; Johnson, S.R.; Cheng, H.Y.; Smith, B.R.; Ward, K.W.; Kopple, K.D., Molecular properties that influence the oral bioavailability of drug candidates. *J Med Chem,* **2002**, *45*, (12), 2615-2623.

[57] Oprea, T.I.; Davis, A.M.; Teague, S.J.; Leeson, P.D., Is there a difference between leads and drugs? A historical perspective. *J Chem Inf Comput Sci,* **2001**, *41*, (5), 1308-1315.

[58] Congreve, M.; Carr, R.; Murray, C.; Jhoti, H., A 'rule of three' for fragment-based lead discovery? *Drug Discov Today,* **2003**, *8*, (19), 876-877.

[59] Denu, J.M., Linking chromatin function with metabolic networks: Sir2 family of NAD(+)-dependent deacetylases. *Trends Biochem Sci,* **2003**, *28*, (1), 41-48.

[60] Sauve, A.A.; Schramm, V.L., SIR2: the biochemical mechanism of NAD(+)-dependent protein deacetylation and ADP-ribosyl enzyme intermediates. *Curr Med Chem,* **2004**, *11*, (7), 807-826.

[61] Keiser, M.J.; Roth, B.L.; Armbruster, B.N.; Ernsberger, P.; Irwin, J.J.; Shoichet, B.K., Relating protein pharmacology by ligand chemistry. *Nat Biotechnol,* **2007**, *25*, (2), 197-206.

[62] Hert, J.; Keiser, M.J.; Irwin, J.J.; Oprea, T.I.; Shoichet, B.K., Quantifying the relationships among drug classes. *J Chem Inf Model,* **2008**, *48*, (4), 755-765.

[63] Wallace, A.C.; Laskowski, R.A.; Thornton, J.M., LIGPLOT: a program to generate schematic diagrams of protein-ligand interactions. *Protein Eng,* **1995**, *8*, (2), 127-134.

[64] Ota, H.; Eto, M.; Kano, M.R.; Ogawa, S.; Iijima, K.; Akishita, M.; Ouchi, Y., Cilostazol inhibits oxidative stress-induced premature senescence via upregulation of Sirt1 in human endothelial cells. *Arterioscler Thromb Vasc Biol,* **2008**, *28*, (9), 1634-1639.

[65] De Clercq, E., Antiviral drug discovery: ten more compounds, and ten more stories (part B). *Med Res Rev,* **2009**, *29*, (4), 571-610.

[66] Trapp, J.; Meier, R.; Hongwiset, D.; Kassack, M.U.; Sippl, W.; Jung, M., Structure-activity studies on suramin analogues as inhibitors of NAD+-dependent histone deacetylases (sirtuins). *ChemMedChem,* **2007**, *2*, (10), 1419-1431.

[67] Kaur, S.; Shivange, A.V.; Roy, N., Structural analysis of trypanosomal sirtuin: an insight for selective drug design. *Mol Divers,* **2010**, *14*, (1), 169-178.

# CAPÍTULO 4

# CONSIDERAÇÕES FINAIS

## 4. CONSIDERAÇÕES FINAIS

As sirtuínas têm sido alvo de estudos intensos desde a descoberta de Sir2 como um fator de longevidade. A função principal das sirtuínas talvez seja promover sobrevivência e resistência ao estresse, resultando em longevidade. Supõe-se que uma vantagem evolutiva que surge da capacidade de modificar a expectativa de vida em resposta ao estresse ambiental talvez tenha permitido a estas enzimas serem conservadas como espécie desenvolvida e aceitarem novas funções em resposta a novas exigências do ambiente. Isto pode explicar por que as sirtuínas têm efeitos marcantes na expectativa de vida em organismos diversos (Sedding e Haendeler, 2007; Vakhrusheva, Braeuer *et al.*, 2008).

Atuando como desacetilases ou ADP-ribosiltransferases, são reguladas pelo cofator NAD e assim podem servir de sensores do estado metabólico da célula e organismo (Longo e Kennedy, 2006). A elucidação de estruturas tridimensionais de diversas sirtuínas tem gerado possibilidades de se estabelecer relações entre estruturas e estudos de atividade, que possibilitam o entendimento dos pontos chaves dos mecanismos de ação de sirtuínas (Finnin, Donigian *et al.*, 2001; Avalos, Boeke *et al.*, 2004; Avalos, Bever *et al.*, 2005; Hoff, Avalos *et al.*, 2006).

As sirtuínas têm recebido notável atenção pela sua influência no metabolismo de mamíferos, estando relacionadas à busca de novas alternativas terapêuticas para doenças associadas ao envelhecimento e ao aumento da expectativa de vida. Através da modulação das rotas das sirtuínas pode-se obter efeitos antienvelhecimento e pode-se prevenir ou retardar doenças decorrentes deste. Estudos diversos apresentam moléculas capazes de modular processos metabólicos e celulares através da inibição de sirtuínas. A inibição de sirtuínas resulta em atividades variadas, incluindo antiparasitária (anti-tripanossomais e anti-leishmania), antiviral (De Clercq, 2009), nas doenças neurodegenerativas, como o Parkinson

(Outeiro, Kontopoulos *et al.*, 2007) e especialmente antitumoral (Bedalov, Gatbonton *et al.*, 2001; Bitterman, Anderson *et al.*, 2002; Avalos, Bever *et al.*, 2005; Napper, Hixon *et al.*, 2005; Olaharski, Rine *et al.*, 2005; Heltweg, Gatbonton *et al.*, 2006; Ota, Tokunaga *et al.*, 2006; Lain, Hollick *et al.*, 2008; Lara, Mai *et al.*, 2009).

A busca por inibidores seletivos de sirtuínas que apresentam como alvo um sítio de ligação específico, e não o do NAD, é importante no sentido de se evitar interferência na atividade de outras proteínas que são dependentes de NAD (Schuetz, Min *et al.*, 2007). O foco se dá especialmente em inibidores específicos de SIRT1, para a qual existe maior número de estudos relacionados ao câncer e na busca de possíveis quimioterápicos. Estudos indicam que inibidores seletivos de SIRT1 aumentam os níveis de p53, aumentando a morte de células tumorais sem efeito tóxico para células normais, sendo estes inibidores bons candidatos para otimização de fármacos anticâncer (Brooks e Gu, 2008; Lain, Hollick *et al.*, 2008; Neugebauer, Uchiechowska *et al.*, 2008).

A ausência de estrutura elucidada por cristalografia de SIRT1 humana em bancos de dados impulsiona pesquisas no campo da modelagem molecular por homologia para que a mesma possa ser utilizada na busca de novos fármacos. Neste trabalho foi possível modelar a SIRT1 humana a partir da Sir2 de *Thermotoga maritima* (PDB: 1YC5) por esta apresentar 38% de identidade sequencial. Como esperado, a estrutura da SIRT1 obtida por modelagem por homologia apresentou um enovelamento clássico de sirtuínas. A estrutura da SIRT1 modelada (SIRT1m) apresentou uma conformação bilobada com o maior domínio consistindo em *Rossmann fold* modificado encontrado em diversas enzimas que se ligam ao NAD(H) e NADP(H), e um menor domínio. Os dois lobos são ligados por quatro cadeias polipeptídicas. Na interface entre os dois domínios existe um grande sulco

formado pelo cruzamento destas quatro cadeias polipeptídicas, duas voltas do maior domínio e um *loop* do menor domínio. O maior lobo é formado por quatro folhas beta (β1-3 e β7). Esta folha beta central é cercada por seis hélices (α1, α2, α4, 5α, α7 e 8). Entre ambos os lobos há uma cavidade a qual o NAD se liga. O menor domínio contém uma folha beta paralela, formada por três folhas beta (β4, β5 e β6) e duas hélices alfa (α3 e α6).

O modelo obtido foi utilizado para o *virtual screening* com um banco de moléculas da família da nicotinamida (477 moléculas) e outro da Sigma-Aldrich (15181 moléculas). O protocolo de *docking* proposto no presente trabalho foi capaz de reproduzir a estrutura cristalográfica de sirtuínas, e os resultados obtidos no *virtual screening* realizado são promissores para o desenvolvimento de novos fármacos moduladores de sirtuínas, indicando novos inibidores em potencial de SIRT1.

A utilização do programa MOLDOCK para a estrutura Sir2 *de Thermotoga maritima* (modelo) em complexo com nicotinamida foi capaz de prever corretamente o posicionamento da nicotinamida no sítio do modelo sendo capaz de reproduzir a estrutura cristalográfica. O menor valor de RMSD da sobreposição foi de 0,73 Å. Protocolos de *docking* flexível similares tem sido utilizados em *virtual screening* com foco em Sir2 de *Leishmania* (Kadam, Tavares et al., 2008).

A nicotinamida tem diversas propriedades estruturais que a torna uma molécula promissora para o procedimento de *virtual screening* baseado em estrutura. Essas propriedades atendem às regras de Lipinski e Veber (Lipinski, Lombardo *et al.*, 2001; Veber, Johnson *et al.*, 2002). O conhecimento de conservação do modelo, aliado ao *virtual screening* baseado em fragmento, tem sido útil como guia na busca de propriedades estruturais na construção de bibliotecas de

moléculas (Oprea, Davis *et al.*, 2001). Este conhecimento está incorporado na regra dos três, a qual estabelece alguns critérios que tornam atrativa uma molécula para construir uma biblioteca para *screening* (Congreve, Carr *et al.*, 2003). Através da observação da estrutura da nicotinamida, constata-se que ela preenche estes requisitos. Tem sido relatado, em diversos estudos, que a nicotinamida é uma molécula que inibe a atividade de desacetilação da SIRT1 (Sauve, Celic *et al.*, 2001; Bitterman, Anderson *et al.*, 2002; Denu, 2003; Avalos, Boeke *et al.*, 2004; Sauve e Schramm, 2004).

A partir dos resultados do *virtual screening* da família nicotinamida com a SIRT1 modelada foi possível selecionar as 10 melhores estruturas acopladas. As simulações de *docking* destas moléculas contra o sítio ativo de SIRT1 tiveram como melhor resultado o ZINC00070123 (6-(3-nitrophenyl)pyrrolo[3,4-b]pyridine-5,7-dione), sendo este o melhor acoplamento, ou seja, de menor *Plant score* (-74.99) e o segundo melhor o ZINC00004778 (11-cyclopropyl-5,11-dihydro-4-methyl-6H-dipyrido [3,2-b:2',3'-e][1,4] diazepin-6-one) (*Plant score*: -74,85), entre os 477 possíveis ligantes testados.

Pela análise do posicionamento do primeiro ligante acoplado na proteína, foi possível constatar que ele apresentou interações de ligação de hidrogênio com a cadeia principal de Ala 20, Phe 31, Leu 201, Leu 202, Val 203 e com a cadeia lateral Gln 103, Ser 199, Asn 104. Já o segundo melhor ligante apresentou interações de ligação de hidrogênio com a cadeia principal de Phe 31 e com a cadeia lateral Asn 104. Observou-se que nos dois melhores acoplamentos, as ligações de hidrogênio, entre os ligantes e a proteína modelada ocorrem com os grupamentos amida dos ligantes, podendo ocorrer tanto com os nitrogênios quanto com os oxigênios destes. Esses resultados sugerem que o grupamento amida deve desempenhar um papel

importante na interação entre a SIRT1m e ligantes. Além disso, os melhores ligantes apresentam algumas características comuns estruturais nas interações intermoleculares entre ligante e proteína. A característica mais marcante é a participação de Phe 31 e Asn 104 em ligações de hidrogênio intermoleculares, o que indica a importância destas interações para o ligante, o que não foi observado em estudos de *virtual screening* publicados anteriormente. Isto pode ter sido observado devido às estratégias de *virtual screening* adotadas e também as diferenças nas bibliotecas de pequenas moléculas utilizadas nas abordagens.

Com o objetivo de estabelecer uma relação entre estrutura e a atividade do melhores resultados obtidos pelo *virtual screening*, foi empregada uma técnica que quantitativamente agrupa e relaciona compostos baseando-se em suas similaridades químicas, utilizando o conjunto de ferramentas de aproximação por similaridade, Similarity Ensamble Approach (SEA). Para tanto foi realizada uma busca para cada um dos compostos que apresentaram menor energia (Keiser, Roth *et al.*, 2007). Para a identificação das atividades relacionadas aos melhores resultados do *virtual screening*, o critério utilizado foi o *e-value,* que representa a probabilidade de se observar um determinado dado de forma aleatória, ou seja, quanto menor o *e-value*, mais intensa será a relação entre o composto e a atividade referenciada. Para garantir uma maior confiabilidade dos resultados, foram selecionadas para a discussão as atividades com um valor de corte para o *e-value* de $10^{-10}$, pois este representa similaridade na relação estrutura-atividade de forma estatisticamente satisfatória (Keiser, Roth *et al.*, 2007; Hert, Keiser *et al.*, 2008).

Foi relatado que diversos inibidores de sirtuínas possuem atividade anti-tumoral, tais como nicotinamida, esplitomicina, sirtinol, cambinol, dihidrocumarina e alguns indóis e salermida (Bedalov, Gatbonton *et al.*, 2001; Bitterman, Anderson *et*

*al.*, 2002; Avalos, Bever *et al.*, 2005; Napper, Hixon *et al.*, 2005; Olaharski, Rine *et al.*, 2005; Heltweg, Gatbonton *et al.*, 2006; Ota, Tokunaga *et al.*, 2006; Lara, Mai *et al.*, 2009). Entretanto o efeito antitumoral que esses compostos apresentam em comum depende em geral do tipo de tumor e das condições de estresse. Além disso, os seus mecanismos de ação ocorrem de forma variada ou ainda não estão completamente elucidados. Lara e colaboradores (2009) descreveram a síntese e o mecanismo de ação de salermida, um potente inibidor de SIRT1 e SIRT2, induzindo a apoptose somente no câncer, preservando as células normais (Lara, Mai *et al.*, 2009).

A partir dos resultados obtidos na pesquisa no SEA para os potenciais inibidores, que relaciona estruturas com suas atividades, não foi possível estabelecer relação com a atividade desempenhada por inibidores de SIRT1, apesar da similaridade estrutural com nicotinamida. Este resultado sugere a necessidade de testes experimentais de atividade com as moléculas de melhor acoplamento para que se possa confirmar a hipótese de que estas inibem efetivamente SIRT1.

Um resultado interessante foi obtido para ZINC00088263. Este indica atividades como estimulante do SNC e antagonista dos receptores AMPA para esta molécula, ambas as atividades relacionadas com neuroproteção. Além disso, estudo recente indicou o envolvimento de SIRT1 na modulação da plasticidade sináptica e formação da memória, o que demonstrou o seu valor como um potencial alvo terapêutico para o tratamento de distúrbios do sistema nervoso central (Gao, Wang *et al.*, 2010). Pelo resultado obtido para o melhor ligante ZINC00070123 e também para o ZINC00099922, temos indícios de que haja atividades anti-inflamatórias e de imunossupressão. Tem sido descrita a relação potencial de inibição SIRT1 na artrite reumatoide, e um estudo recente indicou que a administração terapêutica dos

inibidores da SIRT1 pode seletivamente induzir a apoptose em locais de inflamação na artrite reumatóide (Grabiec, Krausz *et al.*, 2010) . Nossos resultados indicam que ambas as moléculas inibem a SIRT1, e por isso é tentador especular que ambas também podem ser usadas como possíveis fármacos anti-inflamatórios.

Além do ao *virtual screening* com o banco de moléculas derivadas de nicotinamida utilizando-se o protocolo proposto, procedeu-se ao *blind docking*, abrangendo-se toda a proteína modelada (esfera com raio de 32Å). Foi utilizado o mesmo protocolo para os demais parâmetros, com o qual obteve-se um RMSD de 3,1 Å e um Plant *score* de -53,1129. Também foi realizado o *virtual screening* da sirtuína modelada com inibidores conhecidos (Bitterman, Anderson *et al.*, 2002; Marcotte, Richardson *et al.*, 2004; Mai, Massa *et al.*, 2005; Szczepankiewicz e Ng, 2008). O *Plant score* de cada acoplamento foi relacionado às concentrações de inibição a 50% (ICs 50%) referenciadas na literatura. A partir da análise dessa relação é possível constatar que o protocolo de *docking* proposto forneceu resultados coerentes seguindo a mesma ordem lógica dos dados experimentais, como observado na tabela 2

**Tabela 2**. Resultados do *virtual screening* de inibidores conhecidos com a SIRT1m.

| Ligante | Plant *Score* | IC50 (µM) | Referência |
|---|---|---|---|
| Ex527 | -61.8894 | 0,098 | Szczepankiewicz, 2008 |
| Nicotinamida | -46.6765 | < 50 | Bitterman, 2002; Marcotte, 2004 |
| Sirtinol | 50.2177 | 131 | Mai, 2005 |

Além da biblioteca de estruturas derivadas de nicotinamida, a estrutura de SIRT1 modelada foi utilizada para o *virtual screening* contra uma biblioteca de mais de 15.000 compostos obtidos da base de dados da Sigma Aldrich, procedeu-se o mesmo método de análise, sendo que para este grupo utilizou-se o valor de corte de *Plant score* de -75. Assim foi possível demonstrar que as moléculas com melhor

acoplamento resultantes do *virtual screening* apresentaram atividades características de moduladores de SIRT1.

A análise do posicionamento do ligante ZINC02548278 (methyl (3R)-(-)-3-(methyl -1H-indol-3-YL)-3-phenylpropanoate) acoplado na proteína, com melhor valor de Plant *Score*, apresentou uma interação de ligação de hidrogênio com a cadeia principal de Phe 31. Além disso, através do programa LIGPLOT (Wallace, Laskowski *et al.*, 1995), foram identificadas 35 interações de van der Waals. Essas interações apresentadas podem ter contribuído com o alto valor de afinidade de ligação indicada pelo Plant *Score* encontrado através do *virtual screening*.

De acordo com a predição do SEA, a molécula ZINC02548278 (melhor acoplamento) apresentou uma atividade para a qual, a partir da busca de resultados de publicações, não foi possível estabelecer alguma relação (Ota, Eto *et al.*, 2008). Para as demais moléculas que apresentaram um valor inferior ao de corte de -75 de Plant *Score* e de $10^{-10}$ de *e-value*, foram encontradas diversas atividades na literatura a respeito das atividades relacionadas com os resultados da busca realizada através da ferramenta de aproximação SEA. Entre as ações de inibidores sirtuínas, foi possível fazer relação com antidiabética tipo 2, antiviral e antitripanossomal.

Erion e colaboradores demonstram que a inibição da SIRT1 diminui a hiperglicemia hepática e aumenta a sensibilidade à insulina. Também foi relatado por Rodgers e colaboradores (2005) que o *knockdown* de SIRT1 hepática causa hipoglicemia. Esses dados indicam que a SIRT1 hepática é um importante fator para a regulação do metabolismo de glicose e lipídios em resposta a restrição calórica. Assim as moléculas ZINC12957072 e ZINC04078894 possivelmente são inibidoras de SIRT1 e, conforme a busca realizada, possam atuar no tratamento e prevenção

de diabetes tipo 2 e na imunomodulação (Rodgers, Lerin *et al.*, 2005; Erion, Yonemitsu *et al.*, 2009).

Também foram encontradas referências relativas a atividade antiviral e antitripanossomal para a molécula ZINC04078894. Esta informação coincide com a atividade da suramina, uma molécula conhecida como inibidora não específica de SIRT1, que foi identificada como antiviral (De Clercq, 2009). O inibidor suramina também foi identificado experimentalmente como uma molécula antitripanossomal, novamente confirmando os resultados da busca através da ferramenta SEA pela qual foi encontrada essa atividade (Trapp, Meier *et al.*, 2007). Com a identificação de moléculas antitripanossomal, como ZINC04078894, é possível obter informações para o desenvolvimento de inibidores mais específicos através de estudos estruturais detalhados, comparando o acoplamento com sirtuínas humanas e de tripanossomas, sendo estas informações úteis no desenvolvimento de novas estratégias para o desenho de fármacos inibidores seletivos que apresentam maior toxicidade em relação à proteína alvo do parasita e menor toxicidade à proteína humana (King-Keller, Li et al., 2010).

Relacionando a pesquisa da ferramenta SEA e os dados encontrados na literatura, foi possível demonstrar que as moléculas de melhor acoplamento resultantes, de forma global, do *virtual screening* apresentaram atividades características de moduladores de SIRT1. Entre elas, o de protetor neuronal, antiviral e antitripanossomal e anti-inflamatórios, relacionados à inibição de sirtuínas, indicando que estudos experimentais para essas moléculas podem trazer resultados importantes. O protocolo de acoplamento proposto pelo presente trabalho foi capaz de reproduzir a estrutura de cristalográficas de sirtuínas, e os resultados obtidos pelo procedimento de *virtual screening* são promissores na busca de novos inibidores de

sirtuínas, indicando novos potenciais inibidores de SIRT1. Não obstante, o cuidado deve ser exercitado quando são selecionados inibidores de SIRT1, uma vez que esses inibidores podem ter efeitos colaterais indesejáveis, tendo em vista o fato de que a inibição direta da SIRT1 pode afetar a atividade cerebral e também a inibição da plasticidade e da memória, com base nos resultados de previsão SEA. Além disso, a análise dos resultados para a molécula ZINC04078894 sugere atividades antiviral e antiparasitária, ambas relacionadas à inibição de sirtuínas, indicando que estudos experimentais para essa molécula podem trazer resultados promissores. Através desses resultados, pode-se constatar que os possíveis inibidores de sirtuínas encontrados são alvos em potencial na busca de novos fármacos para o tratamento de diversas doenças.

Observando-se os resultados obtidos percebe-se que existem atividades de moduladores de sirtuínas sendo estas de inibidores e ativadores. Entretanto o foco desse trabalho foi a busca de inibidores pois estes já apresentam maior avanço nos estudos estruturais e de mecanismo de ligação. Dessa forma, desperta-se também o interesse no estudo de ativadores que poderão ser investigados em trabalhos futuros.

Estudos de *virtual screening* demonstram alto grau de importância na busca racional de novos fármacos, revelando que é possível fazer uma varredura em tempo relativamente curto em um grande número de moléculas, realizando uma seleção destas para posteriormente serem pesquisadas experimentalmente *in vivo*. Com isso, o processo de busca de novos fármacos agrega agilidade e diminuição considerável em custos experimentais e poupam-se muitas vidas de animais. Com a realização deste trabalho foi possível encontrar algumas moléculas promissoras que necessitam de estudos experimentais para a comprovação das suas atividades aqui

propostas. Além disso, são importantes estudos experimentais com o objetivo de elucidar os mecanismos de ação dessas moléculas. Ainda dentro da bioquímica estrutural temos várias possibilidades de expansão dessa pesquisa *in silico*, como por exemplo na simulação de dinâmica molecular, bem como em experimentação no campo da cristalografia.

# REFERÊNCIAS BIBLIOGRÁFICAS


ALSFORD, S. *et al.* A sirtuin in the African trypanosome is involved in both DNA repair and telomeric gene silencing but is not required for antigenic variation. *Mol Microbiol* [S.I.], v. 63, n. 3, p. 724-36, Feb 2007.

ASHRAF, N. *et al.* Altered sirtuin expression is associated with node-positive breast cancer. *British Journal of Cancer* [S.I.], v. 95, n. 8, p. 1056-1061, Oct 23 2006.

AVALOS, J. L. *et al.* Mechanism of sirtuin inhibition by nicotinamide: altering the NAD(+) cosubstrate specificity of a Sir2 enzyme. *Mol Cell* [S.I.], v. 17, n. 6, p. 855-68, Mar 18 2005.

_____. Structural basis for the mechanism and regulation of Sir2 enzymes. *Mol Cell* [S.I.], v. 13, n. 5, p. 639-48, Mar 12 2004.

BAUR, J. A. *et al.* Resveratrol improves health and survival of mice on a high-calorie diet. *Nature* [S.I.], v. 444, n. 7117, p. 337-42, Nov 16 2006.

BAUR, J. A.; SINCLAIR, D. A. Therapeutic potential of resveratrol: the in vivo evidence. *Nat Rev Drug Discov* [S.I.], v. 5, n. 6, p. 493-506, Jun 2006.

BEDALOV, A. *et al.* Identification of a small molecule inhibitor of Sir2p. *Proc Natl Acad Sci U S A* [S.I.], v. 98, n. 26, p. 15113-8, Dec 18 2001.

BERMAN, H. M. *et al.* The Protein Data Bank. *Nucleic Acids Res* [S.I.], v. 28, n. 1, p. 235-42, Jan 1 2000.

BERNSTEIN, F. C. *et al.* The Protein Data Bank: a computer-based archival file for macromolecular structures. *J Mol Biol* [S.I.], v. 112, n. 3, p. 535-42, May 25 1977.

BITTERMAN, K. J. *et al.* Inhibition of silencing and accelerated aging by nicotinamide, a putative negative regulator of yeast sir2 and human SIRT1. *J Biol Chem* [S.I.], v. 277, n. 47, p. 45099-107, Nov 22 2002.

BORDONE, L. *et al.* Sirt1 regulates insulin secretion by repressing UCP2 in pancreatic beta cells. *PLoS Biol* [S.I.], v. 4, n. 2, p. e31, Feb 2006.

BROOKS, C. L.; GU, W. p53 Activation: a case against Sir. *Cancer Cell* [S.I.], v. 13, n. 5, p. 377-8, May 2008.

_____. Anti-aging protein SIRT1: a role in cervical cancer? *Aging (Albany NY)* [S.I.], v. 1, n. 3, p. 278-80, Mar 2009a.

_____. How does SIRT1 affect metabolism, senescence and cancer? *Nat Rev Cancer* [S.I.], v. 9, n. 2, p. 123-8, Feb 2009b.

CANDURI, F.; DE AZEVEDO, W. F. Protein crystallography in drug discovery. *Curr Drug Targets* [S.I.], v. 9, n. 12, p. 1048-53, Dec 2008.

CHUA, K. F. *et al.* Mammalian SIRT1 limits replicative life span in response to chronic genotoxic stress. *Cell Metab* [S.I.], v. 2, n. 1, p. 67-76, Jul 2005.

CONGREVE, M. *et al.* A 'rule of three' for fragment-based lead discovery? *Drug Discov Today* [S.I.], v. 8, n. 19, p. 876-7, Oct 1 2003.

COSGROVE, M. S. *et al.* The structural basis of sirtuin substrate affinity. *Biochemistry* [S.I.], v. 45, n. 24, p. 7511-21, Jun 20 2006.

DE AZEVEDO, W. F., JR. MolDock applied to structure-based virtual screening. *Curr Drug Targets* [S.I.], v. 11, n. 3, p. 327-34, Mar 2010.

DE AZEVEDO, W. F., JR.; DIAS, R. Computational methods for calculation of ligand-binding affinity. *Curr Drug Targets* [S.I.], v. 9, n. 12, p. 1031-9, Dec 2008.

DE CLERCQ, E. Antiviral drug discovery: ten more compounds, and ten more stories (part B). *Med Res Rev* [S.I.], v. 29, n. 4, p. 571-610, Jul 2009.

DENU, J. M. Linking chromatin function with metabolic networks: Sir2 family of NAD(+)-dependent deacetylases. *Trends Biochem Sci* [S.I.], v. 28, n. 1, p. 41-8, Jan 2003.

DIAS, R.; DE AZEVEDO, W. F., JR. Molecular docking algorithms. *Curr Drug Targets* [S.I.], v. 9, n. 12, p. 1040-7, Dec 2008.

DIAS, R. *et al.* Evaluation of molecular docking using polynomial empirical scoring functions. *Curr Drug Targets* [S.I.], v. 9, n. 12, p. 1062-70, Dec 2008.

EIBEN, A. E.; SMITH, J. E. *Introduction to Evolutionary Computing*. New York: Springer-Verlag, 2003.

ERION, D. M. *et al.* SirT1 knockdown in liver decreases basal hepatic glucose production and increases hepatic insulin responsiveness in diabetic rats. *Proc Natl Acad Sci U S A* [S.I.], v. 106, n. 27, p. 11288-93, Jul 7 2009.

EWING, T. J. *et al.* DOCK 4.0: search strategies for automated molecular docking of flexible molecule databases. *J Comput Aided Mol Des* [S.I.], v. 15, n. 5, p. 411-28, May 2001.

FINNIN, M. S. *et al.* Structure of the histone deacetylase SIRT2. *Nat Struct Biol* [S.I.], v. 8, n. 7, p. 621-5, Jul 2001.

FOGEL, L. J. *et al. Artificial Intelligence through Simulated Evolution.* New York: John Wiley, 1966.

FORD, E. *et al.* Mammalian Sir2 homolog SIRT7 is an activator of RNA polymerase I transcription. *Genes & Development* [S.I.], v. 20, n. 9, p. 1075-1080, May 1 2006.

FORD, J. *et al.* Cancer-specific functions of SIRT1 enable human epithelial cancer cell growth and survival. *Cancer Res* [S.I.], v. 65, n. 22, p. 10457-63, Nov 15 2005.

FRESCAS, D. *et al.* Nuclear trapping of the forkhead transcription factor FoxO1 via Sirt-dependent deacetylation promotes expression of glucogenetic genes. *J Biol Chem* [S.I.], v. 280, n. 21, p. 20589-95, May 27 2005.

FRIESNER, R. A. *et al.* Glide: a new approach for rapid, accurate docking and scoring. 1. Method and assessment of docking accuracy. *J Med Chem* [S.I.], v. 47, n. 7, p. 1739-49, Mar 25 2004.

GAN, L.; MUCKE, L. Paths of convergence: Sirtuins in aging and neurodegeneration. *Neuron* [S.I.], v. 58, n. 1, p. 10-14, Apr 10 2008.

GAO, J. *et al.* A novel pathway regulates memory and plasticity via SIRT1 and miR-134. *Nature* [S.I.], v. 466, n. 7310, p. 1105-9, Aug 26 2010.

GEHLHAAR, D. K. *et al.* Fully automated and rapid flexible docking of inhibitors covalently bound to serine proteases. *Abstracts of Papers of the American Chemical Society* [S.I.], v. 214, p. 155-COMP, Sep 7 1997.

_____. Docking Conformationally Flexible Small Molecules into a Protein-Binding Site through Simulated Evolution. *Abstracts of Papers of the American Chemical Society* [S.I.], v. 209, p. 146-COMP, Apr 2 1995.

GEY, C. *et al.* Phloroglucinol derivatives guttiferone G, aristoforin, and hyperforin: inhibitors of human sirtuins SIRT1 and SIRT2. *Angew Chem Int Ed Engl* [S.I.], v. 46, n. 27, p. 5219-22, 2007.

GLOVER, L. *et al.* Deletion of a trypanosome telomere leads to loss of silencing and progressive loss of terminal DNA in the absence of cell cycle arrest. *Nucleic Acids Res* [S.I.], v. 35, n. 3, p. 872-80, 2007.

GOODSELL, D. S. *et al.* Automated docking of flexible ligands: applications of AutoDock. *J Mol Recognit* [S.I.], v. 9, n. 1, p. 1-5, Jan-Feb 1996.

GRABIEC, A. M. *et al.* Histone deacetylase inhibitors suppress inflammatory activation of rheumatoid arthritis patient synovial macrophages and tissue. *J Immunol* [S.I.], v. 184, n. 5, p. 2718-28, Mar 1 2010.

GREER, E. L.; BRUNET, A. FOXO transcription factors at the interface between longevity and tumor suppression. *Oncogene* [S.I.], v. 24, n. 50, p. 7410-25, Nov 14 2005.

HAIGIS, M. C. *et al.* SIRT4 inhibits glutamate dehydrogenase and opposes the effects of calorie restriction in pancreatic beta cells. *Cell* [S.I.], v. 126, n. 5, p. 941-54, Sep 8 2006.

HALGREN, T. A. *et al.* Glide: a new approach for rapid, accurate docking and scoring. 2. Enrichment factors in database screening. *J Med Chem* [S.I.], v. 47, n. 7, p. 1750-9, Mar 25 2004.

HALLOWS, W. C. *et al.* Sirtuins deacetylate and activate mammalian acetyl-CoA synthetases. *Proc Natl Acad Sci U S A* [S.I.], v. 103, n. 27, p. 10230-5, Jul 5 2006.

HELTWEG, B. *et al.* Antitumor activity of a small-molecule inhibitor of human silent information regulator 2 enzymes. *Cancer Res* [S.I.], v. 66, n. 8, p. 4368-77, Apr 15 2006.

HERT, J. *et al.* Quantifying the relationships among drug classes. *J Chem Inf Model* [S.I.], v. 48, n. 4, p. 755-65, Apr 2008.

HIRSCHEY, M. D. *et al.* SIRT3 regulates mitochondrial fatty-acid oxidation by reversible enzyme deacetylation. *Nature* [S.I.], v. 464, n. 7285, p. 121-5, Mar 4 2010.

HOFF, K. G. *et al.* Insights into the sirtuin mechanism from ternary complexes containing NAD+ and acetylated peptide. *Structure* [S.I.], v. 14, n. 8, p. 1231-40, Aug 2006.

HOFSETH, L. J. *et al.* Taming the beast within: resveratrol suppresses colitis and prevents colon cancer. *Aging (Albany NY)* [S.I.], v. 2, n. 4, p. 183-4, Apr 2010.

HOWITZ, K. T. *et al.* Small molecule activators of sirtuins extend Saccharomyces cerevisiae lifespan. *Nature* [S.I.], v. 425, n. 6954, p. 191-6, Sep 11 2003.

JAIN, A. N. Surflex: fully automatic flexible molecular docking using a molecular similarity-based search engine. *J Med Chem* [S.I.], v. 46, n. 4, p. 499-511, Feb 13 2003.

JANG, M. *et al.* Cancer chemopreventive activity of resveratrol, a natural product derived from grapes. *Science* [S.I.], v. 275, n. 5297, p. 218-20, Jan 10 1997.

JONES, G. *et al.* A genetic algorithm for flexible molecular overlay and pharmacophore elucidation. *J Comput Aided Mol Des* [S.I.], v. 9, n. 6, p. 532-49, Dec 1995.

_____. Development and validation of a genetic algorithm for flexible docking. *J Mol Biol* [S.I.], v. 267, n. 3, p. 727-48, Apr 4 1997a.

_____. Development and validation of a genetic algorithm for flexible docking. *Journal of Molecular Biology* [S.I.], v. 267, n. 3, p. 727-748, Apr 4 1997b.

JOY, S. *et al.* Detailed comparison of the protein-ligand docking efficiencies of GOLD, a commercial package and ArgusLab, a licensable freeware. *In Silico Biol* [S.I.], v. 6, n. 6, p. 601-5, 2006.

KADAM, R. U. *et al.* Structure function analysis of Leishmania sirtuin: an ensemble of in silico and biochemical studies. *Chem Biol Drug Des* [S.I.], v. 71, n. 5, p. 501-6, May 2008.

KAUR, S. *et al.* Structural analysis of trypanosomal sirtuin: an insight for selective drug design. *Mol Divers* [S.I.], v. 14, n. 1, p. 169-78, Feb 2010.

KEISER, M. J. *et al.* Relating protein pharmacology by ligand chemistry. *Nat Biotechnol* [S.I.], v. 25, n. 2, p. 197-206, Feb 2007.

KING-KELLER, S. *et al.* Chemical validation of phosphodiesterase C as a chemotherapeutic target in Trypanosoma cruzi, the etiological agent of Chagas' disease. *Antimicrob Agents Chemother* [S.I.], v. 54, n. 9, p. 3738-45, Sep 2010.

KIVIRANTA, P. H. *et al.* N,N'-Bisbenzylidenebenzene-1,4-diamines and N,N'-Bisbenzylidenenaphthalene-1,4-diamines as Sirtuin Type 2 (SIRT2) Inhibitors. *J Med Chem* [S.I.], v. 49, n. 26, p. 7907-11, Dec 28 2006.

_____. Characterization of the binding properties of SIRT2 inhibitors with a N-(3-phenylpropenoyl)-glycine tryptamide backbone. *Bioorg Med Chem* [S.I.], v. 16, n. 17, p. 8054-62, Sep 1 2008.

KORB, O. *et al.* Empirical scoring functions for advanced protein-ligand docking with PLANTS. *J Chem Inf Model* [S.I.], v. 49, n. 1, p. 84-96, Jan 2009.

KRAMER, B. *et al.* Evaluation of the FLEXX incremental construction algorithm for protein-ligand docking. *Proteins-Structure Function and Bioinformatics* [S.I.], v. 37, n. 2, p. 228-41, Nov 1 1999.

KYRYLENKO, S.; BANIAHMAD, A. Sirtuin family: a link to metabolic signaling and senescence. *Curr Med Chem* [S.I.], v. 17, n. 26, p. 2921-32, 2010.

LAGOUGE, M. *et al.* Resveratrol improves mitochondrial function and protects against metabolic disease by activating SIRT1 and PGC-1alpha. *Cell* [S.I.], v. 127, n. 6, p. 1109-22, Dec 15 2006.

LAIN, S. *et al.* Discovery, in vivo activity, and mechanism of action of a small-molecule p53 activator. *Cancer Cell* [S.I.], v. 13, n. 5, p. 454-63, May 2008.

LANGLEY, B. *et al.* Remodeling chromatin and stress resistance in the central nervous system: histone deacetylase inhibitors as novel and broadly effective neuroprotective agents. *Curr Drug Targets CNS Neurol Disord* [S.I.], v. 4, n. 1, p. 41-50, Feb 2005.

LARA, E. *et al.* Salermide, a Sirtuin inhibitor with a strong cancer-specific proapoptotic effect. *Oncogene* [S.I.], v. 28, n. 6, p. 781-91, Feb 12 2009.

LIPINSKI, C. A. *et al.* Experimental and computational approaches to estimate solubility and permeability in drug discovery and development settings. *Adv Drug Deliv Rev* [S.I.], v. 46, n. 1-3, p. 3-26, Mar 1 2001.

LIU, D. *et al.* Nicotinamide Prevents NAD(+) Depletion and Protects Neurons Against Excitotoxicity and Cerebral Ischemia: NAD(+) Consumption by SIRT1 may Endanger Energetically Compromised Neurons. *Neuromolecular Medicine* [S.I.], v. 11, n. 1, p. 28-42, Mar 2009.

LIU, M.; WANG, S. MCDOCK: a Monte Carlo simulation approach to the molecular docking problem. *J Comput Aided Mol Des* [S.I.], v. 13, n. 5, p. 435-51, Sep 1999.

LONGO, V. D.; KENNEDY, B. K. Sirtuins in aging and age-related disease. *Cell* [S.I.], v. 126, n. 2, p. 257-268, Jul 28 2006.

MAI, A. *et al.* Design, synthesis, and biological evaluation of sirtinol analogues as class III histone/protein deacetylase (Sirtuin) inhibitors. *J Med Chem* [S.I.], v. 48, n. 24, p. 7789-95, Dec 1 2005.

MARCOTTE, P. A. *et al.* Fluorescence assay of SIRT protein deacetylases using an acetylated peptide substrate and a secondary trypsin reaction. *Anal Biochem* [S.I.], v. 332, n. 1, p. 90-9, Sep 1 2004.

MARKS, P. A.; XU, W. S. Histone Deacetylase Inhibitors: Potential in Cancer Therapy. *Journal of Cellular Biochemistry* [S.I.], v. 107, n. 4, p. 600-608, Jul 1 2009.

MICHAN, S.; SINCLAIR, D. Sirtuins in mammals: insights into their biological function. *Biochem J* [S.I.], v. 404, n. 1, p. 1-13, May 15 2007.

MILLER, M. D. *et al.* FLOG: a system to select 'quasi-flexible' ligands complementary to a receptor of known three-dimensional structure. *J Comput Aided Mol Des* [S.I.], v. 8, n. 2, p. 153-74, Apr 1994.

MORÉ, J. J.; WU, Z. Distance Geometry Optimization for Protein Structures. *Journal of Global Optimization* [S.I.], v. 15, n. 3, p. 16, 1999.

MORRIS, G. M. *et al.* Automated docking using a Lamarckian genetic algorithm and a empirical binding free energy funcion. *J. Comput. Chem.* [S.I.], v. 19, p. 1639-62, 1998.

MOSTOSLAVSKY, R. *et al.* Genomic instability and aging-like phenotype in the absence of mammalian SIRT6. *Cell* [S.I.], v. 124, n. 2, p. 315-29, Jan 27 2006.

NAPPER, A. D. *et al.* Discovery of indoles as potent and selective inhibitors of the deacetylase SIRT1. *J Med Chem* [S.I.], v. 48, n. 25, p. 8045-54, Dec 15 2005.

NEMOTO, S. *et al.* SIRT1 functionally interacts with the metabolic regulator and transcriptional coactivator PGC-1 alpha. *Journal of Biological Chemistry* [S.I.], v. 280, n. 16, p. 16456-16460, Apr 22 2005.

NEUGEBAUER, R. C. *et al.* Structure-activity studies on splitomicin derivatives as sirtuin inhibitors and computational prediction of binding mode. *J Med Chem* [S.I.], v. 51, n. 5, p. 1203-13, Mar 13 2008.

OKAWARA, M. *et al.* Resveratrol protects dopaminergic neurons in midbrain slice culture from multiple insults. *Biochemical Pharmacology* [S.I.], v. 73, n. 4, p. 550-560, Feb 15 2007.

OLAHARSKI, A. J. *et al.* The flavoring agent dihydrocoumarin reverses epigenetic silencing and inhibits sirtuin deacetylases. *PLoS Genet* [S.I.], v. 1, n. 6, p. e77, Dec 2005.

OPIE, L. H.; LECOUR, S. The red wine hypothesis: from concepts to protective signalling molecules. *Eur Heart J* [S.I.], v. 28, n. 14, p. 1683-93, Jul 2007.

OPREA, T. I. *et al.* Is there a difference between leads and drugs? A historical perspective. *J Chem Inf Comput Sci* [S.I.], v. 41, n. 5, p. 1308-15, Sep-Oct 2001.

OTA, H. *et al.* Cilostazol inhibits oxidative stress-induced premature senescence via upregulation of Sirt1 in human endothelial cells. *Arterioscler Thromb Vasc Biol* [S.I.], v. 28, n. 9, p. 1634-9, Sep 2008.

_____. Sirt1 inhibitor, Sirtinol, induces senescence-like growth arrest with attenuated Ras-MAPK signaling in human cancer cells. *Oncogene* [S.I.], v. 25, n. 2, p. 176-85, Jan 12 2006.

OUTEIRO, T. F. *et al.* Sirtuin 2 inhibitors rescue alpha-synuclein-mediated toxicity in models of Parkinson's disease. *Science* [S.I.], v. 317, n. 5837, p. 516-9, Jul 27 2007.

PANG, Y. P.; KOZIKOWSKI, A. P. Prediction of the binding site of 1-benzyl-4-[(5,6-dimethoxy-1-indanon-2-yl)methyl]piperidine in acetylcholinesterase by docking studies with the SYSDOC program. *J Comput Aided Mol Des* [S.I.], v. 8, n. 6, p. 683-93, Dec 1994.

PANG, Y. P. *et al.* EUDOC: a computer program for identification of drug interaction sites in macromolecules and drug leads from chemical databases. *J Comput Chem* [S.I.], v. 22, n. 15, p. 1750-1771, Nov 30 2001.

PICARD, F. *et al.* Sirt1 promotes fat mobilization in white adipocytes by repressing PPAR-gamma. *Nature* [S.I.], v. 429, n. 6993, p. 771-6, Jun 17 2004.

PIERCE, B. *et al.* M-ZDOCK: a grid-based approach for Cn symmetric multimer docking. *Bioinformatics* [S.I.], v. 21, n. 8, p. 1472-8, Apr 15 2005.

PORCU, M.; CHIARUGI, A. The emerging therapeutic potential of sirtuin-interacting drugs: from cell death to lifespan extension. *Trends Pharmacol Sci* [S.I.], v. 26, n. 2, p. 94-103, Feb 2005.

RAREY, M. *et al.* A fast flexible docking method using an incremental construction algorithm. *J Mol Biol* [S.I.], v. 261, n. 3, p. 470-89, Aug 23 1996.

RODGERS, J. T. *et al.* Nutrient control of glucose homeostasis through a complex of PGC-1alpha and SIRT1. *Nature* [S.I.], v. 434, n. 7029, p. 113-8, Mar 3 2005.

ROSENFELD, R. J. *et al.* Automated docking of ligands to an artificial active site: augmenting crystallographic analysis with computer modeling. *J Comput Aided Mol Des* [S.I.], v. 17, n. 8, p. 525-36, Aug 2003.

SAUTON, N. *et al.* MS-DOCK: accurate multiple conformation generator and rigid docking protocol for multi-step virtual ligand screening. *BMC Bioinformatics* [S.I.], v. 9, p. 184, 2008.

SAUVE, A. A. *et al.* Chemistry of gene silencing: the mechanism of NAD+-dependent deacetylation reactions. *Biochemistry* [S.I.], v. 40, n. 51, p. 15456-63, Dec 25 2001.

SAUVE, A. A.; SCHRAMM, V. L. SIR2: the biochemical mechanism of NAD(+)-dependent protein deacetylation and ADP-ribosyl enzyme intermediates. *Curr Med Chem* [S.I.], v. 11, n. 7, p. 807-26, Apr 2004.

SAUVE, A. A. *et al.* The biochemistry of sirtuins. *Annu Rev Biochem* [S.I.], v. 75, p. 435-65, 2006.

SCHUETZ, A. *et al.* Structural basis of inhibition of the human NAD+-dependent deacetylase SIRT5 by suramin. *Structure* [S.I.], v. 15, n. 3, p. 377-89, Mar 2007.

SEDDING, D.; HAENDELER, J. Do we age on Sirt1 expression? *Circ Res* [S.I.], v. 100, n. 10, p. 1396-8, May 25 2007.

SMITH, J. S. *et al.* A phylogenetically conserved NAD+-dependent protein deacetylase activity in the Sir2 protein family. *Proc Natl Acad Sci U S A* [S.I.], v. 97, n. 12, p. 6658-63, Jun 6 2000.

SZCZEPANKIEWICZ, B. G.; NG, P. Y. Sirtuin modulators: targets for metabolic diseases and beyond. *Curr Top Med Chem* [S.I.], v. 8, n. 17, p. 1533-44, 2008.

TANG, B. L. Resveratrol is neuroprotective because it is not a direct activator of Sirt1-A hypothesis. *Brain Res Bull* [S.I.], v. 81, n. 4-5, p. 359-61, Mar 16 2010.

TERVO, A. J. *et al.* An in silico approach to discovering novel inhibitors of human sirtuin type 2. *J Med Chem* [S.I.], v. 47, n. 25, p. 6292-8, Dec 2 2004.

THOMSEN, R.; CHRISTENSEN, M. H. MolDock: a new technique for high-accuracy molecular docking. *J Med Chem* [S.I.], v. 49, n. 11, p. 3315-21, Jun 1 2006.

TOTROV, M.; ABAGYAN, R. Flexible protein-ligand docking by global energy optimization in internal coordinates. *Proteins-Structure Function and Bioinformatics* [S.I.], v. Suppl 1, p. 215-20, 1997.

TRAPP, J. *et al.* Adenosine mimetics as inhibitors of NAD(+)-dependent histone deacetylases, from kinase to sirtuin inhibition. *Journal of Medicinal Chemistry* [S.I.], v. 49, n. 25, p. 7307-7316, Dec 14 2006.

_____. Structure-activity studies on suramin analogues as inhibitors of NAD(+)-dependent histone deacetylases (Sirtuins). *Chemmedchem* [S.I.], v. 2, n. 10, p. 1419-1431, Oct 2007.

TSAI, K. C. *et al.* The effect of different electrostatic potentials on docking accuracy: a case study using DOCK5.4. *Bioorg Med Chem Lett* [S.I.], v. 18, n. 12, p. 3509-12, Jun 15 2008.

VAKHRUSHEVA, O. *et al.* Sirt7-dependent inhibition of cell growth and proliferation might be instrumental to mediate tissue integrity during aging. *J Physiol Pharmacol* [S.I.], v. 59 Suppl 9, p. 201-12, Dec 2008.

VAQUERO, A. *et al.* SirT2 is a histone deacetylase with preference for histone H4 Lys 16 during mitosis. *Genes & Development* [S.I.], v. 20, n. 10, p. 1256-1261, May 15 2006.

VEBER, D. F. *et al.* Molecular properties that influence the oral bioavailability of drug candidates. *J Med Chem* [S.I.], v. 45, n. 12, p. 2615-23, Jun 6 2002.

VERDONK, M. L. *et al.* Improved protein-ligand docking using GOLD. *Proteins-Structure Function and Bioinformatics* [S.I.], v. 52, n. 4, p. 609-23, Sep 1 2003.

VERGNES, B. *et al.* Cytoplasmic SIR2 homologue overexpression promotes survival of Leishmania parasites by preventing programmed cell death. *Gene* [S.I.], v. 296, n. 1-2, p. 139-50, Aug 21 2002.

_____. Stage-specific antileishmanial activity of an inhibitor of SIR2 histone deacetylase. *Acta Trop* [S.I.], v. 94, n. 2, p. 107-15, May 2005.

WALLACE, A. C. *et al.* LIGPLOT: a program to generate schematic diagrams of protein-ligand interactions. *Protein Eng* [S.I.], v. 8, n. 2, p. 127-34, Feb 1995.

WESTBROOK, J. *et al.* Validation of protein structures for protein data bank. *Methods Enzymol* [S.I.], v. 374, p. 370-85, 2003.

_____. The Protein Data Bank and structural genomics. *Nucleic Acids Res* [S.I.], v. 31, n. 1, p. 489-91, Jan 1 2003.

_____. PDBML: the representation of archival macromolecular structure data in XML. *Bioinformatics* [S.I.], v. 21, n. 7, p. 988-92, Apr 1 2005.

YAMAMOTO, H. *et al.* Sirtuin functions in health and disease. *Mol Endocrinol* [S.I.], v. 21, n. 8, p. 1745-55, Aug 2007.

YANG, J. M. Development and evaluation of a generic evolutionary method for protein-ligand docking. *J Comput Chem* [S.I.], v. 25, n. 6, p. 843-57, Apr 30 2004.

YANG, J. M.; CHEN, C. C. GEMDOCK: a generic evolutionary method for molecular docking. *Proteins-Structure Function and Bioinformatics* [S.I.], v. 55, n. 2, p. 288-304, May 1 2004.

ZEMZOUMI, K. *et al.* Leishmania major: Cell type dependent distribution of a 43 kDa antigen related to silent information regulatory-2 protein family. *Biology of the Cell* [S.I.], v. 90, n. 3, p. 239-245, Jun 1998.

ZHANG, C. *et al.* Docking prediction using biological information, ZDOCK sampling technique, and clustering guided by the DFIRE statistical energy function. *Proteins-Structure Function and Bioinformatics* [S.I.], v. 60, n. 2, p. 314-318, Aug 1 2005.

ZHANG, H. S. *et al.* Nicotinamide phosphoribosyltransferase/sirtuin 1 pathway is involved in human immunodeficiency virus type 1 Tat-mediated long terminal repeat transactivation. *Journal of Cellular Biochemistry* [S.I.], v. 110, n. 6, p. 1464-70, Aug 15 2010.

# ANEXOS

## ANEXO I: Tabelas

**Tabela 1**. Exemplos de polifenóis com seus respectivos índices de estimulação catalítica da SIRT1.

| COMPOSTO | MID* ± SD | ESQUELETO ESTRUTURAL |
|---|---|---|
| Resveratrol | 13,4 ± 1,0 | 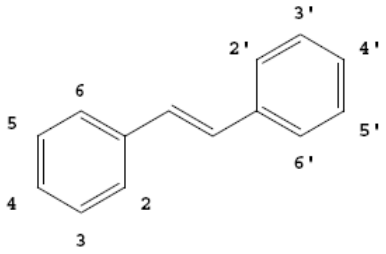 |
| (3,5,4'-Trihidroxi-*trans*-estilbeno) | | |
| Piceatanol | 7,9 ± 0,5 | |
| (3,5,3',4'- Tetrahidroxi-*trans*-estilbeno) | | |
| | | Estilbeno |
| Fisetina | 6.58 ± 0.69 | 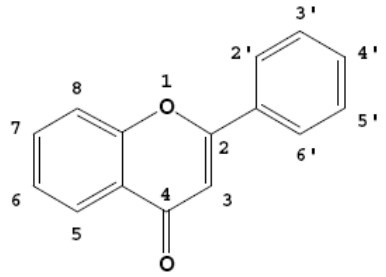 |
| (3,7,3',4'- | | |
| Tetrahidroxiflavona) | | |
| 5,7,3',4',5'- | 6.05 ± 0.98 | |
| Pentahidroxiflavona | | |
| Quercetina | 4.59 ± 0.47 | Flavona |
| (3,5,7,3',4'- | | |
| Pentahidroxiflavona) | | |
| Kamferol | 3.55 ± 0.56 | |
| (3,5,7,4'- | | |
| Tetrahidroxiflavona) | | |
| Apigenina | 2.77 ± 0.40 | |
| (5,7,4'- | | |
| Trihidroxiflavona) | | |
| Buteina | 8.53 ± 0.89 | 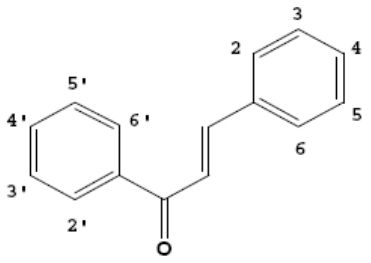 |
| (3,4,2',4'- | | |
| Tetrahidroxichalcona) | | |
| 3,4,2',4',6'- | 2.80 ± 0.32 | |
| Pentahidroxichalcona | | |
| | | Chalcona |

* Média do índice de desacetilação

**Tabela 2**. Estruturas cristalográficas de sirtuínas de microorganismos.

| PDB* | Sirtuína | Organismo | Data |
|---|---|---|---|
| 1ICI | Sir2 | *Archaeoglobus fulgidus* | Maio 2001 |
| 1MA3 | Sir2 | *Archaeoglobus fulgidus* | Outubro 2002 |
| 1M2G | Sir2 | *Archaeoglobus fulgidus* | Abril 2003 |
| 1M2H | Sir2 | *Archaeoglobus fulgidus* | Abril 2003 |
| 1M2J | Sir2 | *Archaeoglobus fulgidus* | Abril 2003 |
| 1M2K | Sir2 | *Archaeoglobus fulgidus* | Abril 2003 |
| 1M2N | Sir2 | *Archaeoglobus fulgidus* | Abril 2003 |
| 1NFH | Sir2 | *Archaeoglobus fulgidus* | Agosto 2003 |
| 1NFJ | Sir2 | *Archaeoglobus fulgidus* | Agosto 2003 |
| 1Q14 | Sir2 | *Saccharomyces cerevisiae* | Setembro 2003 |
| 1Q17 | Sir2 (Hst2) | *Saccharomyces cerevisiae* | Novembro 2003 |
| 1Q1A | Sir2 (Hst2) | *Saccharomyces cerevisiae* | Novembro 2003 |
| 1S5P | Sir2 | *Escherichia coli* | Março 2004 |
| 1S7G | Sir2 | *Archaeoglobus fulgidus* | Março 2004 |
| 1SZC | Sir2 | *Saccharomyces cerevisiae* | Junho 2004 |
| 1SZD | Sir2 | *Saccharomyces cerevisiae* | Junho 2004 |
| 1YC2 | Sir2 | *Archaeoglobus fulgidus* | Março 2005 |
| 1YC5 | Sir2 | *Thermotoga marítima* | Abril 2005 |
| 2H2D | Sir2 | *Thermotoga marítima* | Setembro 2006 |
| 2H4F | Sir2 | *Thermotoga marítima* | Setembro 2006 |
| 2H4H | Sir2 | *Thermotoga marítima* | Setembro 2006 |
| 2H4J | Sir2 | *Thermotoga marítima* | Setembro 2006 |
| 2H59 | Sir2 | *Thermotoga marítima* | Setembro 2006 |
| 2H2G | Sir2 | *Thermotoga marítima* | Novembro 2006 |
| 2H2F | Sir2 | *Thermotoga marítima* | Dezembro 2006 |
| 2H2H | Sir2 | *Thermotoga marítima* | Dezembro 2006 |
| 2H2I | Sir2 | *Thermotoga marítima* | Dezembro 2006 |
| 2OD7 | Sir2 | *Saccharomyces cerevisiae* | Fevereiro 2007 |
| 2OD9 | Sir2 | *Saccharomyces cerevisiae* | Fevereiro 2007 |
| 2OD2 | Sir2 (Hst2) | *Saccharomyces cerevisiae* | Fevereiro 2007 |
| 2QQF | Sir2 (Hst2) | *Saccharomyces cerevisiae* | Outubro 2007 |
| 2QQG | Sir2 (Hst2) | *Saccharomyces cerevisiae* | Outubro 2007 |
| 2HJH | Sir2 | *Saccharomyces cerevisiae* | Abril 2008 |
| 3D4B | Sir2 | *Thermotoga marítima* | Setembro 2008 |
| 3D81 | Sir2 | *Thermotoga marítima* | Setembro 2008 |
| 3JR3 | Sir2 | *Thermotoga marítima* | Setembro 2009 |
| 3JWP | Sir2 | *Plasmodium falciparum* | Outubro 2009 |

*Códigos de acesso PDB.

**Tabela 3**. Estruturas cristalográficas de sirtuínas humanas disponíveis.

| **PDB*** | **Sirtuína** | **Forma / Ligante** | **Data** |
|---|---|---|---|
| 1J8F | SIRT2 | Apo (zinco) | Jul 2001 |
| 2B4Y | SIRT5 | NAD e ácido 4-(2-hidroxietil)-1-piperazina etanosulfônico e zinco | Fev 2006 |
| 2NYR | SIRT5 | Suramina e zinco | Dez 2006 |
| 3GLR | SIRT3 | Acetil-coenzima A sintetase (AceCS2) e zinco | Jun 2009 |
| 3GLS | SIRT3 | Trietilenoglicol e zinco | Jun 2009 |
| 3GLT | SIRT3 | ADPR e AceCS2 e zinco | Jun 2009 |
| 3GLU | SIRT3 | AceCS2 e zinco | Jun 2009 |

*Códigos de acesso PDB.

**Tabela 4**. Programas de *docking* e respectivos algoritmos.

| PROGRAMA | MÉTODO | REFERÊNCIAS |
|---|---|---|
| AUTODOCK | Lamarckian genetic algorithm | (Goodsell, Morris *et al.*, 1996; Rosenfeld, Goodsell *et al.*, 2003) |
| DOCK | Incremental construction | (Ewing, Makino *et al.*, 2001) |
| ZDOCK | Fast Shape Matching | (Zhang, Liu *et al.*, 2005) |
| MS-DOCK | Fast Shape Matching | (Sauton, Lagorce *et al.*, 2008) |
| MCDOCK | Monte Carlo simulations | (Liu e Wang, 1999) |
| ICM | Monte Carlo simulations | (Totrov e Abagyan, 1997) |
| GOLD | Genetic algorithm | (Verdonk, Cole *et al.*, 2003; Joy, Nair *et al.*, 2006) |
| SURFLEX | Incremental construction | (Jain, 2003) |
| FLEXX | Incremental construction | (Rarey, Kramer *et al.*, 1996; Kramer, Rarey *et al.*, 1999) |
| M-ZDOCK | Fast Shape Matching | (Pierce, Tong *et al.*, 2005) |
| SYSDOC | Fast Shape Matching | (Pang e Kozikowski, 1994) |
| EUDOC | Fast Shape Matching | (Pang, Perola *et al.*, 2001) |
| FLOG | Incremental construction | (Miller, Kearsley *et al.*, 1994) |
| GLIDE | Monte Carlo simulations | (Friesner, Banks *et al.*, 2004; Halgren, Murphy *et al.*, 2004) |
| GEMDOCK | Genetic algorithm | (Yang, 2004; Yang e Chen, 2004) |
| MOLDOCK | Differencial evolution | (Thomsen e Christensen, 2006; De Azevedo, 2010) |

**ANEXO II: Comprovantes de submissão e aceite dos artigos científicos**

**Comprovante de aceite do artigo: Bio-inspired algorithms applied to molecular docking simulations**

Porto Alegre, December 8, 2010

Ms. Title: Bio-inspired algorithms applied to molecular docking simulations
(HT-SBJ-CMC-0007)

Dear Graziela Heberlé,

I am glad to inform that your manuscript entitled “Bio-inspired algorithms applied to molecular docking simulations” has been accepted for publication in Current Medicinal Chemistry.
Galley proofs of this manuscript will be sent to the authors soon.

Sincerely,


Guest Editor

Current Medicinal Chemistry (ISSN: 0929-8673)

## Comprovante de submissão do artigo: *In silico* study of SIRT1 inhibitors

November 23, 2010

Dear Dr. Walter

Many thanks for your e-mail and sending the manuscript. I've safely received it and sent to EiC for initial approval.

Feel free to contact me if you have any query.

Kind Regards,
**Ms. Sehrish Ashraf**
Manager Publications
Bentham Science Publishers Ltd.
E-mail: sehrish@benthamscience.org

P.S.: Kindly acknowledge the safe receipt of this message.

---

**From:** Walter Filgueira de A Junior [mailto:walter.junior@pucrs.br]
**Sent:** Monday, November 22, 2010 4:37 PM
**To:** Sehrish
**Cc:** mc@benthamscience.org
**Subject:** RES: Manuscript Submission | BSP-MC-2010-77 | 04-11-2010
**Importance:** High

Dear Ms. Sehrish Ashraf,

Please find attached the requested files. If you need any further information, please feel free to contact.
Please acknowledge the receipt of this message.

Kind regards,

Walter.

Prof. Dr. Walter Filgueira de Azevedo Jr.
Laboratório de Bioquímica Estrutural-LaBioQuest.
Faculdade de Biociências-PUCRS.
Av. Ipiranga, 6681. Porto Alegre-RS
http://azevedolab.net